



저작자표시-비영리-변경금지 2.0 대한민국

이용자는 아래의 조건을 따르는 경우에 한하여 자유롭게

- 이 저작물을 복제, 배포, 전송, 전시, 공연 및 방송할 수 있습니다.

다음과 같은 조건을 따라야 합니다:



저작자표시. 귀하는 원저작자를 표시하여야 합니다.



비영리. 귀하는 이 저작물을 영리 목적으로 이용할 수 없습니다.



변경금지. 귀하는 이 저작물을 개작, 변형 또는 가공할 수 없습니다.

- 귀하는, 이 저작물의 재이용이나 배포의 경우, 이 저작물에 적용된 이용허락조건을 명확하게 나타내어야 합니다.
- 저작권자로부터 별도의 허가를 받으면 이러한 조건들은 적용되지 않습니다.

저작권법에 따른 이용자의 권리는 위의 내용에 의하여 영향을 받지 않습니다.

이것은 [이용허락규약\(Legal Code\)](#)을 이해하기 쉽게 요약한 것입니다.

[Disclaimer](#)

A DISSERTATION FOR THE DEGREE OF DOCTOR OF PHILOSOPHY

**Synthesis and Characterization of Polyester Resin  
and Properties of Polyester Coatings for Multi-coated  
Automotive Pre-coated Metal System**

다층 도장을 위한 폴리에스터 도료 및 다층 도장된 자동차용  
선도장 강판의 성형성과 물성에 미치는 영향 연구

by Yong-Hee Lee

PROGRAM IN ENVIRONMENTAL MATERIALS SCIENCE

GRADUATE SCHOOL

SEOUL NATIONAL UNIVERSITY

FEBRUARY, 2013

A DISSERTATION FOR THE DEGREE OF DOCTOR OF PHILOSOPHY

**Synthesis and Characterization of Polyester Resin  
and Properties of Polyester Coatings for Multi-coated  
Automotive Pre-coated Metal System**

다층 도장을 위한 폴리에스터 도료 및 다층 도장된 자동차용  
선도장 강판의 성형성과 물성에 미치는 영향 연구

**Advisor : Hyun-Joong Kim**

**by Yong-Hee Lee**

PROGRAM IN ENVIRONMENTAL MATERIALS SCIENCE

GRADUATE SCHOOL

SEOUL NATIONAL UNIVERSITY

FEBRUARY, 2013

SEOUL NATIONAL UNIVERSITY  
GRADUATE SCHOOL  
PROGRAM IN ENVIRONMENTAL MATERIALS SCIENCE

WE HEREBY RECOMMEND THE THESIS BY  
Yong-Hee Lee

ENTITLED

Synthesis and Characterization of Polyester Resin and Properties of  
Polyester Coatings for Multi-coated Automotive Pre-coated Metal System

BE ACCEPTED IN FULFILLMENT OF THE REQUIREMENTS  
FOR THE DEGREE OF DOCTOR OF PHILOSOPHY

December, 2012

COMMITTEE ON FINAL EXAMINATION

Chairman Jyongsik Jang  
Prof. Jyongsik Jang

Co-Chairman Hyun Joong Kim  
Prof. Hyun-Joong Kim

Member Hee chon Choi  
Ph.D Hee-Chon Choi

Member Young-Wook Chang  
Prof. Young-Wook Jang

Member Youngchul Kim  
Ph.D Young-Chul Kim

## **Abstract**

# **Synthesis and Characterization of Polyester Resin and Properties of Polyester Coatings for Multi-coated Automotive Pre-coated Metal system**

Yong-Hee Lee

Program in Environmental Materials Science

Graduate School

Seoul National University

The automotive industry is faced with environmental regulations. These regulations require to reduce organic solvents, wastes of industrial products, and to recycle end-of-life vehicles. Therefore, overcoming environmental regulations are important issues in the automotive industry, which have been tried new coating process such as wet-on-wet coating and continuous roll coating.

Pre-coated metal system (PCM) is manufactured in a sheet or coil coating line and assembled in factories for household, electric appliances, building materials and others. In this system, a wet coating process can be abbreviated by a roll coating application, so the problem of solvent evaporation can be eliminated. PCM offers other advantages such as productivity improvement and energy saving. Based on these

reasons, the automotive pre-coated metal system (automotive PCM) has been investigated to remove the wet coating process. Multi-coated layers in automotive PCM should have high flexibility and formability to overcome the harsh conditions which are the cutting, pressing, and stamping processes. Polyester can be controlled physical properties and curing conditions with various curing agents such as melamine formaldehyde (MF) resin and blocked isocyanate pre-polymer.

Flexible polyester resins were synthesized using polycarbonate diol which has long alkyl chain to extend the polymer chains of the resins. The characteristics, viscoelastic behavior and flexibility of the resins were measured by dynamic mechanical analysis (DMA) and tensile test. Flexible polyester coatings were coated on the cold roll steel sheets to verify formability using a deep drawing test, and to determine corrosion resistance. Results showed that storage modulus decreased, and the glass transition temperature shifted to a lower temperature with increasing contents of polycarbonate diol. So, polycarbonate diol provides lower stiffness and higher softness to the polyester coatings. Values of tensile strength and strain exerted on the coatings in the cylindrical deep drawing, were calculated 5.1 MPa and 23.4 % for 90 s, respectively. From those tests, the polyester/melamine coatings of CPC-2 which had 2 mol of polycarbonate diol had good formability and anti-corrosion property. So, it would be an appropriate coatings as a primer for pre-coated metal system.

Nanoclay (organic modified montmorillonite, OMMT) can contribute barrier property and anti-corrosion property. PE/OMMT nanocomposites were synthesized by the in-situ polymerization with

high speed homogenizer process at the various contents of organoclay, which can be dispersed into the polyester matrix. The dispersion of organoclay was examined by small angle X-ray scattering (SAXS) and transmission electron microscopy (TEM). The absence of reflection pattern of OMMT by SAXS and TEM study revealed that exfoliated clay layers are well dispersed into the polymer chain. Mechanical property of PE/OMMT nanocomposites coatings improved the tensile strength and formability at the deep drawing test. The viscoelastic behavior of PE/OMMT nanocomposites coatings were observed by dynamic mechanical analysis (DMA). When the content of organoclay was increased, the stiffness of the PE/OMMT nanocomposites coatings increased considerably and  $T_g$  of each cured coatings shifted to a lower temperature. Anti-corrosion property was examined by the salt spray test. CNC-3 had little rust after 600 h, implying that nano-sized layered silicate of OMMT effectively increases the length of the diffusion pathways water molecules. And nano-sized layered silicate of organoclay may decrease the permeability and can make higher corrosion resistance. From those results, CNC-3 which had 3 wt % of organoclay had good formability in the deep drawing and also had good anti-corrosion property. So, CNC-3 would be an appropriate coatings as a primer for automotive pre-coated metal system.

Cyclic structure contained polyester resins were synthesized, using 1,4-cyclohexanedicarboxylic acid (1,4-CHDA). These resins were formulated to make polyester/melamine heat-cured coatings to control formability, and to have good stone-chip resistance. The characteristics, viscoelastic behavior and flexibility of the resins were measured by

DMA and tensile test. Stone-chip resistance was measured by the chipping resistance test at -20 °C. Cyclic structure contained polyester coatings were coated on the cold roll steel sheets to verify formability, using a cylindrical deep drawing test. Results showed that storage modulus decreased, and glass transition temperatures shifted to lower temperatures with increasing contents of 1,4-CHDA. So, 1,4-CHDA provides lower stiffness and higher softness to the polyester coatings. To have good formability, the tensile strength value of the polyester coatings should be larger than 5.1 MPa, to overcome stresses during the deep drawing test, while the strain value should exceed 23.4 % for 90 s, by the creep test. The cyclic structure of 1,4-CHDA has better elasticity than that of aromatic structure. BCHDA-20 which had 20 mol of 1,4-CHDA had good formability in the deep drawing testing, and also had good results in the chipping resistance test. So, it would be appropriate coatings as a basecoat for automotive pre-coated metals.

Silicone-modified polyester resins were synthesized for cleanable characteristics with silicone intermediate, which has a long chain for extending the polymer chains of the resins. These resins were formulated to make polyester/melamine heat-cured coatings to control the formability. The characteristics, viscoelastic behavior and flexibility of the resins were measured by DMA and tensile test. The contact angle measurement can be determined by the water repellence of the coating surface, which is a standard method to evaluate cleanable characteristics. The surface free energy was calculated by the contact angle measurement, and the surface analysis of each cured coatings was evaluated using an XPS. Silicone-modified polyester coatings were

coated on the cold roll steel sheets to verify their formability, using a deep drawing test. Results showed that the storage modulus decreased, and the glass transition temperature shifted to a lower temperature with increasing contents of silicone intermediate. So, silicone intermediate provides lower stiffness and higher softness to the polyester coatings. To have good formability, the tensile strength of polyester coatings should be larger than 5.1 MPa to overcome stresses during the deep drawing test, while the strain should exceed 23.4 % for 90 s. CSiPE-3 and CSiPE-5 offered good formability, and had 5.1 MPa of stress by tensile strength, and over 30 % of strain by the creep test. So, it implied that silicone intermediate can give a low surface energy and peel strength to polyester coatings. From those tests, the polyester/melamine coatings of CSiPE-5 which had 0.5 mol of silicone intermediate had good formability and low peel strength, which are semi-removable characteristics. So, it could be an appropriate coatings as a topcoat for automotive pre-coated metals.

**Keywords** : Automotive, Polyester, Pre-coated metal (PCM), Formability, Deep drawing, Polycarbonate diol, Nanoclay, Nanocomposites, Cyclic structure, Silicone intermediate

***Student Number : 2008-30330.***

# Contents

<b>Chapter 1. Introduction</b> .....	<b>1</b>
<b>1. Backgrounds</b> .....	<b>2</b>
1.1. Pre-coated metal system (PCM) .....	4
1.2. Automotive pre-coated metal system (PCM) .....	7
1.3. Primer of Automotive PCM .....	10
1.4. Basecoat of Automotive PCM .....	11
1.5. Topcoat/clearcoat of Automotive PCM .....	13
1.6. Polyester resin .....	15
<b>2. Objectives</b> .....	<b>17</b>
2.1. Formability of flexible polyester coatings with polycarbonate diol for automotive pre-coated metals ....	17
2.2. Synthesis of polyester-nanocomposites and characterization of polyester-nanocomposites coatings for automotive pre-coated metals .....	18
2.3. Synthesis and chracterization of cyclic structure contained polyester resin as a basecoat for automotive pre-coated metals .....	19
2.4. Synthesis and chracterization of silicone-modified polyester resin as a topcoat for automotive pre-coated metals .....	20
<b>3. Literature review</b> .....	<b>22</b>
3.1. Flexible chain effects .....	22

3.2. Barrier effects .....	23
3.3. Cyclic structure effects .....	24
3.4. Silicone-contained polymer .....	26
3.5. Formability .....	27

**Chapter 2. Formability of Flexible Polyester Coating  
with Polycarbonate diol for Automotive Pre-coated  
Metals ..... 29**

<b>1. Introduction .....</b>	<b>30</b>
<b>2. Experimental .....</b>	<b>32</b>
2.1. Materials .....	32
2.2. Synthesis of flexible polyester with polycarbonate diol	32
2.3. Preparation of flexible polyester coatings .....	36
2.4. Characterization .....	38
2.4.1. Fourier transform infrared spectroscopy ( <i>FT-IR</i> ) .....	38
2.4.2. Gel permeation chromatography ( <i>GPC</i> ) .....	38
2.4.3. Dynamic mechanical analysis ( <i>DMA</i> ) .....	38
2.4.4. Creep compliance properties .....	39
2.4.5. Tensile properties .....	39
2.4.6. Deep drawing .....	40
2.4.7. Electrochemical Impedance Spectroscopy ( <i>EIS</i> ) .....	41
2.4.8. Salt spray test .....	42

2.4.9. Video image enhanced evaluation of weathering ( <i>VIEEW</i> ) .....	42
<b>3. Results and Discusion .....</b>	<b>47</b>
3.1. Chracterization of flexible polyester resin .....	47
3.2. Viscoelastic behavior .....	50
3.3. Creep behavior .....	52
3.4. Flexibility .....	54
3.5. Formability .....	56
3.6. Water uptake .....	61
3.7. Anti-corrosion property .....	63
<b>4. Conclusions .....</b>	<b>67</b>

## **Chapter 3. Synthesis of Polyester-nanocomposites and Characterization of Polyester-nanocomposites Coatings for Automotive Pre-coated Metals ..... 69**

<b>1. Introduction .....</b>	<b>70</b>
<b>2. Experimental .....</b>	<b>72</b>
2.1. Materials .....	72
2.2. Synthesis of PE/OMMT nanocomposites .....	72
2.3. Preparation of PE/OMMT nanocomposites coatings ...	76
2.4. Charactrization .....	78
2.4.1. Small angle X-ray scattering ( <i>SAXS</i> ) .....	78
2.4.2. Transmission electron microscope ( <i>TEM</i> ) .....	78
2.4.3. Dynamic mechanical analysis ( <i>DMA</i> ) .....	78

2.4.4. Creep compliance properties .....	79
2.4.5. Tensile properties .....	79
2.4.6. Deep drawing .....	79
2.4.7. Electrochemical Impedance Spectroscopy ( <i>EIS</i> ) .....	80
2.4.8. Salt spray test .....	80
<b>3. Results and Discussion .....</b>	<b>81</b>
3.1. Small angle X-ray scattering of PE/OMMT nanocomposites .....	81
3.2. Transmission electron microscope of PE/OMMT nanocomposites .....	83
3.3. Viscoelastic behavior .....	85
3.4. Creep behavior .....	87
3.5. Flexibility .....	89
3.6. Formability .....	91
3.7. Water uptake .....	95
3.8. Anti-corrosion property .....	97
<b>4. Conclusions .....</b>	<b>100</b>

## **Chapter 4. Synthesis and Characterization of Cyclic Structure Contained Polyester Resin as a Basecoat for Automotive Pre-coated Metals ..... 101**

<b>1. Introduction .....</b>	<b>102</b>
<b>2. Experimental .....</b>	<b>104</b>

2.1. Materials .....	104
2.2. Synthesis of cyclic structure contained polyester resin .....	104
2.3. Preparation of cyclic structure contained polyester coatings .....	108
2.4. Charactrization .....	110
2.4.1. Fourier transform infrared spectroscopy ( <i>FT-IR</i> ) .....	110
2.4.2. Gel permeation chromatography ( <i>GPC</i> ) .....	110
2.4.3. Dynamic mechanical analysis ( <i>DMA</i> ) .....	110
2.4.4. Creep strain properties .....	111
2.4.5. Tensile properties .....	111
2.4.6. Deep drawing .....	111
2.4.7. Chipping resistance test .....	112
2.4.8. Video image enhanced evaluation of weathering ( <i>VIEEW</i> ) .....	112
<b>3. Results and Discusion .....</b>	<b>114</b>
3.1. Chracterization of cyclic structure contained polyester resin .....	114
3.2. Viscoelastic behavior .....	117
3.3. Flexibility .....	119
3.4. Formability .....	121
3.5. Chipping resistance .....	126
<b>4. Conclusions .....</b>	<b>130</b>

**Chapter 5. Synthesis and Characterization of Silicone-modified Polyester Resin as a Topcoat for Automotive Pre-coated Metals ..... 131**

**1. Introduction .....132**

**2. Experimental .....134**

    2.1. Materials ..... 134

    2.2. Synthesis of silicone-modified polyester resin ..... 134

    2.3. Preparation of silicone-modified polyester coatings .. 138

    2.4. Charactrization ..... 140

        2.4.1. Fourier transform infrared spectroscopy (*FT-IR*)  
                ..... 140

        2.4.2. Gel permeation chromatography (*GPC*) ..... 140

        2.4.3. Dynamic mechanical analysis (*DMA*) ..... 140

        2.4.4. Creep strain properties..... 141

        2.4.5. Tensile properties ..... 141

        2.4.6. Deep drawing ..... 141

        2.4.7. Surface free energy ..... 141

        2.4.8. X-ray photoelctron spectroscopy (*XPS*) ..... 143

        2.4.9. Measurements of cleanable characteristics using  
                180° peel test ..... 143

**3. Results and Discusion .....146**

    3.1. Chracterization of silicone-modified polyester resin .. 146

    3.2. Viscoelastic behavior ..... 149

    3.3. Flexibility ..... 151

3.4. Formability .....	153
3.5. Analysis of X-ray photoelectron spectroscopy .....	158
3.6. Surface free energy .....	160
3.7. Cleanable characteristics as a topcoat .....	163
<b>4. Conclusions .....</b>	<b>166</b>
<b>Chapter 6. Concluding Remarks .....</b>	<b>167</b>
<b>References .....</b>	<b>173</b>
<b>초록 .....</b>	<b>180</b>

## List of Tables

<b>Table 1-1.</b> Properties of test compounds .....	25
<b>Table 2-1.</b> Formulations used for synthesis of flexible polyester resin .....	35
<b>Table 2-2.</b> Formulations of flexible polyester coatings .....	37
<b>Table 2-3.</b> Conditions for deep drawing test of PCM .....	46
<b>Table 2-4.</b> Characterization of flexible polyester resin .....	49
<b>Table 2-5.</b> Calculated values from tensile test and creep test of flexible polyester coatings .....	59
<b>Table 3-1.</b> Formulations used for synthesis of PE/OMMT nanocomposites .....	75
<b>Table 3-2.</b> Formulations of PE/OMMT nanocomposites coatings .....	77
<b>Table 3-3.</b> Calculated values from tensile test and creep test of PE/OMMT nanocomposites coatings .....	93
<b>Table 4-1.</b> Formulations used for synthesis of cyclic structure contained polyester resin .....	107
<b>Table 4-2.</b> Formulations of cyclic structure contained polyester resin as a basecoat .....	109
<b>Table 4-3.</b> Chip stone types of chipping resistance test .....	113
<b>Table 4-4.</b> Characterization of cyclic structure contained polyester resin .....	116
<b>Table 4-5.</b> Calculated values from tensile test and creep test of cyclic structure contained polyester coatings .....	125
<b>Table 5-1.</b> Formulations used for synthesis of silicone-modified	

polyester resin .....	136
<b>Table 5-2.</b> Formulations of the silicone-modified polyester resin as a topcoat .....	139
<b>Table 5-3.</b> Characterization of the silicone-modified polyester resin .....	148
<b>Table 5-4.</b> Calculated values from tensile test and creep test of silicone-modified polyester coatings .....	156
<b>Table 5-5.</b> Contact angle and surface free energy of silicone- modified polyester coatings .....	162
<b>Table 5-6.</b> Classification of pressure-sensitive adhesive vs. peel adhesion .....	165

## List of Figures

<b>Figure 1-1.</b> Coating processes in automotive production .....	3
<b>Figure 1-2.</b> Suggested of new processes in automotive industry .....	4
<b>Figure 1-3.</b> Process and products of pre-coated meals .....	5
<b>Figure 1-4.</b> Manufacturing of pre-coated metal sheets using a roll coating process .....	6
<b>Figure 1-5.</b> Technology development of automotive pre-coated metal system .....	8
<b>Figure 1-6.</b> Automotive PCM vs. conventional process in an automotive industry .....	9
<b>Figure 1-7.</b> Corrosion developed of barrier coating using nanoclay after exposing to salt spray for 500 h. (A) 0 wt %, (B) 1 wt %, (C) 3 wt %, (D) 5 wt % .....	11
<b>Figure 1-8.</b> SEM micrograph of typical damage of stone chipping .....	12
<b>Figure 1-9.</b> Types of polymer network structures and their application in automotive coating .....	13
<b>Figure 1-10.</b> Sol-gel process of polysiloxane .....	14
<b>Figure 1-11.</b> Typical raw materials for polyester resin .....	16
<b>Figure 1-12.</b> Chemical structure of polycarbonate diol .....	17
<b>Figure 1-13.</b> Structure of montmorillonite .....	19
<b>Figure 2-1.</b> Procedure of a deep drawing .....	44
<b>Figure 2-2.</b> Schematic diagram of specimens in a cylindrical drawing test .....	45

<b>Figure 2-3.</b> IR spectra of flexible polyester resin with polycarbonate diol (1240, 1760 $\text{cm}^{-1}$ : carbonate group) ..	48
<b>Figure 2-4.</b> Viscoelastic properties of flexible polyester coatings (a) storage modulus and (b) $\tan \delta$ .....	51
<b>Figure 2-5.</b> Creep compliance of flexible polyester coatings .....	53
<b>Figure 2-6.</b> Stress-strain curve of flexible polyester coatings .....	55
<b>Figure 2-7.</b> Formability of flexible polyester coatings on the cold roll steel sheet .....	58
<b>Figure 2-8.</b> Strain of flexible polyester coatings by the creep test .....	60
<b>Figure 2-9.</b> Water uptake (vol %) of electro coatings and flexible polyester coatings by the capacitance method under the immersion .....	62
<b>Figure 2-10.</b> Corrosion resistance of electro coatings and flexible polyester coatings by salt spray test for 500 h .....	64
<b>Figure 2-11.</b> VIEEW images of electro coatings and flexible polyester coatings after salt spray test .....	65
<b>Figure 3-1.</b> SAXS patterns of organoclay powder and PE/OMMT nanocomposites .....	82
<b>Figure 3-2.</b> TEM images of PE/OMMT nanocomposites coatings with organoclay (a) 1 wt % and (b) 3 wt % .....	84
<b>Figure 3-3.</b> Viscoelastic properties of PE/OMMT nanocomposites coatings (a) storage modulus and (b) $\tan \delta$ .....	86
<b>Figure 3-4.</b> Creep compliance of PE/OMMT nanocomposites coatings .....	88

<b>Figure 3-5.</b> Stress-strain curve of PE/OMMT nanocomposites coatings .....	90
<b>Figure 3-6.</b> Formability of PE/OMMT nanocomposites coating on the cold roll steel sheet .....	92
<b>Figure 3-7.</b> Strain of PE/OMMT nanocomposites coating by the creep test .....	94
<b>Figure 3-8.</b> Water uptake (vol %) of PE/OMMT nanocomposites coatings by the capacitance method under immersion .....	96
<b>Figure 3-9.</b> Corrosion resistance of PE/OMMT nanocomposites coatings by salt spray test for 600 h (a) CNC-0 and (b) CNC-3.....	98
<b>Figure 4-1.</b> IR spectra of cyclic structure contained polyester resin with 1,4-cyclohexanedicarboxylic acid (aromatic ring : 728, 1286 $\text{cm}^{-1}$ , cyclic ring : 1036, 1138 $\text{cm}^{-1}$ ) .....	115
<b>Figure 4-2.</b> Viscoelastic properties of cyclic structure contained polyester coatings (a) storage modulus and (b) $\tan \delta$ ...	118
<b>Figure 4-3.</b> Stress-strain curve of cyclic structure contained polyester coatings .....	120
<b>Figure 4-4.</b> Formability of cyclic structure contained polyester coatings on the cold roll steel sheet .....	123
<b>Figure 4-5.</b> Strain of cyclic structure contained polyester coatings by the creep test .....	124
<b>Figure 4-6.</b> Chipping resistance of cyclic structure contained polyester coatings on the cold roll steel	

(before test : -20°C x 3 h).....	128
<b>Figure 4-7.</b> Calculated removed area of cyclic structure contained polyester coatings by the VIEEW .....	129
<b>Figure 5-1.</b> Measurement of cleanable characteristics using 180° peel test .....	145
<b>Figure 5-2.</b> IR spectra of silicone-modified polyester resin (Si-O-Si : 800 cm <sup>-1</sup> , Si-O : 1083 cm <sup>-1</sup> ) .....	147
<b>Figure 5-3.</b> Viscoelastic properties of silicone-modified polyester coatings (a) storage modulus and (b) tan δ .....	150
<b>Figure 5-4.</b> Stress-strain curve of silicone-modified polyester coatings .....	152
<b>Figure 5-5.</b> Formability of silicone-modified polyester coatings on the cold roll steel sheet .....	155
<b>Figure 5-6.</b> Strain of silicone-modified polyester coatings by the creep test .....	157
<b>Figure 5-7.</b> XPS curves of silicone-modified polyester coatings .....	159
<b>Figure 5-8.</b> Surface free energy and contact angle of silicone- modified polyester coatings .....	161
<b>Figure 5-9.</b> Peel strength of silicone-modified polyester coatings .....	164

## List of Schemes

<b>Scheme 2-1.</b> Synthesis scheme of flexible polyester resin with polycarbonate diol .....	34
<b>Scheme 3-1.</b> Synthesis scheme of PE/OMMT nanocomposites .....	74
<b>Scheme 4-1.</b> Synthesis scheme of cyclic structure contained polyester resin with 1,4-cyclohexanedicarboxylic acid ..	106
<b>Scheme 5-1.</b> Synthesis scheme of silicone-modified polyester resin .....	135

# **Chapter 1**

## **Introduction**

## 1. Backgrounds

In the automotive industry, amount of waste water and solvent, derived from wet coating process are restricted by environmental regulations. The wet coating process consists of a pre-treatment, a dip coating and a spray coating for an electrocoating, a primer, a basecoat, and a clearcoat. These process discharges mixture of water and organic/inorganic materials, hence the needs for purification of waste water and solvent capturing. Many increasingly stringent environmental legislations such as the European Unions' Directive 2000/53/EG, the 'Registration, Evaluation, Authorization and Restriction of Chemicals' (REACH) and the Biocidal Products Directive 98/8/EC have been made around the world (Streitberger and Dossel, 2008).

These legislations also affect manufacturing sectors that employ coating process. Pre-painted or coil-coated metals (PCM) provide an opportunity to eliminate coating processes. The PCMs are manufactured to be subsequently processed and assembled in factories based on the principle "finish first-fabricate later". PCMs also offer many other advantages such as increased productivity, effective use of space in the factories, and reduced VOCs (Streitberger and Dossel, 2008). These PCMs are pre-manufactured in a continuous process-coils of flat steel sheets are decoiled, cleaned, pre-treated, coated and re-coiled ([www.eccacoil.com](http://www.eccacoil.com), 2006).

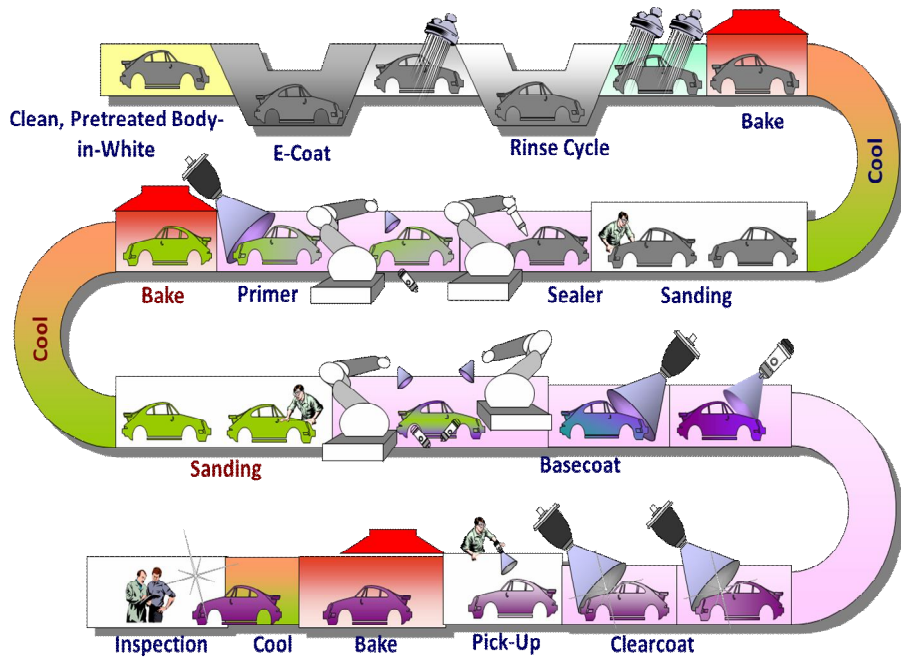


Figure 1-1. Coating processes in automotive production (Streitberger, 2008).

In a consolidated process, the operation is concluded in a shorter process times, the primer application is dispensed with, and coats are applied wet-on-wet, without lengthy drying. The pre-primed process in the consolidated systems, is an environmentally friendly process because replaces wet coating processes such as pre-treatment and electrocoating which are usually performed to attain anti-corrosion and good interfacial adhesion between coating layers (Jandel and Meuthen, 2005).

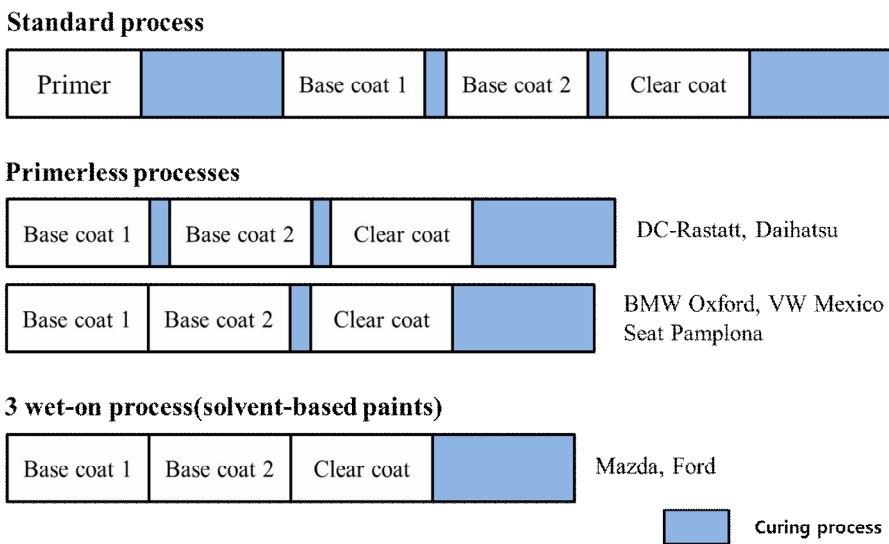


Figure 1-2. Suggested of new processes in automotive industry (Jandel, 2005).

### 1.1. Pre-coated metal system (PCM)

Pre-painted or coil-coated metals (PCM) produced in sheet or coil coating process are been applied in many fields such as building

materials and home appliances. In many cases, the coils are cut, formed, and fabricated before they are coated, as in production of automobiles. In other cases, metal coils coated in advance and later fabricate the final product from the pre-coated metal system.

In the pre-coated metal sheets using roll coating process, the exhaust air from the hoods over the coaters, and particularly from the oven, contains solvents and volatile organic compounds (VOCs). The exhausted streams are used to burn the gas to heat the ovens or are fed through an oxidizer. In this way, part of the residual heat from the oven exhaust is recycled and the solvents and volatile organic compounds are burned. Burning the solvent essentially eliminates VOCs emissions, and the energy cost to heat up the oven can be reduced.

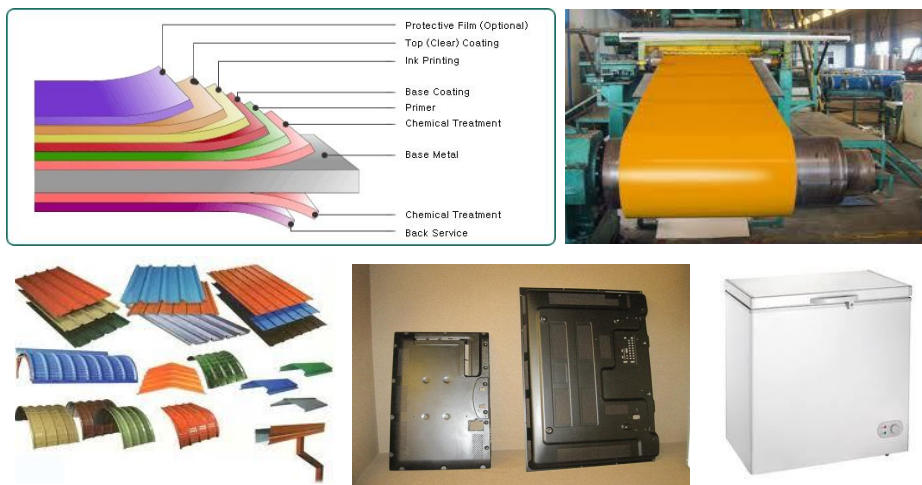


Figure 1-3. Process and products of pre-coated metals ([www.gobizkorea.com](http://www.gobizkorea.com))

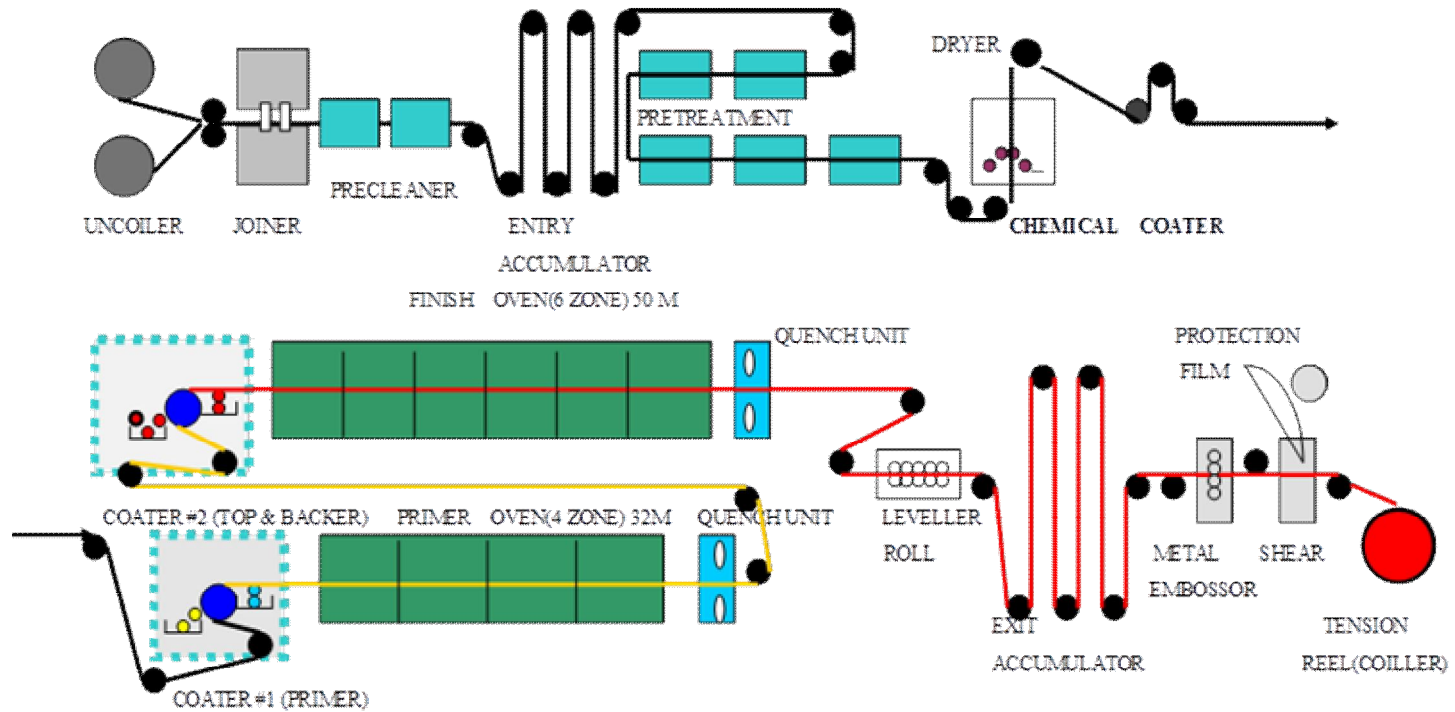


Figure 1-4. Manufacturing of pre-coated metal sheets using a roll coating application (Goldschmidt *et al.*, 2007).

## **1.2. Automotive pre-coated metal system (PCM)**

Automotive industries have tried many attempts to reduce VOCs or pollutions such as waste water and oils. Pre-primed system also has been investigated to overcome environmental regulation unifying both pre-treatment and primer process.

An automotive pre-coated metal system has been investigated to remove the wet coating process, such as pre-treatment, dip coating and spray coating. In this system, all coating layers must have high flexibility and formability to overcome the harsh conditions due to the cutting, press and stamping process. As automotive PCMs are formed after coating, formability is one of the most important performances (Stroiszniigg *et al.*, 2009; Husbands *et al.*, 1987; Yin *et al.*, 1998).

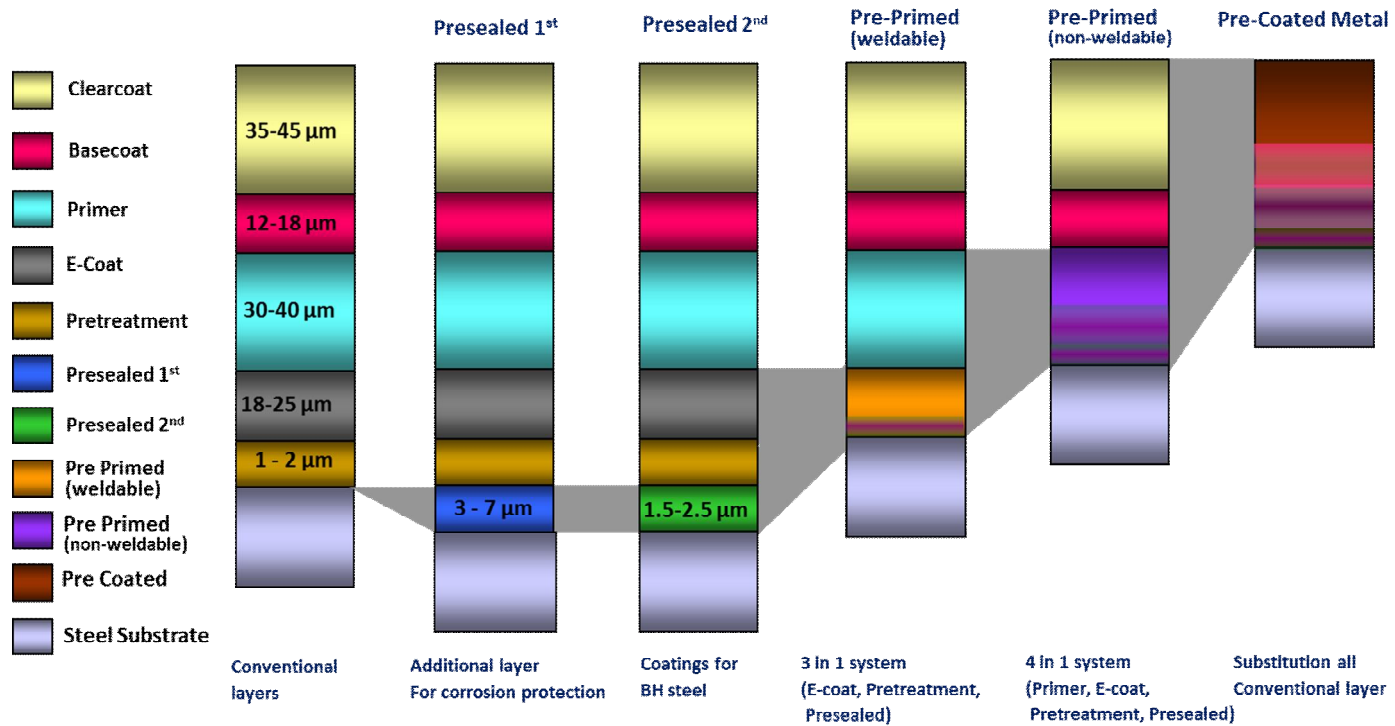


Figure 1-5. Technology development of automotive pre-coated metal system (Moon et al., 2012).

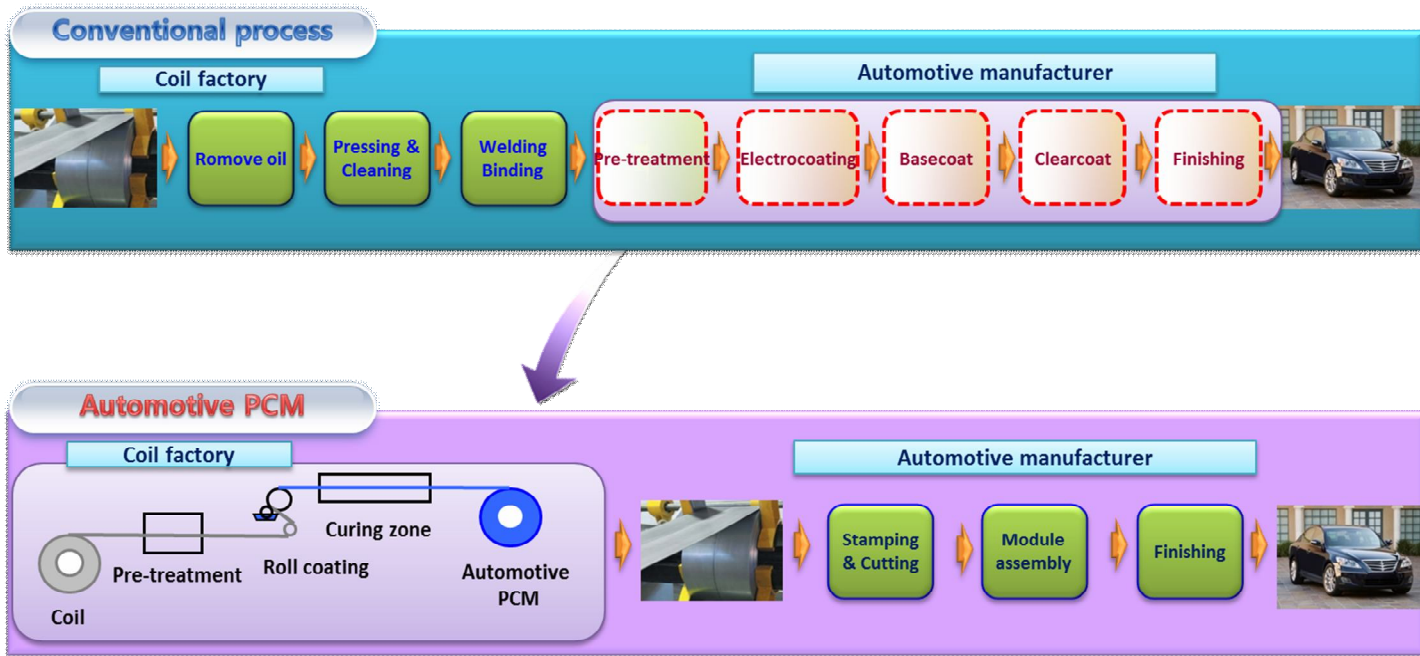


Figure 1-6. Automotive PCM vs. conventional process in an automotive industry (Moon *et al.*, 2012)

### 1.3. Primer of Automotive PCM

Primer of automotive coatings is specially designed to fulfill the demanding requirements such anti-corrosion, durability and adhesion to metal. The most important performance is an anti-corrosion. The prevention of corrosion can be provided by three different mechanisms as follows (Wicks *et al.*, 2007).

- (a) Electrochemical inhibitors
- (b) Sacrificial coatings
- (c) Barrier coatings

Inhibitive pigments like chromates used in the first generation of passivate the metal surface by generating an oxide film. But chromates are toxic materials and it can not used any more. Sacrificial coatings such as zinc or zinc-rich primers uses a less passive anode and render steel in a continuous cathodic and prevent steel.

Barrier coatings are blocking the permeability of corrosion factors such as  $H_2O$ ,  $O_2$  and  $H^+$  into coating interface. Corrosion factors can lead to blistering on the surface, reduce stability of the adhesion bond, increase the speed of catodic reaction and degradation of coatings (Bagherzadeh and Mahdavi, 2007).

Anti-corrosion property is an essential part of coating damages from environmental cause, and is one of the major concern and warranty problem in the automotive industry. Recently many efforts have been tried to improve anti-corrosion properties of automotive PCM of primer such as: modifying epoxy coating using silane-coupling agents, using

epoxy-siloxane hybrid binder, nanocomposite using nanoclay.

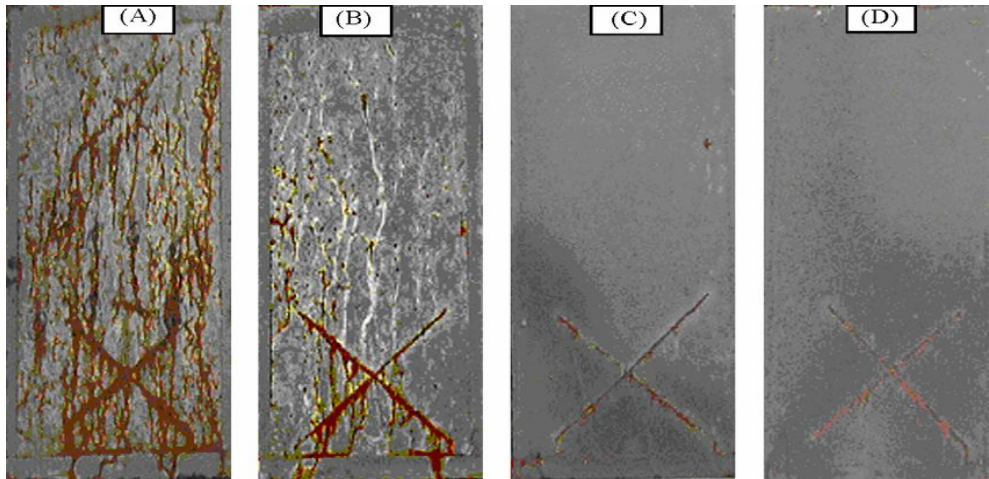


Figure 1-7. Corrosion developed of barrier coating using nanoclay after exposing to salt spray for 500 h. (A) 0 wt %, (B) 1 wt %, (C) 3 wt %, (D) 5 wt % (Bagherzadeh and Mahdavi, 2007).

#### 1.4. Basecoat of Automotive PCM

Basecoat of automotive coatings is specially designed to fulfill the demanding requirements such chipping resistance, color maintaining and adhesion between primer and clearcoat. The most important performance is a chipping resistance and it can be improved by two different ways as follows (Wicks *et al.*, 2007).

- (a) Improve intercoat adhesion to the primer
- (b) Improve energy absorption in the coating

To improve the energy absorption, polymer structure and the cross-linking density are the major factors. Polyester and polyurethanes are the favorites of the polymers and rubber domains can be incorporated to reach of energy absorption.

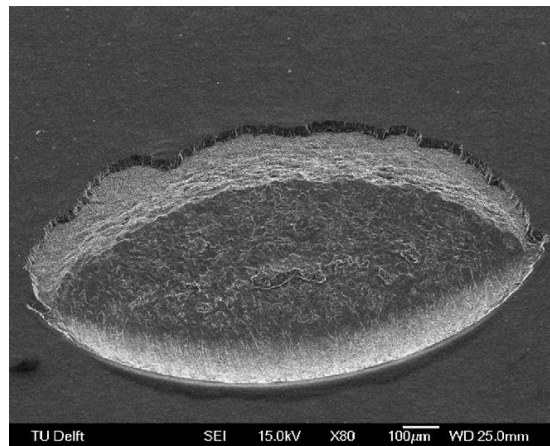


Figure 1-8. SEM micrograph of typical damage of stone chipping (Lonyuk and Bosma, 2008).

Chipping resistance is related to cross-linking density and elasticity of the polymer network as shown in Figure 1-9. Type A represents a highly etch resistant coating having a poor scratch resistance because of low cross-link density. Type B represents a highly flexible coating, as used for plastic coatings, having improved scratch resistance. Type C represents a glasslike inorganic network, which has good scratch resistance, but is too brittle to be used on automobiles. Type D represents a new type of scratch resistant coating.

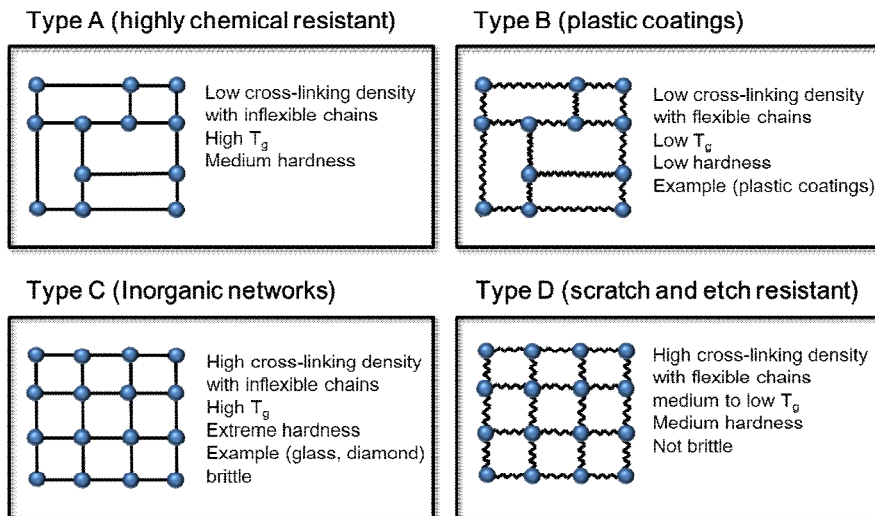


Figure 1-9. Types of polymer network structures and their application in automotive coating (Streitberger and Dossel, 2008).

### 1.5. Topcoat/clearcoat of Automotive PCM

Automotive coatings are specially designed to fulfill the demanding requirements such high gloss and good appearance. The most important performances are weathering resistance, scratch resistance and environmental etch resistance.

The most important performance is weathering resistance and it can be improved by three different ways as follows (Wicks, 2007).

- (a) Higher cross-link density
- (b) Lower water permeability
- (c) Using HALS

Weathering resistance can be improved using organic-inorganic hybrid resin with silicone. Interest in developing organic-inorganic hybrid coatings has been increased because of the unique properties from combining inorganic and organic components into a single coating system. One approach is a sol-gel process involving the hydrolysis and condensation reaction of metal alkoxides (Frings and Meinema, 1998) Sol-gel process provides an easy, cost-effective and efficient way to incorporate inorganic components into an organic binder. The other approach is using nanoparticles which can be dispersed in an organic binder (Zhou and Wu, 1998). The incorporation of inorganic nanofillers in organic coating is often reported. Organic-inorganic hybrid materials exhibit improved properties such as toughness, impact strength, tensile strength and thermal stability (Chattopadhyay and Webster, 2009).

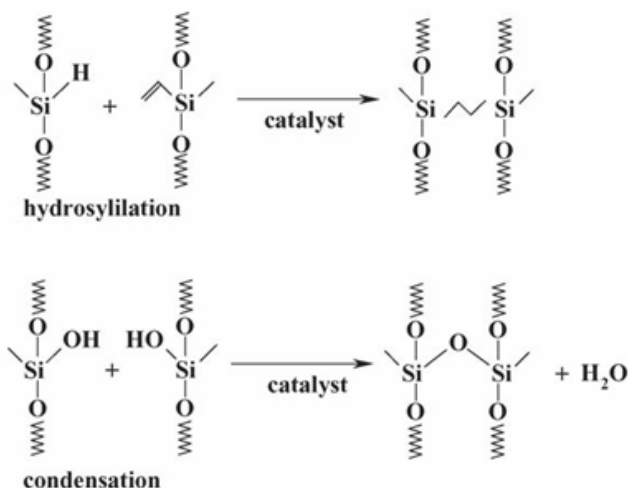
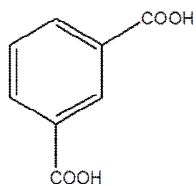


Figure 1-10. Sol-gel process of polysiloxane (Zielecka and Bujnowaska, 2006).

## 1.6. Polyester resin

Polyesters are polymers containing the recurring ester unit. Polyesters are formed by a condensation reaction between carboxyl and hydroxyl containing compounds. The esterification reaction is an equilibrium reaction, the polybasic alcohols is usually added to excess, resulting in a detectable proportion of this excess component remaining in the end product. In addition, polyesters can be controlled physical properties and curing condition using various curing systems such as melamine formaldehyde (MF) and blocked isocyanate. Most hydroxy-terminated polyesters have been made by co-esterifying four types of monomers: two polyols (a diol and a triol) and two diacids (an aliphatic dibasic acid or anhydride and an aromatic dicarboxylic acid). The ratio of moles of dibasic acid to polyol must be less than 1 to give hydroxyl-terminated polyester and to avoid gelation during the synthesis.

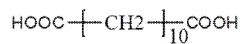
Polyesters have been used many fields such as automotive, general metal finishing, architectural and can coating. Because polyester give coatings with better adhesion to metal substrate and better impact resistance than thermosetting acrylics (Percec, 1991).



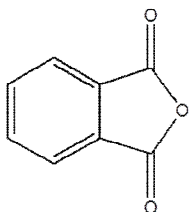
Isophthalic acid



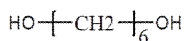
Terephthalic acid



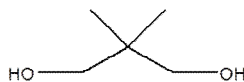
Dodecadicarboxylic acid



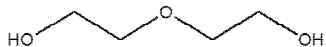
Phthalic anhydride



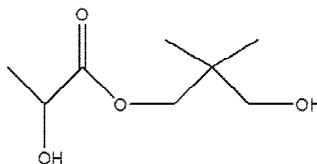
1,6-Hexandiol



Neopentylglycol



Diethylene glycol



Hydroxy pivalinic acid neopentylglycol ester

Figure 1-11. Typical raw materials for polyester resin (Streitberger and Dossel, 2008).

## 2. Objectives

### 2.1. Formability of flexible polyester coatings with polycarbonate diol for automotive pre-coated metals

Polycarbonate diol is an esterification product, formed by a reaction of carbonic acid with polyols. The aliphatic polycarbonates are employed as the main segment in superior polyurethane coatings due to the physical properties such as low viscosity, good toughness, weather stability and excellent hydrolysis resistance (Westhuse, 2007). Owing to the hydroxyl group, polycarbonate diol can be used as an alcohol during the synthesis of polyester resin. In particular, polycarbonate diol consists of a long alkyl chain which is contained many flexible rod-like group such as  $-\text{CH}_2$ . An aliphatic C-C bond is most flexible than an aromatic C-C, C-O and C-N bond because of low rotation barrier energy (Percec and Zuber, 1991). In addition, polycarbonate has a low glass transition temperature and a low Young's modulus, supporting flexibility and formability of the polyester coatings (Hou *et al.*, 2009).

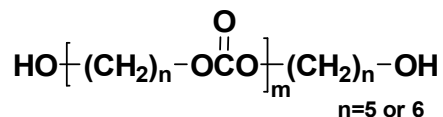


Figure 1-12. Chemical structure of polycarbonate diol .

The polyester resin was designed to control the flexibility for an automotive pre-coated metal system using polycarbonate diol. The

viscoelastic behavior and flexibility were measured to determine the flexible segment effect of polycarbonate diol for an automotive pre-coated metal system.

## **2.2. Synthesis of polyester-nanocomposites and characterization of polyester-nanocomposites coatings for automotive pre-coated metals**

Nanoclay are layered silicates such as smectite, montmorillonite and saponite are the effective and reinforcing agents in making polymer clay composites. Pristine-layered silicates, which contain layered  $\text{Na}^+$  or  $\text{K}^+$  ions, are only miscible with hydrophilic polymers. Through ion-exchange reactions with cationic surfactants layered silicates render miscible with other polymers. Cations reduce the surface energy of the organic host and improve wetting characteristics of polymer, resulting in a larger interlayer spacing.

Several types of morphologies may occur when the polymer is mixed with layered silicates (Zhang *et al.*, 2004)

- (a) conventional composites
- (b) intercalated nanocomposites
- (c) exfoliated nanocomposites

Their differences can be related to the polymer permeation between clay layers and dispersion uniformity of silicate sheets in polymer matrix. The high aspect ratio of silicate layers plays an important role in production of anti-corrosive coating systems. Polyester resin will be

synthesized with nanoclay to control the permeability of corrosion factors such as H<sub>2</sub>O and O<sub>2</sub>. Nanoclay can be well dispersed in the polymer network and it has high aspect ratio which can make long pathway. The high aspect ratio can reduce permeability of corrosion factors.

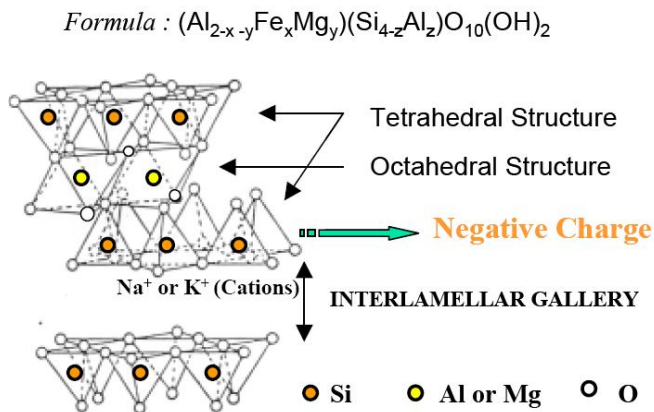


Figure 1-13. Structure of montmorillonite (Zhang *et al.*, 2004).

### 2.3. Synthesis and characterization of cyclic structure contained polyester resin as a basecoat for automotive pre-coated metals

Polyester resins were synthesized with polycarbonate diol to control the flexibility for an automotive PCM. The resins were designed to demonstrate the flexible chain effect, using polycarbonate diol. Cyclic structure contained polyester resin system had been investigated to improve the chipping resistance and impact resistance for an automotive PCM. Those resins were designed to increase the stiffness of coatings using 1,4-cyclohexanedicarboxylic acid. Cyclohexane is a

stiff molecule of chair form consisting of C-C single bonds which has maximum rotational barrier at  $\pm 60^\circ$ . For the reason, cycloheptane and cyclooctane are soft molecules in comparison with cyclohexane (Toshiyuki *et al.*, 1994; Hata *et al.*, 1998).

The cyclic structure contained polyester resins were synthesized with different contents of 1,4-cyclohexanedicarboxylic acid. The viscoelastic behavior, flexibility, formability and chipping resistance were measured to determine the effect of a cyclic structure for an automotive PCM as a basecoat.

#### **2.4. Synthesis and characterization of silicone-modified polyester resin as a topcoat for automotive pre-coated metals**

Topcoat should have good gloss, hardness and good chemical resistance. Silicone-modified polyester resins will be designed higher cross-linking density using TMP and cyclo-structured alcohols to control the elasticity for an automotive PCM. Silicone intermediate has good chemical resistance and gloss retention. And it has higher molecular weight than other materials and gives the flexibility to the polymer network.

Silicone-modified polyester resin will be designed to have the flexible chain effect using silicone intermediate. Those resins will be controlled to increase anti-weathering property and low surface free energy with different content of silicone intermediate.

The curing and viscoelastic behavior will be measured by dynamic mechanical analysis. Flexibility and formability will be tested to

determine the flexible segment effect of silicone intermediate and scratch resistance will be measured to determine optimum content for a pre-coated metal system. Surface morphology will be measured by X-ray photoelectron spectroscopy (XPS) and surface tension will be measured by peel test.

### 3. Literature review

#### 3.1. Flexible chain effects

Percec and Zuber *et al.* (1991) suggested a classification in rigid rod-like groups (the rod-like shape of the molecule is rigid although there is free rotation about some of its C-C bonds), semi-rigid or semi-flexible rod-like groups (conformationally flexible but of medium rotational energy barrier like for example aromatic esters and amides) and flexible rod-like groups.

Yin *et al.* (1998) studied polyimides containing long flexible chains in the backbone to improve the processability of polyimides. They synthesized polyimides based on di(4-aminophenoxy)alkanes. It can be observed that  $T_g$  of a polyimide exhibits a basically linear decrease with the increase of the length of the long flexible chains. The introduction of the long flexible chains increases the flexibility of the polyimide backbone and thus the mobility of the molecular chains.

Moon *et al.* (2012) reported the polyester resin was designed to control the flexibility for an automotive pre-coated metal system using polycarbonate diol. In addition, low viscosity of polycarbonate diol can be expected to apply a high-solid coating system. The curing and viscoelastic behavior, flexibility and scratch resistance were measured to determine the flexible segment effect of polycarbonate diol for an automotive pre-coated metal system. With increasing polycarbonate

diol content, the final frequency and the storage modulus increased and the  $T_g$  of the coatings decreased. This is related to the high mobility of the chain segment in polycarbonate diol.

### **3.2. Barrier effects**

Bagherzadeh *et al.* (2007) studied epoxy-clay nanocomposite with a quaternary ammonium modified montmorillonite clay and anti-corrosion properties of the nanocomposite were investigated using salt spray and electrochemical impedance spectroscopy. It can be observed an improvement in the barrier property and anti-corrosive characteristics by increasing content of a quaternary ammonium modified montmorillonite clay.

Heidaian *et al.* (2010) reported that the synthesis of polyurethane organoclay nanocomposites and PU/OMMT nanocomposite coatings were superior to the neat PU in corrosion protection effects which the improved coating properties such as adhesion and barrier property. The anticorrosive properties of PU/OMMT nanocomposite coatings were characterized by electrochemical impedance spectroscopy and PU/OMMT nanocomposite was observed that the corrosion protection was improved as the clay loading is increased up to 3 wt. %.

Singh-Beemat *et al.* (2012) studied corrosion resistance of epoxy ester coatings with addition of cloisite 15A. The surface contact angle of the coatings decreased with increasing weight percent of clay. The surface

roughness decreased with the addition of clay up to 1 wt % by the measurement of atomic force microscope. The reinforcement of epoxy ester with organoclay resulted in a significant increase in the glass transition temperature. However, there was no significant change in the height of the tangent of the loss angle. Tan delta with variation in the clay concentration indicated that there was no significant change in the damping behavior of the epoxy ester coatings as a result of reinforcement by organoclay.

### 3.3. Cyclic structure effects

Heta and Tsubouchi *et al.* (1998) reported that cyclohexane is a stiff molecule of chair form, and on the other side, cycloheptane and cyclooctane are soft molecules in comparison with cyclohexane, comparing the correlation between  $\mu@20\text{ }^{\circ}\text{C}$  and  $E_{\text{rot}}$  of cyclohexane, cycloheptane and cyclooctane.

Moon *et al.* (2012) reported that the polyester resin was designed to control the elasticity using 1,4-cyclohexanediol. With increasing content of 1,4-cyclohexanediol, the final frequency decreased and the storage modulus and  $T_g$  of the coatings increased. This is related to the high stiffness of the cyclohexane structure of 1,4- cyclohexanediol and scratch resistance has been increased due to the restoring force of the stiff structure of 1,4-cyclohexanediol. Cyclohexane structure is a good factor for improving the scratch resistance and reflow property of the polyester coatings.

Table 1-1. Properties of test compounds (Hata *et al.*, 1998)

Compound	Cyclohexane	Cycloheptane	Cyclooctane
$\mu@20\text{ }^{\circ}\text{C}$	0.0718	0.0244	0.0342
$E_{\text{rot}}$ (kJ/mol)	27.9	11.0	12.2

### 3.4. Silicone contained polymer

Maria *et al.* (2007) studied the properties of silicone-containing polymer matrices as coating materials such as fluoropolymers, polyolefins and acrylic resins. It has showed good correlation of application properties of these coating materials and their surface properties such as high dynamic contact angle, low surface free energy, surface morphology. The surface properties of protective coatings obtained from silicone containing polymer matrices were studied based on wettability, morphology and chemical composition of the surface nanolayer. Morphology, roughness and structural regularity of protective coatings showed the effect of organic component on the surface properties. The application properties of such coatings materials were tested based on anti-soiling tests, water vapor permeability, water absorption and weathering resistance

Murillo *et al.* (2011) reported hyperbranched alkyd–silicone nanoresins (ASiHBRs) with high solid content were synthesized by etherification reaction between a hyperbranched alkyd resin (HABR) and Z-6018 silicone. NMR spectra show the presence of aromatic rings, –Si–O and –C–O; grafting was successful. The molar masses of ASiHBRs determined by GPC are higher than that of HABR. The hydroxyl values decrease with increasing silicone content. Hydrodynamic dimensions, refractive indices, glass transition temperatures, gloss and hardness of ASiHBRs increase with increasing silicone contents.

### 3.5. Formability

Ueda *et al.* (2001) studied the relationship between the forming of PCM and properties of paint films and the following results were obtained. In the drawing mode in which steel sheets are subjected to both tensile and compressive strain, the paint film should have higher elongation and smaller elastic strain energy stored in the paint film during the forming process.

The main defect developed in compressive deformation is the buckling of coating films followed by wrinkle formation, and the development of buckling is dominated by the elastic strain energy stored in the paint film during deformation.

Ueda *et al.* (2002) also studied rheological measurements such as dynamic viscoelasticity, relaxation and creep to determine relationship between formability and properties of polyester/melamine paint for PCMs. Dependence of the formability of PCMs in deep drawing on these viscoelastic properties was considered and the following conclusions were obtained. Drawing of PCM was performed at the temperature below the  $T_g$  of paint films of PCMs, the formability was excellent because the stress developed in the film in such a condition was easily relaxed to small values in a short time by large deformation. The destruction of network structure occurs and then plastic deformation easily develops in the paint film which exhibits good formability in deep drawing. This mechanism was also supported by

the high steady-state compliance and the low creep viscosity of such a paint film.

Moon *et al.* (2002) also studied prediction of formability in deep drawing of automotive PCM, three types of polyester resin with different crosslink density and controlled testing conditions of deep drawing tester, universal testing machine (UTM) and dynamic mechanical analysis (DMA) to find correlation between flexibility and formability.

## **Chapter 2**

### **Formability of Flexible Polyester Coatings with Polycarbonate diol for Automotive Pre-coated Metals**

## 1. Introduction

Many environmental legislations that are increasingly stringent have been made around the world. In the automotive industries, the amount of waste water and solvent, derived from wet coating process are restricted by environmental regulations (Ueda *et al.*, 2001). These legislations also affect other manufacturing sectors that employ coating process. Pre-painted or coil-coated metals (PCM) provide an opportunity to eliminate coating processes. PCM have been used in many applications such as household electric appliances, building materials and others. In this system, wet coating process can be eliminated by using a roll coating process, making it possible to circumvent the problem of air pollution arising from evaporation. In addition, a pre-coated metal system offers other advantages such as improved productivity and energy saving thus the use of PCM has been spreading (Ueda *et al.*, 2002; Moon *et al.*, 2012).

The most important property of PCM is formability. If the film on the coated PCM parts is damaged, the products are rendered useless (Kanda *et al.*, 1998). The characteristic of coated films for good formability is dependent on the maximum strain and tensile strength of PCMs in deep drawing (Jandel *et al.*, 2005). However, the requirement for higher formability of PCM is increasing nowadays. A published study reveals that the formability of a material is correlated to its molecular chain length and crosslink density (Yin *et al.*, 1998). However, using polybasic alcohols such as 1,6-hexanediol and 2-methyl 1,3-propanediol to capitalize the chain length effect did not

effectively improve the formability of the pre-coated metal systems.

In this study, we used polycarbonate diol in the synthesis of polyester resin to control the formability of the resulted resin. Polycarbonate diol is an esterification product from the reaction of carbonic acid with polyols. It consists of a long alkyl chain with contains much flexible rod-like group such as  $-\text{CH}_2$  (Percec *et al.*, 1991). Aliphatic polycarbonates have been employed as the main segment in superior polyurethane coatings. We opted to use polycarbonate diol because it can also function as an alcohol during the synthesis of polyester resin.

Overall, this chapter reports the design of a polyester resin for pre-coated metals using polycarbonate diol in the resin. The elongation, tensile strength and viscoelastic properties of free coated film were measured. The formability of PCMs was evaluated using a cylindrical drawing test. Stress and strain of the coatings were calculated from the deep drawing results. Finally, the relationship between the contents of polycarbonate diol and formability of the polyester coatings was discussed.

## 2. Experimental

### 2.1. Materials

A polycarbonate diol (PCDL,  $M_n = 500$ , Asahi Kasei Chemicals Corp., Japan) was prepared to control the flexibility of the main chain. 1,4-cyclohexanedicarboxylic acid (1,4-CHDA, Tokyo Chemical Industry, Japan), adipic acid (AA, Samchun Pure Chemical, Republic of Korea), and isophthalic acid (IPA, Junsei Chemical Corp., Japan), trimethylol propane(TMP, Tokyo Chemical Industry, Japan), 1,6-hexandiol (1,6-HD, Samchun Pure Chemical, Republic of Korea), 1,4-cyclohexanedimethanol (1,4-CHDM, Tokyo Chemical Industry, Japan), and MPD (2-methyl 1,3-propanediol, Tokyo Chemical Industry, Japan) were used without further purification. Butylstannoic acid (FASCAT 4100, Arkema Inc., USA) was used as a catalyst to catalyze polymerization and prevent a transesterification reaction during the polymerization (Hamada *et al.*, 1997).

Hexamethoxy-methylmelamine (HMMM, Cytec Industries Inc., USA) was used as the curing agent and blocked acid catalyst (NACURE 1953, King Industries, Inc., USA) was used.

### 2.2. Synthesis of flexible polyester with polycarbonate diol

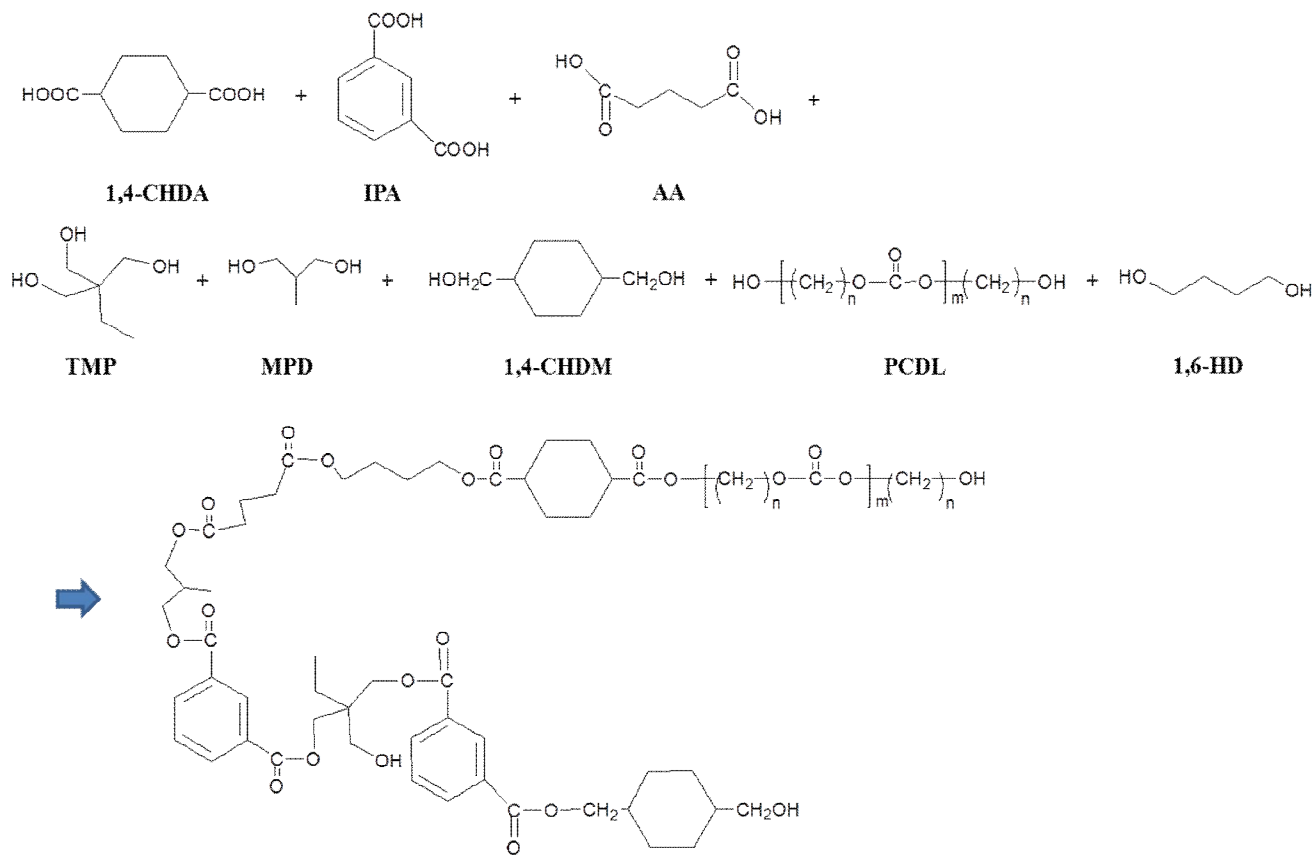
The synthesized scheme of flexible polyester with polycarbonate diol is shown in scheme 2-1 and the formulations are shown in Table 2-1. Polyester was synthesized from polybasic alcohols and polybasic acids with the following procedure which consisted of two synthesis processes. One was the fusion process and the other was the solvent

process. The synthesis took place in a 500 mL round bottom flask equipped with a four-necked flask having a mechanical stirrer, thermometer, condenser and water trap. The condenser and water trap were meant to remove condensed water during the poly-condensation reaction between alcohols and acids.

Isophthalic acid has two carboxyl groups, one of which reacts at around 190 °C and the second one reacts at a temperature above 210 °C. It therefore requires a high reaction temperature. Polycarbonatediol could decompose at around 210 °C. To avoid decomposition of polycarbonate diol, a modified synthesis process was carried out as follows.

Firstly, IPA, TMP, 1,6-HD, 1,4-CHDM, and MPD were charged into a dried reactor and the reaction temperature was set to 150 °C with stirring for 2 h under N<sub>2</sub> purge. Subsequently, the reaction temperature was increased from 150 °C to 210 °C at the rate of 0.5 °C/min. During the fusion process, all raw materials were melted and the condensed water was collected.

After that 1,4-CHDA, AA, and PCDL were charged into the reactor containing melt prepared from the preceding step and the reaction temperature was set to 130 °C with stirring for 2 h under N<sub>2</sub> purge. Subsequently, the reaction temperature was increased from 130 °C to 180 °C at the rate of 0.3 °C/min. The reaction temperature was maintained for several hours to collect condensed water.



Scheme 2-1. Synthesis scheme of flexible polyester resin with polycarbonate diol.

Table 2-1. Formulations used for synthesis of flexible polyester resin.

(unit : mole of monomer)

Contents	PC-0	PC-1	PC-2	PC-3
Polycarbonate diol	0	1	2	3
2-methyl 1,3-propanediol	6	5	4	3
Trimethylol propane	3	3	3	3
1,6-hexanediol	5	5	5	5
1,4- cyclohexanedimethanol	11	11	11	11
1,4-cyclohexanedicarboxylic acid	7	7	7	7
Adipic acid	2	2	2	2
Isophthalic acid	15	15	15	15

The fusion process was then converted into solvent process by adding xylene. The solvent process was carried out to collect condensed water and to make low acid value. The reaction temperature was set to 180 °C. During the solvent process, the acid value was measured by 0.1 N KOH solution. The reaction temperature was maintained for several hours until the acid value was under 3 mg KOH/g resin (Hamada *et al.*, 1997).

### **2.3. Preparation of flexible polyester coatings**

Synthesized flexible polyester resin was mixed with HMMM, additives, and solvents. Four different formulations were prepared as listed Table 2-2.

Free film : The coating formulations were casted on to an aluminum pan and dried to evaporate solvent in the oven at 60 °C for 12 h and then baked at 150 °C (oven temperature) for 1 h. The thickness of the baked films ranged from 150 to 200  $\mu\text{m}$ . The resulted films became the samples for tensile strength and dynamic mechanical analysis

PCM : Cold roll steel sheets (thickness of 0.8 mm) were coated with alkali solution and baked at the 150 °C for 5 min for a pre-treatment. The cured pre-treated films were 5  $\mu\text{m}$  in thickness. The flexible polyester coatings as a primer were coated on the cured pre-treated film and then baked at 180 °C for 20 min. The thickness of those cured film was 15  $\mu\text{m}$ . The total film thickness was 20  $\mu\text{m}$ .

Table 2-2. Formulations of flexible polyester coatings.

(unit : wt %)

Contents	CPC-0	CPC-1	CPC-2	CPC-3
* PC-0	53.4	-		-
* PC-1	-	53.8		-
* PC-2	-	-	54.1	-
* PC-3	-	-		54.3
Aromatic solvent	25.4	25.2	25.1	25.2
TiO <sub>2</sub>	4.0	4.0	4.0	4.0
** MA 100	0.7	0.7	0.7	0.7
Shieldex C303	10.0	10.0	10.0	10.0
HMMM	5.0	4.8	4.6	4.3
Additives	1.0	1.0	1.0	1.0
Nacure	0.5	0.5	0.5	0.5

\* Solid content of polyester resins : 75 %

\*\* Black pigment

## **2.4. Characterization**

### **2.4.1. Fourier transform infrared spectroscopy (*FT-IR*)**

Infrared spectra were obtained using a JASCO FT/IR-6100 (Jasco, Japan) spectrometer which is equipped with a Miracle accessory, and attenuated total reflectance (ATR) setup. The ATR crystal was made of diamond and its refractive index was 2.4 at 8500-2500  $\text{cm}^{-1}$  and 1700-300  $\text{cm}^{-1}$ . The spectra were collected using ATR mode in the wavenumber range of 4000-650  $\text{cm}^{-1}$  and the resolution of the spectra recorded was 4  $\text{cm}^{-1}$ .

### **2.4.2. Gel permeation chromatography (*GPC*)**

The molecular weight and polydispersity of the synthesized elastomeric polyester resins were measured using an YL9100 GPC SYSTEM (Young Lin, Republic of Korea) apparatus consisting of a pump and a RI detector. Tetrahydrofuran (THF) was used as the eluent, and the flow rate was 1 mL/min.

### **2.4.3. Dynamic mechanical analysis (*DMA*)**

The glass transition temperature and viscoelastic properties of the polyester/melamine heat-cured films were analyzed using a dynamic mechanical analysis (Q800, TA Instruments). The crosslink density ( $\nu_c$ ) was derived from a following equation (Hill 1997; Stroisznigg *et al.*, 2009):

$$v_c = \frac{E'_{\min}}{3RT_{E'_{\min}}}$$

where,  $E'_{\min}$  is the minimum storage modulus,  $T_{E'_{\min}}$  is temperature in °K corresponding to the minimum storage modulus in the rubbery plateau region, and R is the gas constant.

Rectangular specimens with 20 mm in length, 6.45 mm in width and 200  $\mu\text{m}$  in thickness were used for the test. The specimens were tested in tension mode at a frequency of 1 Hz and strain of 0.3 % at the temperature levels from -50 °C to 150 °C at a scanning rate of 2 °C/min.

#### **2.4.4. Creep compliance properties**

The creep and creep recovery tests of the free coated films were performed using a dynamic mechanical analysis (Q800, TA Instruments). Rectangular specimens of, 20 mm in length, 6.45 mm in width and 200  $\mu\text{m}$  in thickness were used for the test. The time-dependence of creep compliance of the free coated films were obtained at a stress level of  $5.1 \times 10^6$  Pa. The tests were performed at 25 °C, and with a loading time of 90 s followed by recovery time is 120 s. The 90's of creep time is designed to correspond to the deep drawing testing time.

#### **2.4.5. Tensile properties**

Tensile properties was measured using a Universal Testing Machine (Zwick Corp.) at a crosshead speed of 20 mm/min which is designed to correspond to the deep drawing testing speed at ambient temperature.

The tensile specimens prepared from free coated films were 40 mm in length (span length), 6.45 mm in width and 200  $\mu\text{m}$  in thickness. The tensile strength value was calculated by dividing the maximum load in newtons (N) by the average original cross-sectional areas in the gage length of the specimen in square meters. The percent elongation (strain %) was calculated by dividing the change in gage length by the original specimen gage length, expressed as a percentage (%) (ASTM D638-10).

#### 2.4.6. Deep drawing

A cylindrical deep drawing test was performed to examine formability of the heat-cured coatings as shown Figure 2-1 and 2-2. The shape of PCM before deep drawing was a disk and its diameter was 105 mm. The shape of the punch was circle and its diameter was 40 mm, the shoulder radius of the punch and the corner radius of the punch were 5 mm.

Specific conditions of the deep drawing were listed in Table 2-3. The speed of punch was 20 mm/min and the drawing testing time was 90 s. The blank force was  $4.9 \times 10^4$  N and this test was performed at 25 °C. Value of stress on PCM specimens can be calculated using Eq. (1):

Stress on PCM specimen =

$$\frac{\text{blank force (N)}}{\text{total areas of specimen before drawing test (mm}^2\text{)}} \quad (1)$$

where, blank force is  $4.9 \times 10^4$  N and the total areas of specimen before drawing test is 8,659  $\text{mm}^2$

Also, the value of strain on PCM specimens can be calculated using Eq. (2):

Strain on PCM specimens =

$$\frac{(\text{total areas of specimens after drawing test} - \text{total areas of specimens before drawing test}) (\text{mm}^2)}{\text{total areas of specimens before drawing test} (\text{mm}^2)} \quad (2)$$

where, the total areas of specimen before drawing test is 8,659 mm<sup>2</sup> and total areas of specimen after drawing test is 10,681 mm<sup>2</sup> (see Fig. 2. for schematic diagram of the PCM before and after deep drawing test). From Eq. (1) and Eq. (2), the calculated stress is 5.1 MPa and strain is 23.4 %.

#### 2.4.7. Electrochemical Impedance Spectroscopy testing (EIS)

EIS measurements of each PCM specimens and conventional electro coatings were carried out in the unstirred 3.5 wt % NaCl solution using a frequency range of 10<sup>5</sup> down to 10<sup>-2</sup> Hz using 10 mV amplitude (Solartron SI 1260, UK). The electrical capacitance of the coatings (C) were measured every 2 minutes for 3 h. The water uptake values of samples obtained from Brasher-Kingsbery equation:

$$\text{Water uptake} = \frac{\log ( C_t / C_0 )}{\log 80}$$

where  $C_t$  is the electrical capacitance of the coatings during  $t$  time of immersion and is  $C_0$  the electrical capacitance of the coating before immersion (Bagherzadeh *et al.*, 2007).

#### **2.4.8 Salt spray test**

The anti-corrosion property of polyester coatings on PCM and conventional electro deposition coatings were measured using salt spray test. All specimens were first prepared on the cold roll steel sheets and a cross-scratch line was made on the coating surface with a sharp instrument. The salt spray test condition was according to ASTM B-117 in a 5 wt % NaCl solution at 35 °C. After 500 h, changes of surface morphology, especially around the cross-line on the coating and surface defects were examined via VIEEW<sup>TM</sup> digital image analyzer (VIEEW<sup>TM</sup>, Atlas Electric Devices Co., USA) (Choi *et al.*, 2006; Howard *et al.*, 1999).

#### **2.4.9 Video image enhanced evaluation of weathering (VIEEW)**

After salt spray test, surface defects were evaluated by VIEEW<sup>TM</sup> system. VIEEW<sup>TM</sup> is capable of capturing digital images of samples under various lighting schemes optimized to highlight and enhance surface defects to digitally process images. It is also capable of measuring and counting defects with a comprehensive statistical profile. The VIEEW<sup>TM</sup> incorporates two different illumination methods: (1) diffuse, chromatic (color) lighting for the detection of variations in chromatic contrast; and (2) direct lighting to measure variations in geometric reflection (gloss) and its textural characteristics. The area under the scan was selected and lights for the reflection were optimized using Atlas imaging software. Sample images were analyzed for surface texture and smooth by grayscale. The value of corrosion area of

specimens was calculated by dividing the corrosion area by the tested area (%) (Atul, 2007).

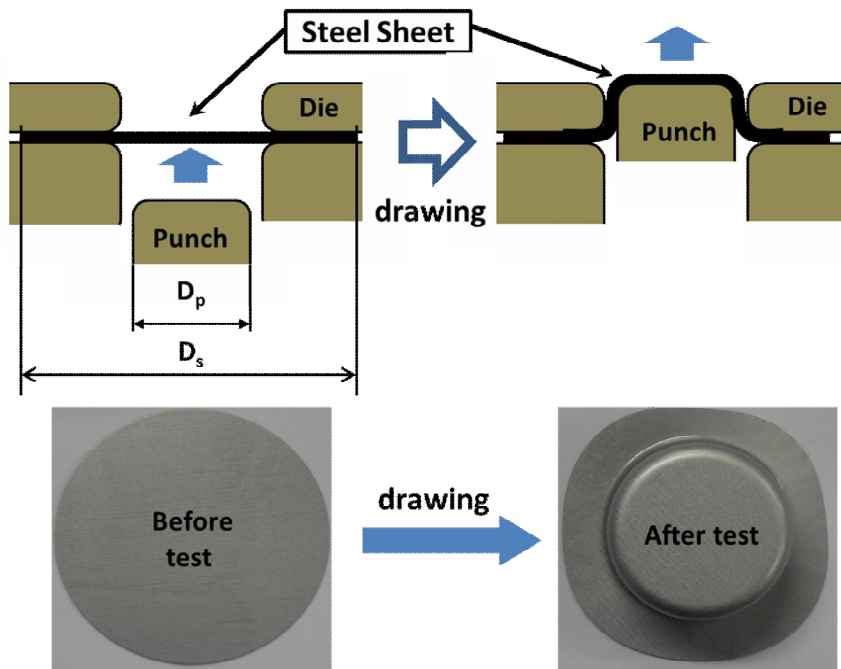
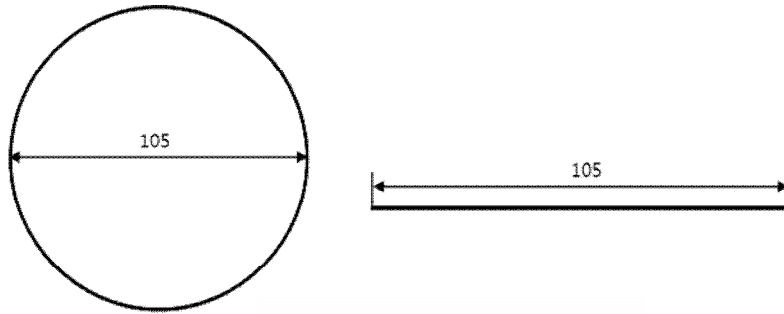
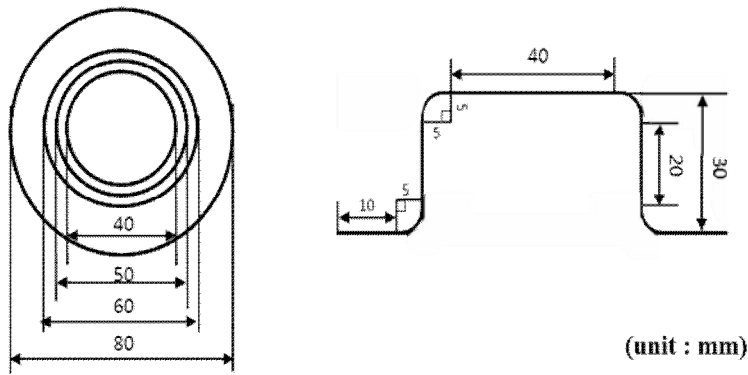


Figure 2-1. Procedure of a deep drawing test (Ueda *et al.*, 2002).



**Before drawing test**



(unit : mm)

**After drawing test**

Figure 2-2. Schematic diagram of specimens for a cylindrical drawing test (Moon *et al.*, 2012).

Table 2-3. Conditions for deep drawing test of PCM (Moon *et al.*, 2012).

Shape of punch	Cylindrical
Corner radius of punch (mm)	5
Should radius of punch (mm)	5
Size of punch (mm)	40
Size of PCM (mm)	105
Drawing height (mm)	30
Drawing of speed (mm/min)	20

### 3. Results and Discussion

#### 3.1. Characterization of flexible polyester resin

Polyester resins were synthesized with different content of polycarbonate diol. The carbonate group in the synthesized polyester resin was determined using FT-IR. As shown in Figure 2-3, the carbonated group was detected at 1240 and 1760  $\text{cm}^{-1}$  and the intensity of these bands increased with increasing content of polycarbonate diol (Nakano *et al.*, 1999).

Table 2-4 listed the molecular weight and polydispersity of the synthesized polyester resin. Theoretical hydroxyl number of polyester resin ( $n_{\text{OH}}$ ) was decreased with increasing content of polycarbonate diol which has higher molecular weight than 2-methyl 1,3-propanediol (MPD). Also, the ratio between the number average molecular weight and hydroxyl number ( $M_n/n_{\text{OH}}$ ) indicates the length of the repeating unit in the crosslink network of the synthesized polyester resin (Stroisz nigg *et al.*, 2009). The value of  $M_n/n_{\text{OH}}$  was observed to increase with increasing content of polycarbonate diol, thus indicating decreasing crosslinking density.

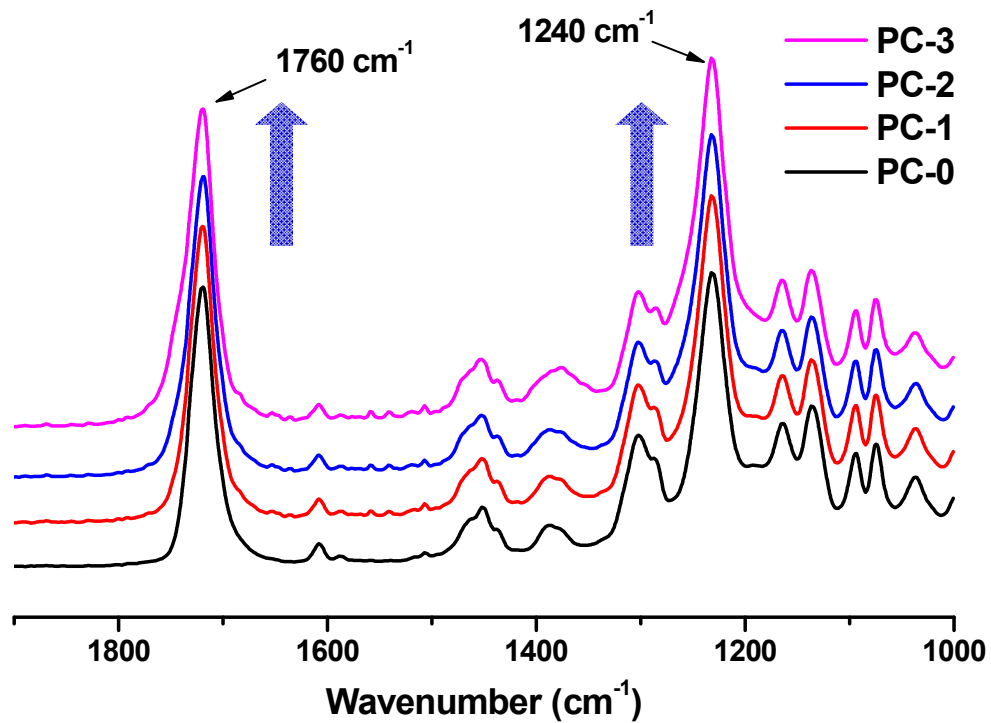


Figure 2-3. IR spectra of flexible polyester resin with polycarbonate diol (1240, 1760  $\text{cm}^{-1}$  : carbonate group).

Table 2-4. Characterization of flexible polyester resin.

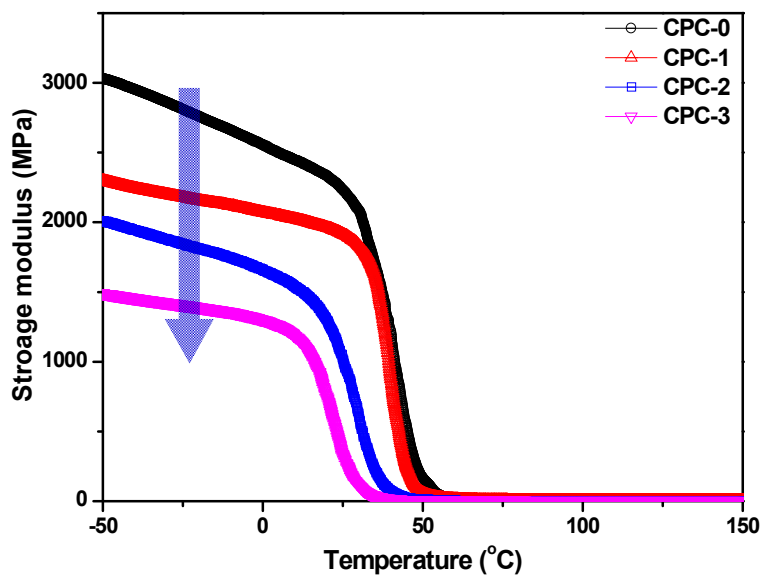
Property	PC-0	PC-1	PC-2	PC-3
Number average M.W. ( $M_n$ )	5,670	5,940	6,950	7,390
Polydispersity index ( $M_w/M_n$ )	4.2	4.7	4.6	4.7
* $n_{OH}$ (mg KOH/g)	44.9	42.1	39.7	37.9
$M_n/n_{OH}$ (g/mg KOH)	126	141	175	194
Crosslink density ( $10^{-3}$ mol/cm <sup>3</sup> )	0.626	0.568	0.410	0.231

\*  $n_{OH}$  -Theoretical hydroxyl number of polyester resins

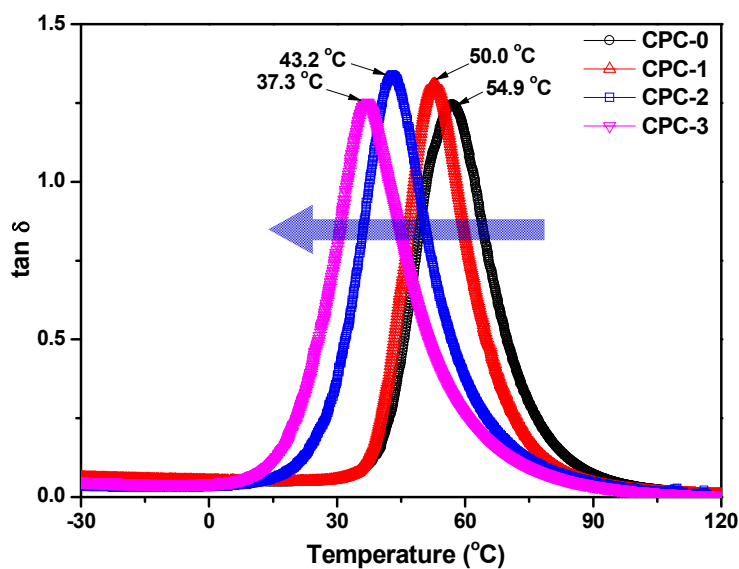
### 3.2. Viscoelastic behavior

Dynamic mechanical analysis (DMA) is a convenient method to study thermal and mechanical viscoelastic properties of polymeric materials. The DMA data allow observations of changes in loss and storage modulus, glass transition temperature ( $T_g$ ), and crosslink density (Hou *et al.*, 2009).

Figure 2-4(a) shows storage modulus as a function of temperature for synthesized polyester resins with polycarbonate diol. The storage modulus decreased with increasing contents of polycarbonate diol, i.e. CPC-0 > CPC-1 > CPC-2 > CPC-3. Polycarbonate diol has long alkyl chain compared to MPD; it is generally recognized that the mobility and flexibility of polymer chain increased with the length of linear alkyl chain segment (Moon *et al.*, 2002). In addition, the storage modulus decreased with the increase of the ratio between the number average molecular weight and hydroxyl number ( $M_n/n_{OH}$ ) (Stroisznnigg *et al.*, 2009). As listed in Table 2-4, a longer length between crosslinks corresponds to a lower crosslink density, thus explaining the lower modulus of the resin. Also, the  $T_g$  shifted to a lower temperature as shown in Figure 2-4(b) with increasing content of polycarbonate diol (Hou *et al.*, 2009). From the dynamic mechanical analysis, polycarbonate diol would favorably provide lower stiffness and higher softness to polyester coatings (Moon *et al.*, 2002).



(a) Storage modulus



(b)  $\tan \delta$

Figure 2-4. Viscoelastic properties of flexible polyester coatings (a) storage modulus and (b)  $\tan \delta$ .

### 3.3. Creep behavior

Creep behavior can estimate changes in the molecular network structure during the deformation by the stress (Mezger, 2006). Results of creep measurements at a stress level of 5.1 MPa and creep time is 90 s are shown in Figure 2-5. Creep compliance increased with increasing content of polycarbonate diol. The steady-state compliance,  $J_e$  can be determined by the interception of the extrapolation of the linear relation. Ueda *et al* reported that  $J_e$  increases with an increasing and deformation occurs easily when the molecular weight increases the polyester resin (Ueda *et al.*, 2002). Agreeing with their finding, CPC-3 had the highest molecular weight among the polyester resins. Also, it has the highest deformation, because it contained the highest amount of polycarbonate diol which has long alkyl chain. CPC-3 has the longest molecular segment length between crosslinks thus, it has the lowest crosslink density. It means that CPC-3 has the highest compliance among the samples investigated, and it was developed a permanent strain more easily by the stress. Conversely, CPC-0 exhibited the lowest deformation, and it was hardly developed a permanent strain by the stress. From the creep test, the compliance in an ascending order : CPC0 < CPC-1 < CPC-2 < CPC-3, and this trend agrees with the increasing contents of polycarbonate diol. It means that polycarbonate diol would favorably provide higher softness and lower stiffness to polyester coatings.

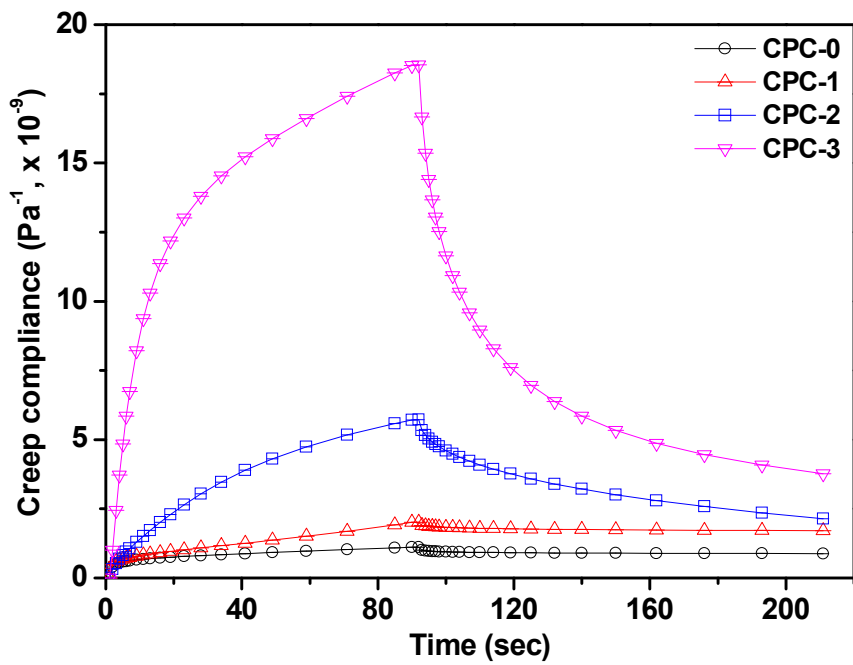


Figure 2-5. Creep compliance of flexible polyester coatings.

### 3.4. Flexibility

Flexibility is the most important property for cutting, pressing and stamping processes in the pre-coated system. Tensile strength tests are carried out to study basic mechanical properties - modulus, tensile strength, elongation at break, and toughness of polymeric materials (Levine *et al.*, 2010). Figure 2-6 presents effects of the contents of polycarbonate diol on tensile behaviors of the synthesized resins. The tensile strength decreased with an increased content of polycarbonate diol (CPC-0 > CPC-1 > CPC-2 > CPC-3). In contrast, the maximum strain increased when the content of polycarbonate diol was increased (CPC-0 < CPC-1 < CPC-2 < CPC-3). The tensile strength of CPC-2 was 16.7 MPa and that of CPC-3 was 8.7 MPa, with maximum strain of 178 % and 195 %, respectively. These values represent a high flexibility and high breaking strain, which were a consequence of the high stretchability imparted by the soft segments of the polycarbonate diol in flexible polyester resins. Compared to the chain length between polycarbonate diol and MPD, polycarbonate diol has 5.5 times longer than MPD and it would provide soft segments of polymer network. Therefore it could be implied that polycarbonate diol can give to a flexibility and would favorably provide lower stiffness and higher softness to polyester coatings (Moon *et al.*, 2012).

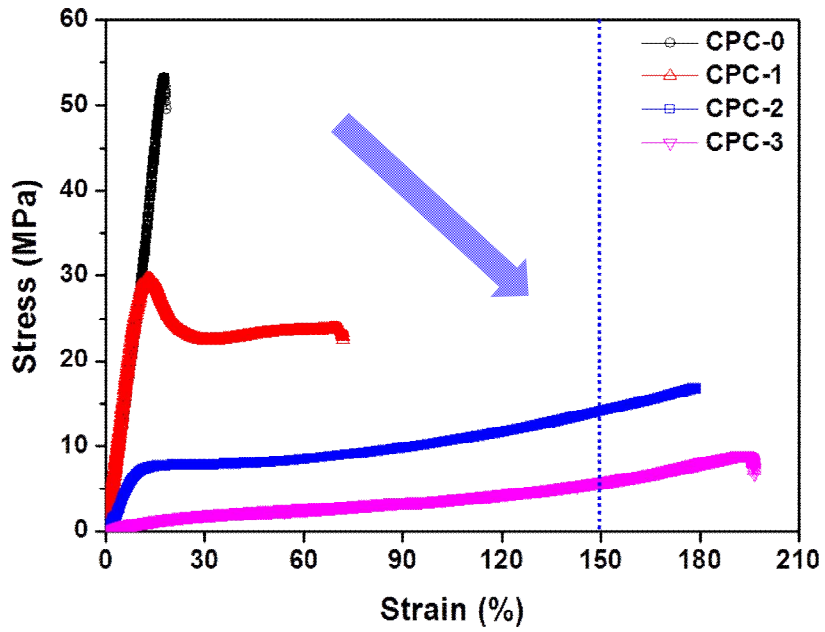


Figure 2-6. Stress-strain curve of flexible polyester coatings.

### 3.5. Formability

The deep drawing test is a common method for determining formability in pre-coated metals. During the deep drawing test which took 90 s to complete, the calculated stress was 5.1 MPa and strain was 23.4 % on the PCM. Stress of polyester coatings should have larger than 5.1 MPa of deep drawing and strain should stretch out 23.4 % for 90 s to have good formability.

Figure 2-7 shows formability resulted from the deep drawing. CPC-0 had cracks and delamination even though it exhibited the highest tensile strength value from the flexibility test as shown in Figure 2-6, CPC-0 was not flexible enough to be stretched out during the deep drawing. Also, CPC-3 exhibited cracks and delamination even though it had the highest percent elongation value from the flexibility test. The tensile strength of CPC-3 was lower than 5.1 MPa at the strain of 23.4 % (see Figure 2-6); hence CPC-3 was not strong enough to overcome stress exerted on PCM during the deep drawing. Even though flexibility tests revealed sufficient tensile strength and elongation values for CPC-1, some smaller cracks still developed in the specimen. This behavior of CPC-1 can be explained by the DMA creep test whose results are shown in Figure 2-8. The creep test, which was performed at a tensile stress of 5.1 MPa for 90 s to simulate the condition of deep drawing that the strain developed in CPC-1 was 10.0 %. This strain value is lower than the 23.4 % strain that would be exerted on a specimen in the 90 s of the deep drawing condition. Therefore, CPC-1 was not flexible enough to be stretched out during the deep drawing.

CPC-2 exhibited good formability. It had sufficient tensile strength

and elongation values based on the flexibility test. It also had sufficient flexibility based on the creep test as shown in Figure 2-8. The developed strain was 29.1 % for 90 s. So, CPC-2 can be stretched without being damaged during the deep drawing test. This result agreed to our previous study, formability could be predicted from the tensile test and creep test. A forming coefficient based on strain energy ( $F_U$ ) should be larger than 1, and a forming coefficient based on strain ( $F_\epsilon$ ) should be larger than 1 (Moon *et al.*, 2012).  $F_U$  and  $F_\epsilon$  were calculated, and are listed in Table 2-5. The  $F_U$  of CPC-2 was 1.49 and that of  $F_\epsilon$  was 1.26. So, CPC-2 can be stretched out without being damaged during the deep drawing.

From the deep drawing test, tensile strength of polyester coatings should be larger than 5.1 MPa to overcome tensile stressed and strain of polyester coatings should be larger than 23.4 % for 90 s to have good formability. Also, polycarbonate diol would favorably provide lower stiffness and higher softness to polyester coatings, but it would make weaker of the polyester coatings. The short crosslink between long chain segments had been made intramolecular crosslink, so called loop crosslink which is a weaken point of the polymer network (Tonelli *et al.*, 1974; Simon *et al.*, 1991). So, it is important to have appropriate amounts of polycarbonate diol in the polyester coatings to have good formability.



Figure 2-7. Formability of flexible polyester coatings on the cold roll steel sheet.

Table 2-5. Calculated values from tensile test and creep test of flexible polyester coatings (Moon *et al.*, 2012).

Sample	$U_T$	$U_C$	$F_U (U_C/U_T)$	$\varepsilon_C$ (%)	$F_\varepsilon (\varepsilon_C/R_f)$
CPC-0	253.10	28.30	0.11	5.55	0.24
CPC-1	227.58	71.87	0.32	14.09	0.60
CPC-2	101.15	150.9	1.49	29.42	1.26
CPC-3	20.23	472.01	23.33	92.55	3.96

$U_T$ : strain energy at 23.4% in tensile test

$U_C$ : strain energy of coating film in creep test

$F_U (U_C/U_T)$  : forming coefficient based on strain energy

$\varepsilon_C$ : strain at 5.1 MPa during the creep test

$F_\varepsilon (\varepsilon_C/R_f)$  : forming coefficient based on strain

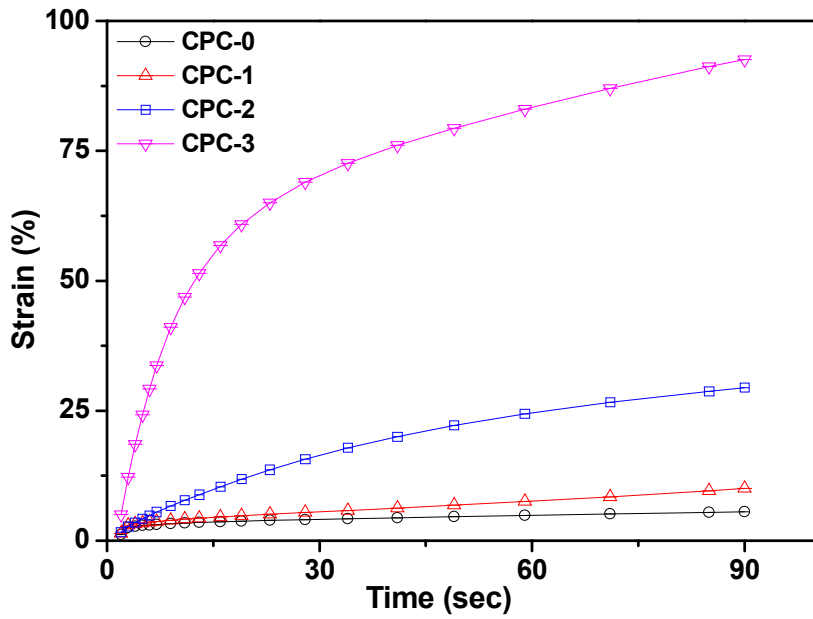


Figure 2-8. Strain of flexible polyester coatings by the creep test.

### 3.6. Water uptake

One of the important roles of coating is to block the environmental factors such as Water and oxygen. Coating capacitance has been represented water uptake of coatings and it is measured by alternating current impedance method of electrochemical impedance spectroscopy (EIS). When water is penetrating the coating, the value of coating capacitance is started. The value of water uptake of coating is calculated from Brasher-Kingbury equation .

The water uptake behavior of the conventional electro coatings and polyester coatings are shown in Figure 2-9. The coating thickness of electro coatings is 10  $\mu\text{m}$  and polyester coatings are 20  $\mu\text{m}$ . The water uptake of electro coating was continuously increased for 3 h. But, those of polyester coatings were greatly increased for 10 min and then were gradually increased. They were reached equilibrium state after 1 h. The value of electro coatings is 28.5 vol % . CPC-0, CPC-1, and CPC-2 are almost same and those value are 4 vol % . However, CPC-3 has larger than other polyester coatings. It is 6 vol % , because CPC-3 has the highest amount of polycarbonate diol which would make weaker of the coating.

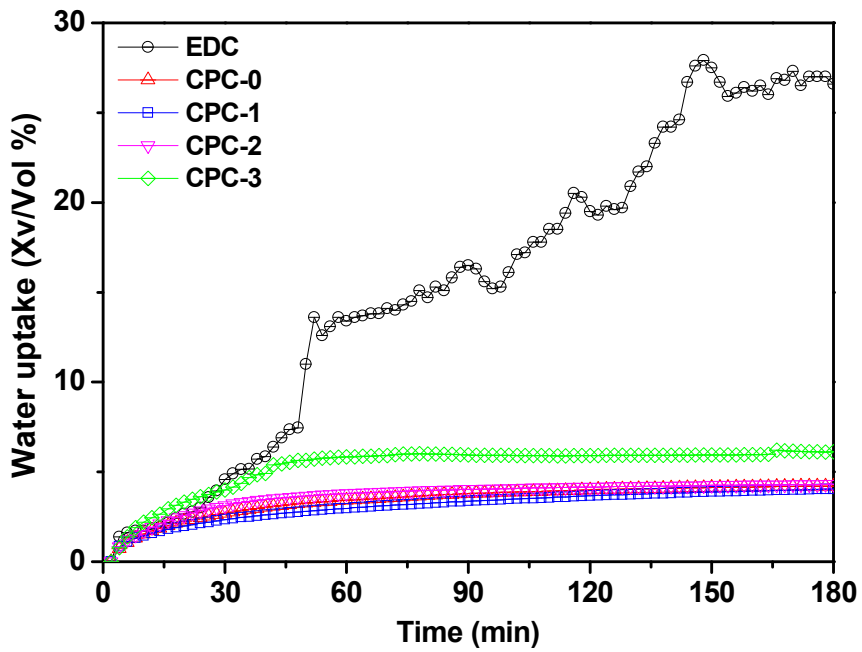


Figure 2-9. Water uptake (vol %) of electro coatings and flexible polyester coatings by the capacitance method under the immersion.

### 3.7. Anti-corrosion property

The anti-corrosion property is one of the physical properties of pre-coated metals. Conventional electro coatings and polyester coatings were tested via salt spray for 500 h. As shown in Figure 2-10, all specimens had red rusts around X-cut. Electro coatings had the much amounts of red rusts around X-cut among the specimens, but the surface was clear where there was no X-cut. CPC-0 had lots of small size blistering and CPC-1 had some of small size blistering around X-cut. CPC-3 had a big size blistering around X-cut. However, CPC-2 was relatively clear surface around X-cut and the surface was relatively clear where there was no X-cut. Those results agree with water uptake test. Electro coatings had the highest value of the water uptake, so it could not block the corrosion factors during the salt spray test. CPC-3 had the highest value of the water uptake among the polyester coatings. It means that CPC-3 could not block the corrosion factors during the salt spray test compared to other polyester coatings. Also, it had the lowest value of tensile strength among the polyester coatings. So, it was not strong enough to overcome the harsh conditions.

Figure 2-11 presents surface morphology of all specimens by VIEEW<sup>TM</sup> images. All specimens had damaged around X-cut. CPC-0 and CPC-1 can see the blistering of the surface and CPC-3 also can see a large size of blistering. CPC-2 has relatively clear surface around X-cut. Corrosion area of specimens can be calculated from the VIEEW images.

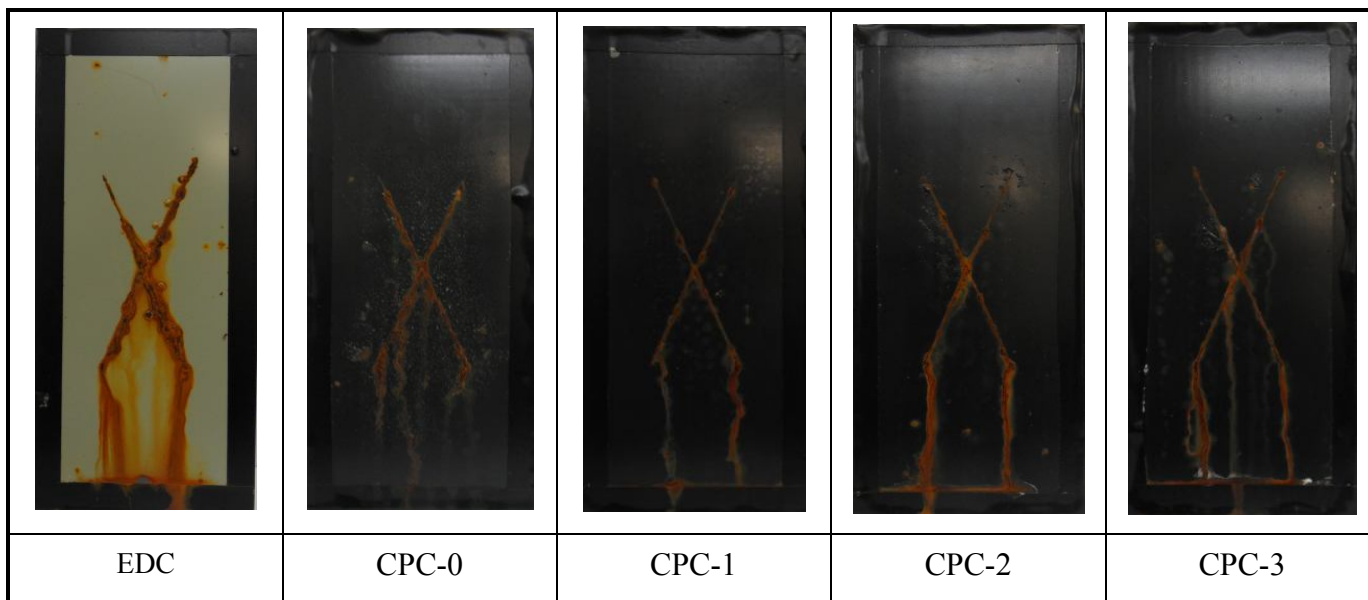


Figure 2-10. Corrosion resistance of electro coatings and flexible polyester coatings by salt spray test for 500 h.

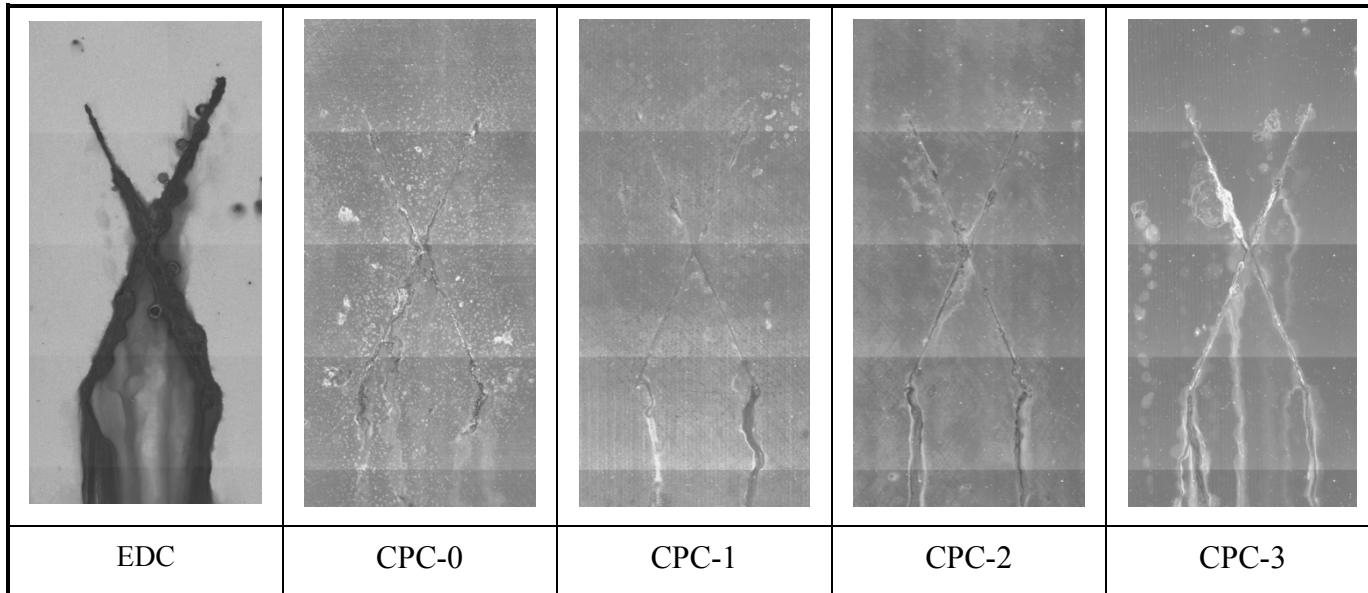


Figure 2-11. VIEEW images of electro coatings and flexible polyester coatings after salt spray test.

Corrosion area of electro coatings was 3.3 % and polyester coatings were less than 3.0 %. Those of polyester coatings are as the followings : CPC-0 is 2.4 %, CPC-1 2.2 %, CPC-2 is 2.1 %, and CPC-3 is 2.7 % respectively. Those results agree with water uptake test. An electro coatings had the highest value of the water uptake, so it has largest value of corrosion area. CPC-3 had the highest value of the water uptake among the polyester coatings, so it has largest value of corrosion area. From the salt spray test, polyester coatings have better an anti-corrosion property than electro coatings.

#### 4. Conclusions

Four types of flexible polyester resins with polycarbonate diol were synthesized and formulated to control formability for pre-coated metal systems. These resins were designed to show the flexibility of long alkyl chain. The viscoelastic behavior, flexibility and formability were measured to determine the long alkyl chain effect on the flexibility of the pre-coated metal system.

When the content of long alkyl chain of polycarbonate diol was increased in the resins synthesized, the stiffness of the product decreased considerably and  $T_g$  of each cured coatings shifted to a lower temperature. Therefore, polycarbonate diol is a major factor to improve flexibility and formability of the polyester coatings. To make good formability of polyester coatings for the pre-coated metals, tensile stress of polyester coatings should be larger than 5.1 MPa to overcome stressed during the deep drawing and strain should stretch out 23.4 % for 90 s.

CPC-2 which had 2 mol of polycarbonate diol had good formability in the deep drawing and also had good anti-corrosion property compared to electro coatings. So, CPC-2 would be an appropriate coatings as a primer for automotive pre-coated metals.



## **Chapter 3**

### **Synthesis of Polyester-nanocomposites and Characterization of Polyester-nanocomposites Coatings for Automotive Pre-coated Metals**

## 1. Introduction

Pre-painted or coil-coated metals (PCM) have been used in many applications such as household electric appliances, building materials and others. In this system, wet coating process can be eliminated by using a roll coating process, making it possible to circumvent the problem of air pollution arising from evaporation. In addition, a pre-coated metal system offers other advantages such as improved productivity and energy saving, thus the use of PCM has been spreading (Ueda *et al.*, 2002; Moon *et al.*, 2012). One of the most important properties of PCM is formability. If the film on the coated PCM parts is damaged, the products are rendered useless (Kanda *et al.*, 1998). Also, the most important property of PCM is anti-corrosion property. Many researchers have been reported that the incorporation of layered silicate fillers into polymers leads to improved properties such as stiffness, strength, heat resistance, and decreased moisture absorption and permeability, when compared to micro-scale composites (Wang *et al.*, 2007). One of the major properties is to decrease moisture absorption and permeability which can protect corrosion of metals which can prevent the diffusion of corrosive factors such as water and oxygen (Heidarian *et al.*, 2010).

Polymer/layered silicate nanocomposites have been widely investigated. Especially polyurethane/clay nanocomposites have been tried to overcome low thermal stability and barrier property (Ray *et al.*, 2003). Those properties can be improved by adding clay such as organoclay to the polymer. The incorporation of organoclay into the

polymer matrix improved coating properties such as adhesion (Ahamadi *et al.*, 2007), hardness (Ahamadi *et al.*, 2007; Lv *et al.*, 2008), barrier property Choi *et al.*, 2004; Spirkova *et al.*, 2008), and corrosion resistance (Chen-Yang *et al.*, 2004).

In this study, we used organoclay such as Cloisite 30B with modified with a quaternary ammonium salt (organic modified montmorillonite, OMMT) and it has -OH group. PE/OMMT nanocomposites were synthesized by in situ polymerization with high speed homogenizer process of the various contents of organoclay. The major purpose is to study the effect of well dispersed nano-layered silicates on corrosion performance. Small angle X-ray scattering (SAXS) and transmission electron microscopy (TEM) were employed to characterize the structure of organoclay dispersions. Another purpose is formability using polycarbonate diol in the synthesis of polyester. Polycarbonate diol consists of a long alkyl chain with contains much flexible rod-like group such as -CH<sub>2</sub> (Percec *et al.*, 1991).

Overall this chapter reports the design of a polyester resin for automotive pre-coated metal using organoclay and polycarbonate diol in the resin formulation. The elongation, tensile strength and viscoelastic properties of free coated film were measured. The formability of PCMs was evaluated using a cylindrical drawing test. Salt spray and electrochemical impedance spectroscopy were employed to investigate the corrosion performance of PE/OMMT nanocomposites coating and the effect of the concentration of organoclay into the polyester matrix.

## 2. Experimental

### 2.1. Materials

A polycarbonate diol (PCDL,  $M_n = 500$ , Asahi Kasei Chemicals Corp., Japan) was prepared to control the flexibility of the main chain. 1,4-cyclohexanedicarboxylic acid (1,4-CHDA, Tokyo Chemical Industry, Japan), adipic acid (AA, Samchun Pure Chemical, Republic of Korea), and isophthalic acid (IPA, Junsei Chemical Corp., Japan), trimethylol propane(TMP, Tokyo Chemical Industry, Japan), 2,2,4-trimethyl-1,3-pentanediol (TMPD, Tokyo Chemical Industry, Japan), 1,4-cyclohexanedimethanol (1,4-CHDM, Tokyo Chemical Industry, Japan), and Closite 30B (Southern Clay Products, Inc., USA) were used without further purification. Butylstannic acid (FASCAT 4100, Arkema Inc., USA) was used as a catalyst to catalyze polymerization and prevent a transesterification reaction during the polymerization (Hamada *et al.*, 1997).

Hexamethoxymethyl-melamine (HMMM , Cytec Industries Inc., USA) was used as the curing agent and blocked acid catalyst (NACURE 1953, King Industries, Inc., USA) was used.

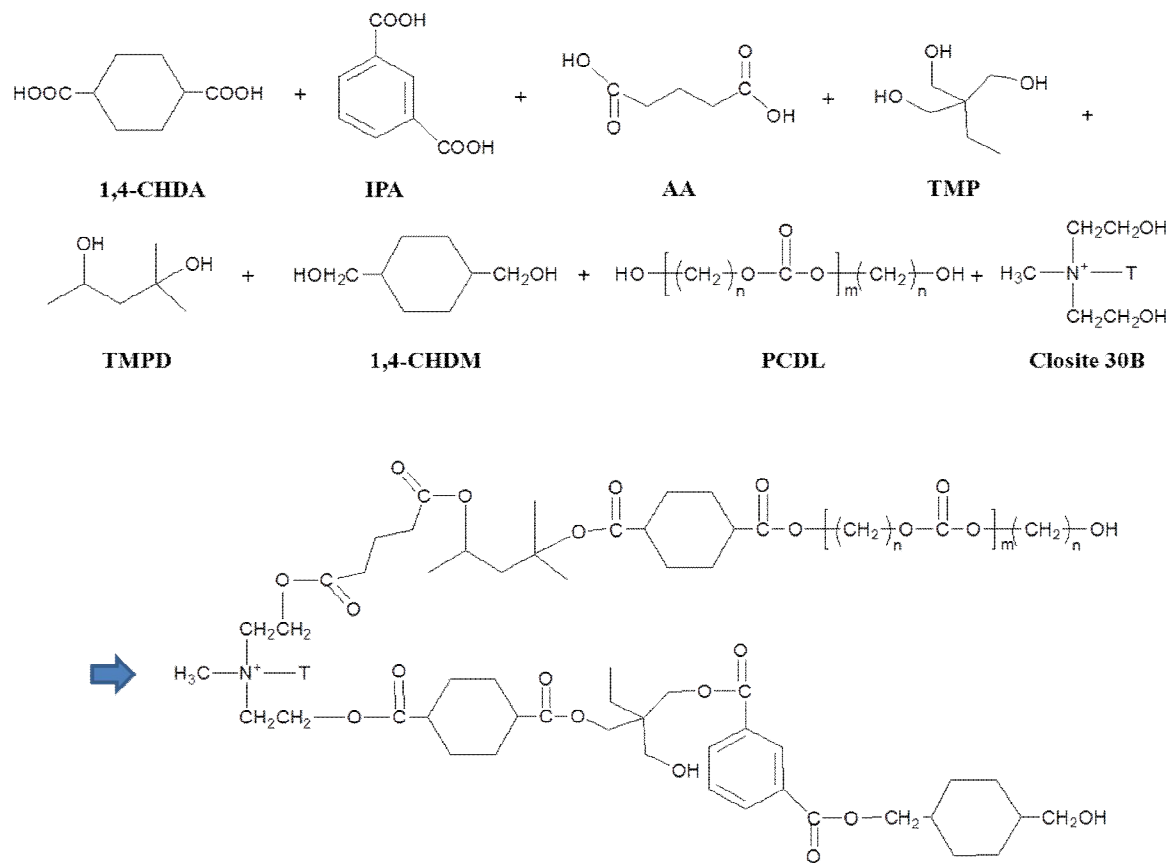
### 2.2. Synthesis of PE/OMMT nanocomposites

The synthesized scheme of PE/OMMT nanocomposites with Closite 30B polycarbonate diol is shown in scheme 3-1 and the formulations are shown in Table 3-1. PE/OMMT nanocomposites were synthesized from polybasic alcohols and polybasic acids with the following procedure which consisted of two synthesis processes. One was the

fusion process and the other was the solvent process. Synthesis equipments were same in chapter 2.

Organoclay dispersion : Cloisite 30B is inorganic materials. It needs to disperse before using. Organoclay was dispersed in cyclohexanone with high speed homogenizer. Organoclay, PCDL, and cyclohexanone were charged into a vessel and dispersed for 30 min with 10,000 rpm and pre-dispersed organoclay was 10 wt %.

Firstly, IPA, TMP, TMPD, 1,4-CHDM, and pre-dispersed organoclay(10 wt%) were charged into a dried reactor and the reaction temperature was set to 150 °C with stirring for 2 h under N<sub>2</sub> purge. Subsequently, the reaction temperature was increased from 150 °C to 210 °C at the rate of 0.5 °C/min. During the fusion process, all raw materials were melted and the condensed water was collected. After that 1,4-CHDA, AA, and PCDL were charged into the reactor containing melt prepared from the preceding step and the reaction temperature was set to 130 °C with stirring for 2 h under N<sub>2</sub> purge. Subsequently, the reaction temperature was increased from 130 °C to 180 °C at the rate of 0.3 °C/min. The reaction temperature was maintained for several hours to collect condensed water.



Scheme 3-1. Synthesis scheme of PE/OMMT nanocomposites.

Table 3-1. Formulations used for synthesis of PE/OMMT nanocomposites.

(unit : mole of monomer)

Contents	NC-0	NC-1	NC-2	NC-3
Polycarbonate diol	1	1	1	1
Trimethylol propane	3	3	3	3
2,2,4-trimethyl-1,3-pentanediol	10	10	10	10
1,4- cyclohexanedimethanol	11	11	11	11
1,4-cyclohexanedicarboxylic acid	10	10	10	10
Adipic acid	2	2	2	2
Isophthalic acid	12	12	12	12
Closite 30B (wt %)	0	1	2	3

The fusion process was then converted into solvent process by adding xylene. The solvent process was carried out to collect condensed water and to make low acid value. The reaction temperature was set to 180 °C. During the solvent process, the acid value was measured by 0.1 *N* KOH solution. The reaction temperature was maintained for several hours until the acid value was under 3 mg KOH/g resin (Hamada *et al.*, 1997). The solid content of synthesized PE/OMMT nanocomposites was 70 %.

### **2.3. Preparation of PE/OMMT nanocomposites coatings**

Synthesized PE/OMMT nanocomposites were mixed with HMMM, additives, and solvents. Four different formulations were prepared as listed in Table 3-2.

Free film : Preparing free film was same in chapter 2. The resulted films became the samples for tensile strength and dynamic mechanical analysis

PCM : Cold roll steel sheets (thickness of 0.8 mm) were coated with alkali solution and baked at the 150 °C for 5 min for a pre-treatment. The cured pre-treated films were 5  $\mu\text{m}$  in thickness. The PE/OMMT nanocomposites coatings were coated on the cured pre-treated film and then baked at 150 °C for 30 min. The thickness of those cured film was 20  $\mu\text{m}$ . The total thickness of those cured film was 25  $\mu\text{m}$ .

Table 3-2. Formulations of PE/OMMT nanocomposites coatings.

(unit : wt %)

Contents	CNC-0	CNC-1	CNC-2	CNC-3
NC-0	61.8	-		-
NC-1	-	61.8		-
NC-2	-	-	61.8	-
NC-3	-	-		61.8
HMMM	6.5	6.5	6.5	6.5
* Additives	1.0	1.0	1.0	1.0
Nacure	0.5	0.5	0.5	0.5
**Solvent	30.2	30.2	30.2	30.2

\* Additives

- Defoamer : Afcona 3770, Leveling agent : Afcona 3777

\*\*Solvent : solvesso #100

## 2.4. Characterization

### 2.4.1. Small angle X-ray scattering (SAXS)

Small angle X-ray scattering analysis of Cloisite 30B powders and PE/OMMT nanocomposites were performed using a Bruker X-ray diffractometer (equipped with a 2-D detector) in reflection mode. Tests were carried out with  $2\theta$  scanned between  $2.0^\circ$  and  $9^\circ$  nickel-filtered  $\text{CuK}_{\alpha 1}$  radiation ( $\lambda = 0.15418$  nm) under a voltage of 40 kV and a current of 40 mA.

### 2.4.2. Transmission electron microscope (TEM)

Degree of clay exfoliation in nanocomposites was observed with a transmission electron microscope (TEM). Specimens with thickness of 80 nm were cut using a RMC ultra-microtome MT 7000. The morphology of PE/OMMT nanocomposites coating was examined by a JEOL JEM-3010 TEM with operating at an accelerating voltage 300 kV

### 2.4.3. Dynamic mechanical analysis (DMA)

The glass transition temperature and viscoelastic properties of the polyester/melamine heat-cured films were analyzed using a dynamic mechanical analysis (Q800, TA Instruments). The crosslink density ( $\nu_c$ ) was derived from a following equation (Hill 1997; Stroisznigg *et al.*, 2009):

$$\nu_c = \frac{E'_{\min}}{3RT_{E'_{\min}}}$$

Rectangular specimens with 20 mm in length, 6.45 mm in width and 200  $\mu\text{m}$  in thickness were used for the test. The test conditions were same in chapter 2.

#### **2.4.4. Creep compliance properties**

The creep and creep recovery tests of the free coated films were performed using a dynamic mechanical analysis instrument (Q800, TA Instruments). Rectangular specimens of, 20 mm in length, 6.45 mm in width and 200  $\mu\text{m}$  in thickness were used for the test. The time-dependence of creep compliance of the free coated films were obtained at a stress level of  $5.1 \times 10^6$  Pa. The test conditions were same in chapter 2.

#### **2.4.5. Tensile properties**

Tensile properties was measured using a Universal Testing Machine (UTM, Zwick Corp.) at a crosshead speed of 20 mm/min which is designed to correspond to the deep drawing testing speed at an ambient temperature. The tensile specimens prepared from free coated films were 40 mm in length (span length), 6.45 mm in width and 200  $\mu\text{m}$  in thickness. The test conditions were same in chapter 2.

#### **2.4.6. Deep drawing**

A cylindrical deep drawing test was performed to examine formability of the heat-cured coatings as shown Figure 2-1 and 2-2 in chapter 2. The shape of PCM before deep drawing was a disk and its diameter was 105 mm. The shape of the punch was circle and its

diameter was 40 mm, the shoulder radius of the punch and the corner radius of the punch were 5 mm.

Specific conditions of the deep drawing are shown Table 2-3 in chapter 2. In our previous study, calculated value of stress is 5.1 MPa and calculated value of strain is 23.4 % (Lee *et al.*, 2012)

#### **2.4.7. Electrochemical Impedance Spectroscopy (EIS)**

EIS measurements of PE/OMMT nanocomposites coatings were carried out in the unstirred 3.5 wt % NaCl solution. The electrical capacitance of the coatings (C) were measured every 2 minutes for 3 h. The water uptake values of samples obtained from Brasher-Kingsbery equation:

$$\text{Water uptake} = \frac{\log ( C_t / C_0 )}{\log 80}$$

where,  $C_t$  is the electrical capacitance of the coatings during  $t$  time of immersion and is  $C_0$  the electrical capacitance of the coatings before immersion (Bagherzadeh *et al.*, 2007). The test conditions were same in chapter 2.

#### **2.4.8 Salt spray test**

The anti-corrosion property of PE/OMMT nanocomposites coatings were measured using salt spray test. All specimens were first prepared on cold roll steel sheets. The salt spray test condition was according to ASTM B-117 in a 5 wt % NaCl solution at 35 °C. After 600 h, changes of surface morphology and surface defects were examined (Choi *et al.*, 2006; Howard *et al.*, 1999).

### 3. Results and Discussion

#### 3.1. Small angle X-ray scattering of PE/OMMT nanocomposites

PE/OMMT nanocomposites were synthesized based on different content of pre-dispersed organoclay. Degree of intercalation or exfoliation of organoclay in polyester matrix was characterized by small angle X-ray scattering (SAXS) patterns as shown Figure 3-1. Pure organoclay has one diffraction peak at  $2\theta = 4.78^\circ$ . This peak is related to the d-spacing of clay and d-spacing of clay is 18.48 Å by the Bragg's law. PE/OMMT nanocomposites coating specimens containing 1, 2 and 3 wt % of organoclay, there is no peak at  $4.78^\circ$  on SAXS patterns. It means that organoclay of silicate layers were well dispersed and exfoliated into the polyester matrix during the synthesized process. This result is in a good agreement with the data reported by Heidarian *et al.* (Heidarian *et al.*, 2010).

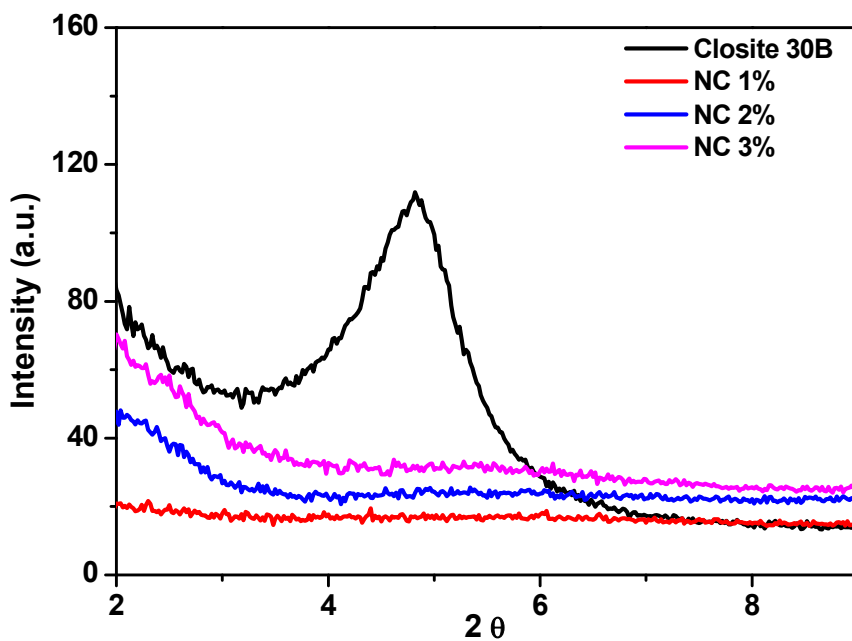


Figure 3-1. SAXS patterns of organoclay powder and PE/OMMT nanocomposites.

### **3.2. Transmission electron microscope of PE/OMMT nanocomposites**

TEM image of PE/OMMT nanocomposites containing with organoclay was taken to confirm the data obtained from SAXS. TEM micrograph of PE/OMMT nanocomposites coating containing of 1 wt % and 3 wt % of organoclay is shown in Figure 3-2. CNC-1 has 1 wt % and CNC-3 has 3 wt % of organoclay. The parallel silicate layers are seen at the organoclay layers. Those TEM micrograph showed the existence of well-dispersed silicate layers and exfoliation of organoclay layers into the polymer chains. The reason is that the strong interactions between the carboxylic ester group of polyester matrix and –OH group of organoclay. From the TEM micrograph, the exhibited morphology can be classified as an exfoliation because the individual organoclay layers were observed (Konwar *et al.*, 2011).

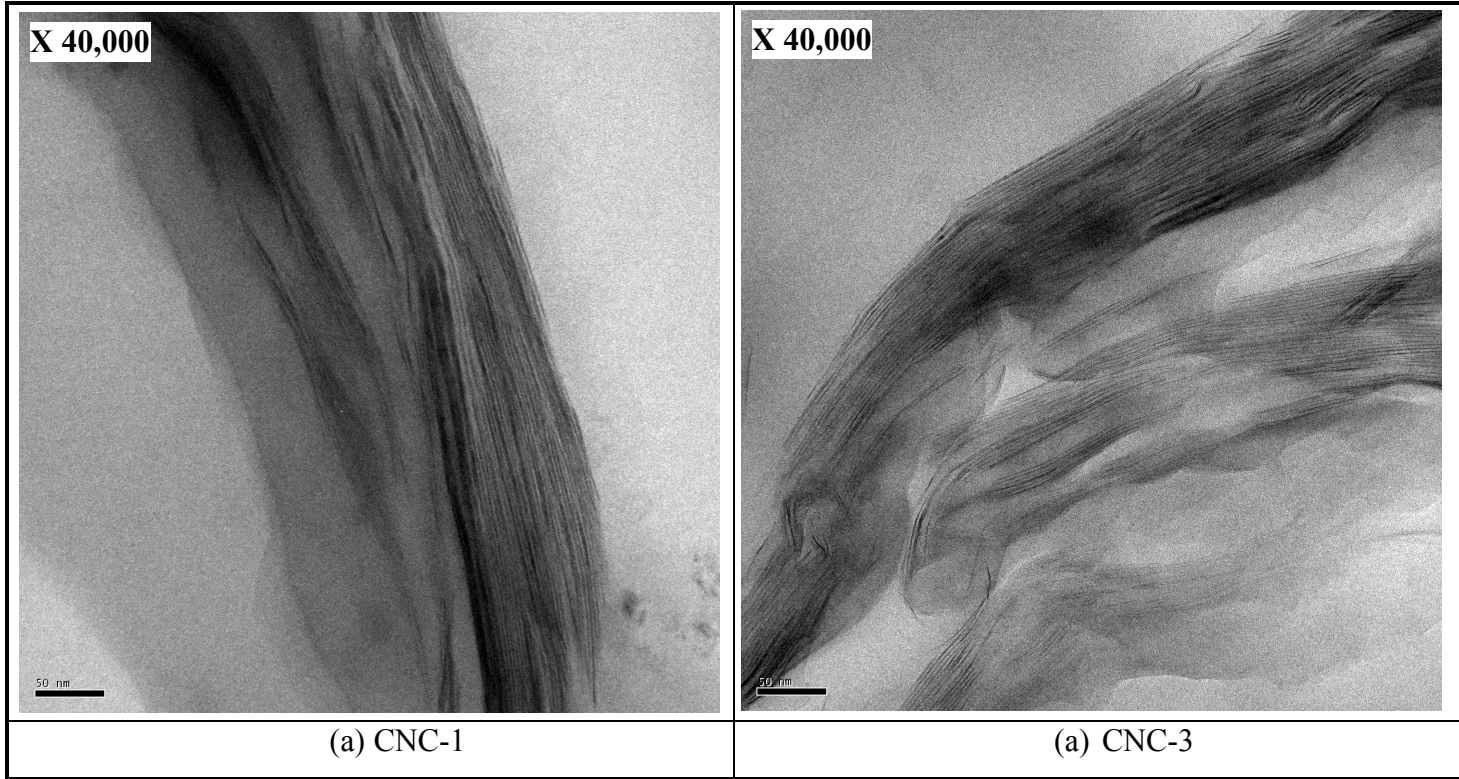
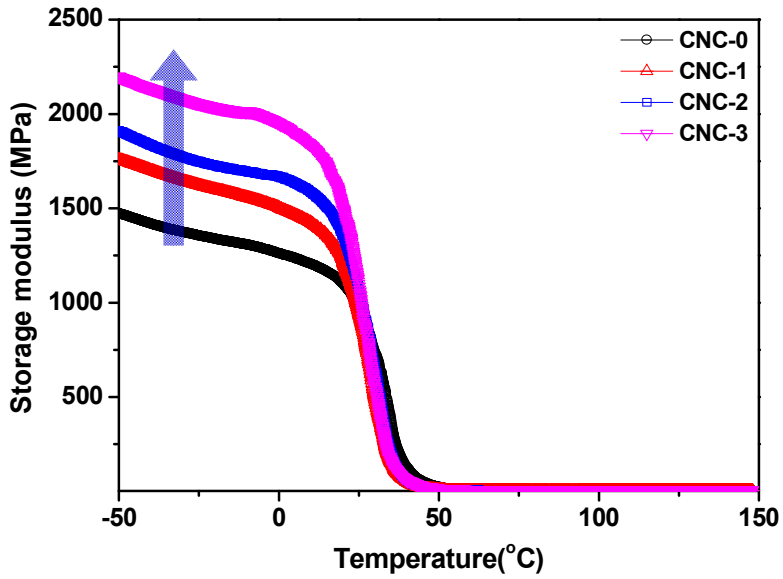


Figure 3-2. TEM images of PE/OMMT nanocomposites coatings (a) CNC-1 and (b) CNC-3

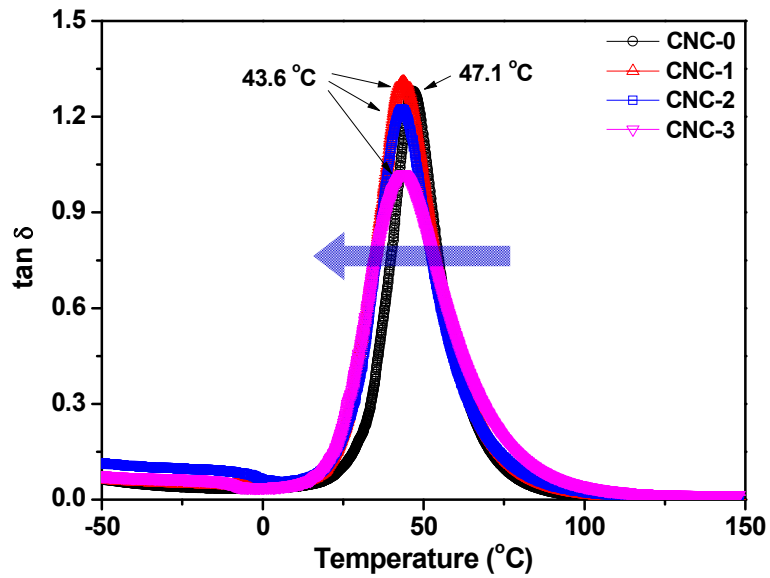
### 3.3. Viscoelastic behavior

Dynamic mechanical analysis (DMA) is a convenient method to study thermal and mechanical viscoelastic properties of polymeric materials. The DMA data allow observations of changes in loss and storage modulus, glass transition temperature ( $T_g$ ), and crosslink density (Hou *et al.*, 2009).

Figure 3-3(a) shows storage modulus as a function of temperature for polyester coatings and PE/OMMT nanocomposites coatings. Storage modulus increased with increasing content of organoclay, i.e. CNC-0 < CNC-1 < CNC-2 < CNC-3. With an addition of 3.0 wt % of organoclay, the storage modulus of PE/OMMT nanocomposites coatings increased about 50 % in the glassy state compared to no addition of organoclay. However, the glass transition temperature of PE/OMMT nanocomposites coatings is lower than PE coating as shown Figure 3-3(b). It causes reduction in crosslink density and lacked surrounding entanglement between the nano-sized layered silicate of organoclay and polyester matrix at the interface.



(a) Storage modulus



(b)  $\tan \delta$

Figure 3-3. Viscoelastic properties of PE/OMMT nanocomposites coatings (a) storage modulus and (b)  $\tan \delta$ .

### 3.4. Creep behavior

Creep behavior can estimate changes in the molecular network structure during the deformation by the stress (Mezger, 2006). Results of creep measurements at a stress level of 5.1 MPa and creep time is 90 s are shown in Figure 3-4. Creep compliance increased with increasing content of organoclay. CNC-0 has the highest compliance among the samples investigated, and it was developed a permanent strain more easily by the stress. Conversely, CNC-3 exhibited the lowest deformation, and it was less easily developed a permanent strain by the stress. From the creep test, the compliance in an order : CNC-0 > CNC-1 > CNC-2 > CNC-3, and this trend agrees with the increasing contents of organoclay of PE/OMMT nanocomposites coatings. CNC-0 had the lowest storage modulus and it could be easily deformed at the stress of 5.1 MPa, so it had the highest creep compliance. But, CNC-3 had the highest storage modulus and it could not be easily deformed at the stress. It means that organoclay would provide stiffness to the PE/OMMT nanocomposites coatings.

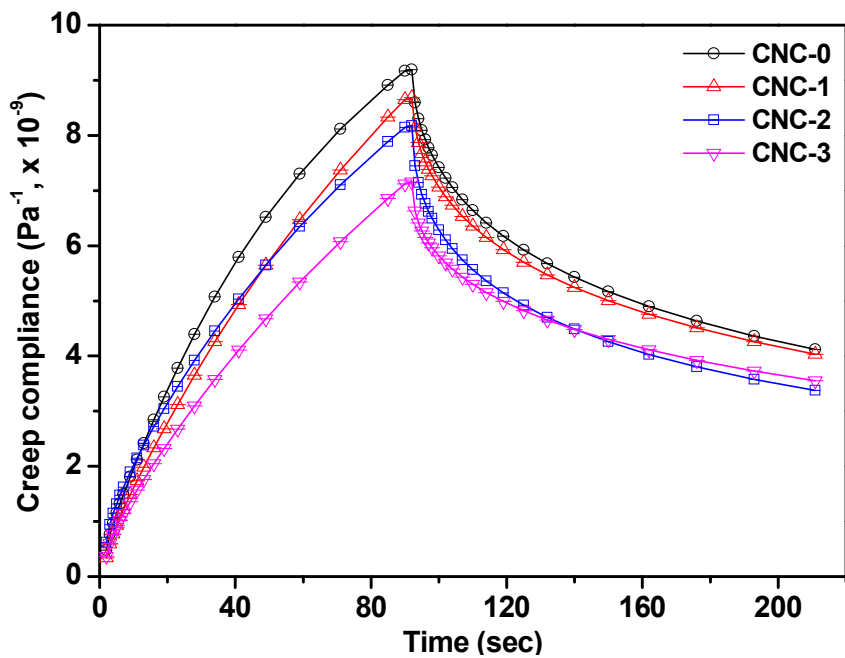


Figure 3-4. Creep compliance of PE/OMMT nanocomposites coatings.

### 3.5. Flexibility

Flexibility is the most important property for cutting, pressing and stamping processes in the pre-coated system. Tensile strength tests are carried out to study basic mechanical properties - modulus, tensile strength, elongation at break, and toughness of polymeric materials (Levine *et al.*, 2010). Figure 3-5 presents effects of the contents of organoclay on the tensile behaviors of the PE/OMMT nanocomposites coatings. The tensile strength increased with an increased content of organoclay and the maximum strain decreased when the content of organoclay was increased. Compared to CNC-0 and CNC-3, the maximum tensile strength of CNC-0 was 20.2 MPa and that of CNC-3 was 22.0 MPa, with maximum strain of 185 % and 166 %, respectively. The maximum tensile strength of CNC-3 is increased by 9 % and the maximum strain is decreased by 11 % in comparison with CNC-0. It means that nano-sized layered silicate of organoclay dispersed homogeneously into the polyester matrix inhibit the mobility. This result was also reported by Chang *et al.* (Chang *et al.*, 2002). It could be implied that organoclay can give stiffness to the PE/OMMT nanocomposites coatings.

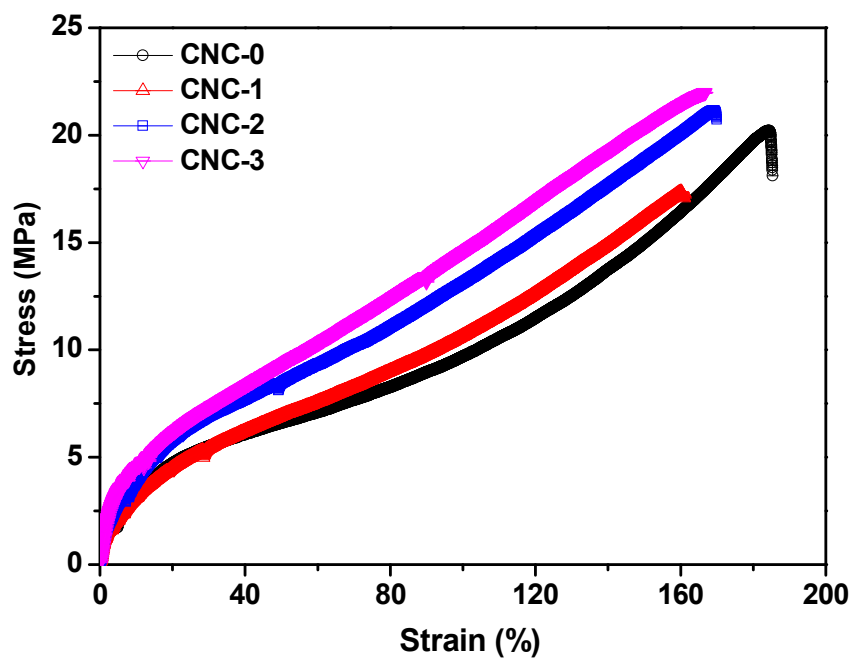


Figure 3-5. Stress-strain curve of PE/OMMT nanocomposites coatings.

### 3.6. Formability

The deep drawing test is a common method for determining formability in pre-coated metals. During the deep drawing test which took 90 s to complete, the calculated stress was 5.1 MPa and strain was 23.4 % on the PCM. Stress of polyester coatings should have larger than 5.1 MPa and strain should stretch out 23.4 % for 90 s to have good formability (Lee *et al.*, 2012).

Figure 3-6 shows formability resulted from the deep drawing test. All tested specimens have good formability and do not have any cracks. Because those specimens had sufficient tensile strength and elongation values based on the flexibility test. And it also had sufficient flexibility based on the creep test as shown in Figure 3-7. The developed strain was over than 30 % for 90 s. So, those specimens can be stretched without being damaged during the deep drawing.

In our previous study, formability could be predicted from the tensile test and creep test. A forming coefficient based on strain energy ( $F_U$ ) should be larger than 1, and a forming coefficient based on strain ( $F_\epsilon$ ) should be larger than 1 (Moon *et al.*, 2012).  $F_U$  and  $F_\epsilon$  were calculated, and are listed in Table 3-3. The  $F_U$  of all specimens were larger than 1, and the  $F_\epsilon$  of all specimens were also larger than 1. So, all specimens can be stretched without being damaged during the deep drawing. Those results agreed with our previous study.

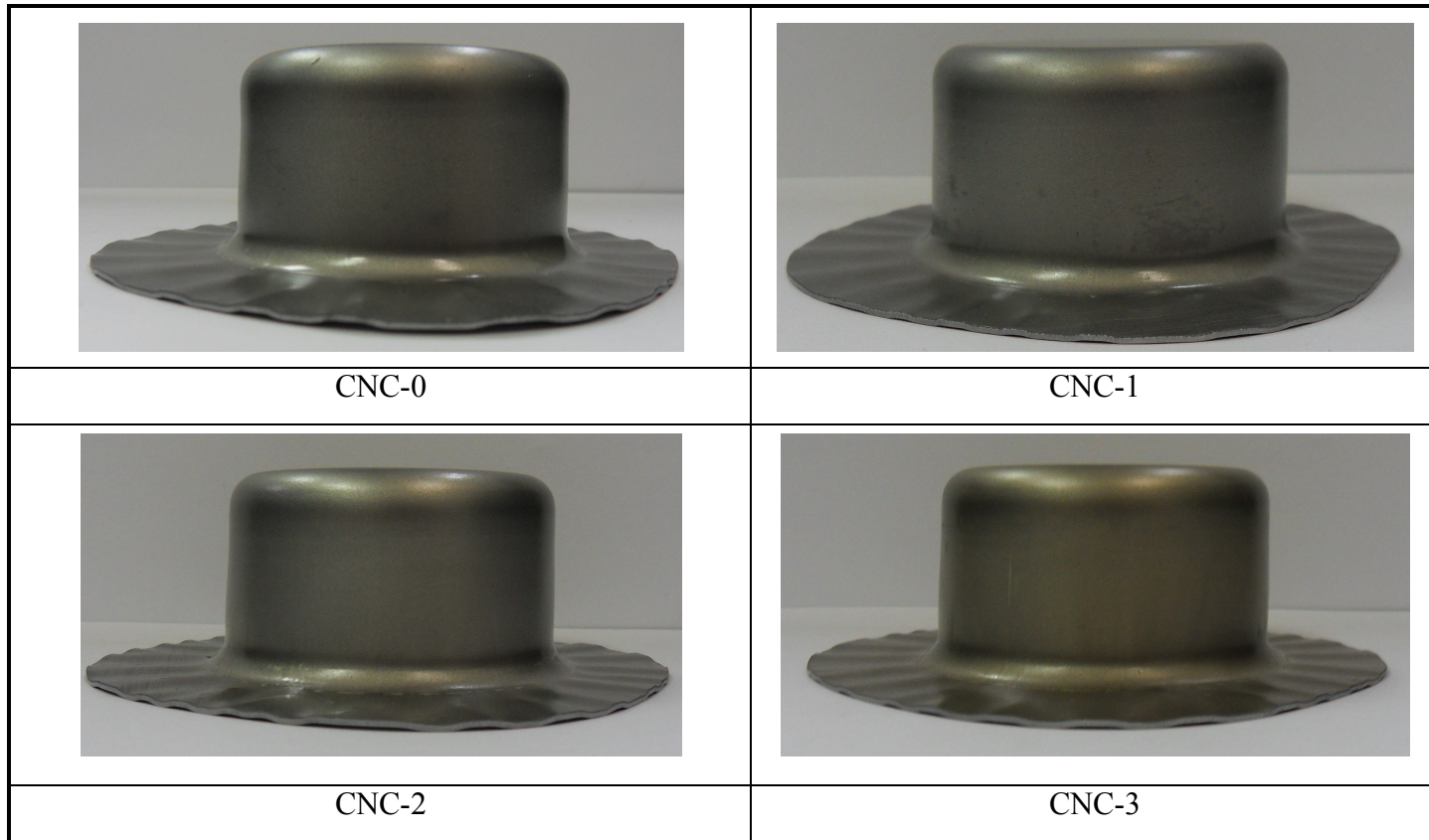


Figure 3-6. Formability of PE/OMMT nanocomposites coating on the cold roll steel sheet.

Table 3-3. Calculated values from tensile test and creep test of PE/OMMT nanocomposites coatings (Moon *et al.*, 2012).

Sample	$U_T$	$U_C$	$F_U (U_C/U_T)$	$\varepsilon_C$ (%)	$F_\varepsilon (\varepsilon_C/R_f)$
CNC-0	93.10	215.21	2.31	42.27	1.81
CNC-1	75.60	192.32	2.54	37.78	1.61
CNC-2	101.11	191.54	1.89	37.56	1.61
CNC-3	107.12	185.51	1.73	36.31	1.55

$U_T$ : strain energy at 23.4% in tensile test

$U_C$ : strain energy of coating film in creep test

$F_U (U_C/U_T)$  : forming coefficient based on strain energy

$\varepsilon_C$ : strain at 5.1 MPa during the creep test

$F_\varepsilon (\varepsilon_C/R_f)$  : forming coefficient based on strain

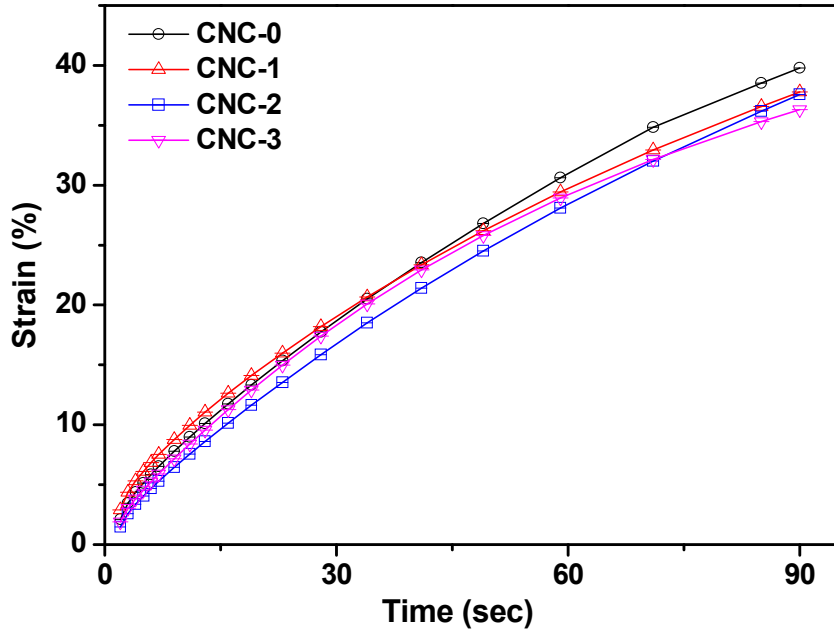


Figure 3-7. Strain of PE/OMMT nanocomposites coatings by the creep test.

### 3.7. Water uptake

One of the important roles of coating is to block the environmental factors such as water and oxygen. Coating capacitance has been represented water uptake of coatings and it is measured by alternating current impedance method of electrochemical impedance spectroscopy (EIS). When water is penetrating the coating, the value of coating capacitance is started. The value of water uptake of coating is calculated from Brasher-Kingsbury equation (Bagherzadeh *et al.*, 2007).

The water uptake behavior of PE/OMMT nanocomposites coatings are shown in Figure 3-8. The coating thickness of PE/OMMT nanocomposites coatings are 20  $\mu\text{m}$ . The water uptake of PE/OMMT nanocomposites coatings were rapidly increased for 10 min and then were gradually increased. They were reached equilibrium state after 1 h. The value of water uptake is in order : CNC-0 > CNC-1 > CNC-2 > CNC-3. Compared to CNC-0 and CNC-3 the value of water uptake of CNC-3 was less than 2 vol % and CNC-0 was almost 4 vol %. It means that nano-sized layered silicate of organoclay is dispersed homogeneously into the polyester matrix and can make longer pathways of water molecules to pass through the network of PE/OMMT nanocomposites coatings.

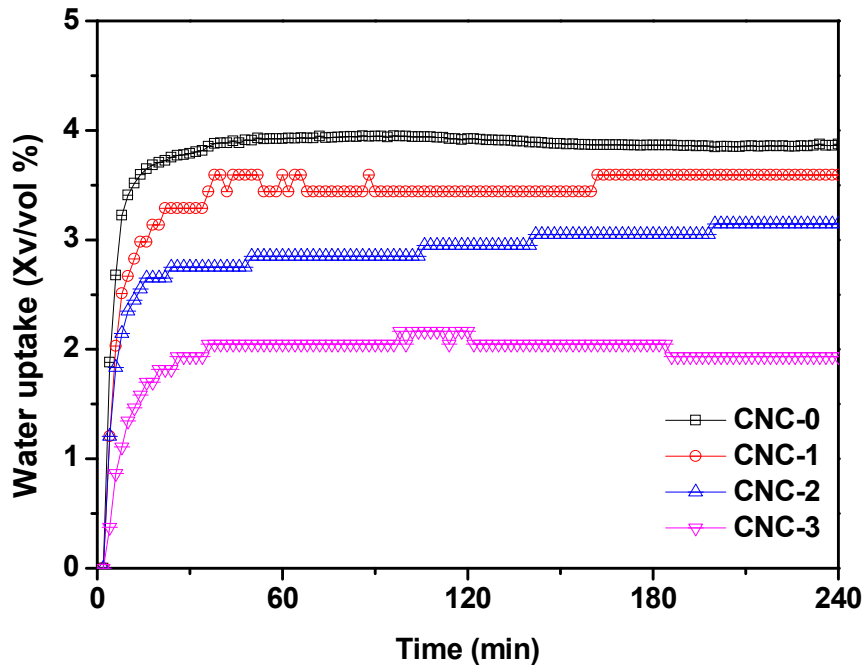
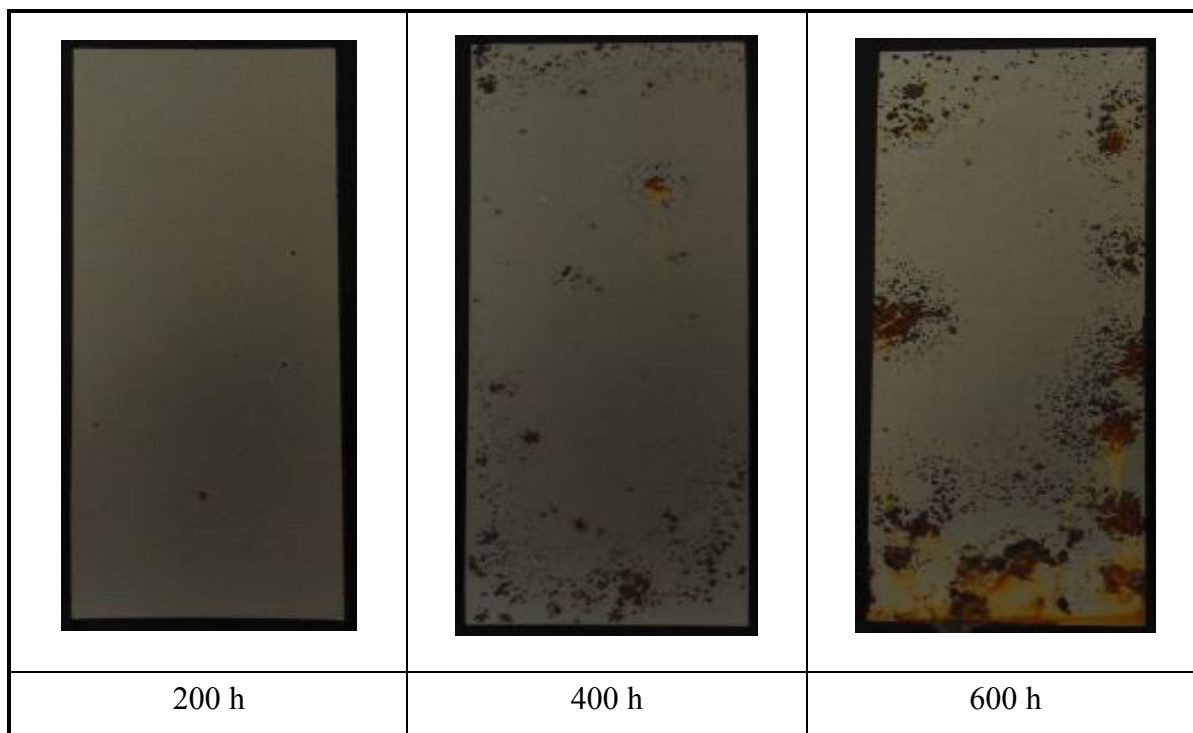


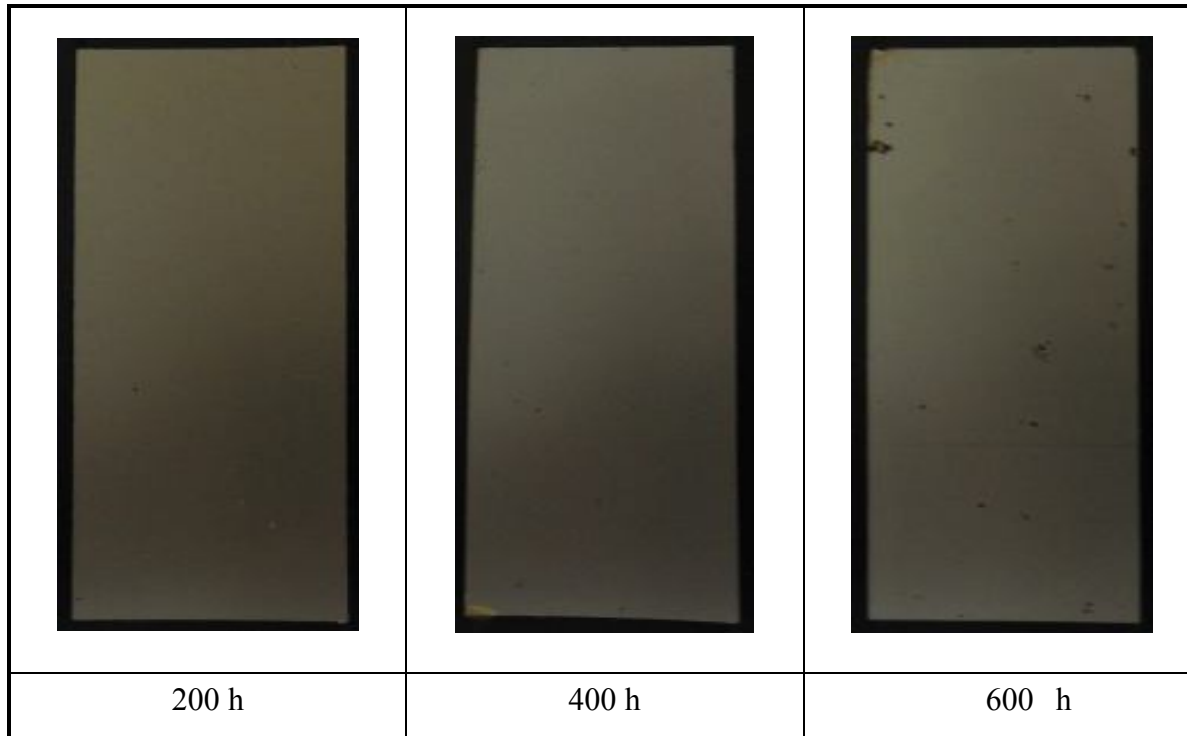
Figure 3-8. Water uptake (vol %) of PE/OMMT nanocomposites coatings by the capacitance method under the immersion.

### **3.8. Anti-corrosion property**

The anti-corrosion property is one of the physical properties of pre-coated metals. PE/OMMT nanocomposites coatings were tested via salt spray for 600 h. As shown in Figure 3-9, CNC-0 significantly increased red rust and blistering on the surface with increasing salt spray testing time. It has lots damaged areas after 400 h salt spray test. However, CNC-3 had little rust on the surface with increasing salt spray testing time. It has small damaged areas after 600 h salt spray test. Those results agree with water uptake test. The value of water uptake of CNC-3 was less than 2 vol %, but CNC-0 was almost 4 vol %. It implies that nano-sized layered silicate of organoclay effectively increases the length of the diffusion pathways environmental factors such as water and oxygen. And it also means that nano-sized layered silicate of organoclay might be decreased permeability and can make higher corrosion resistance of coatings.



**(a) CNC-0**



**(b) CNC-3**

Figure 3-9. Corrosion resistance of PE/OMMT nanocomposites coatings by salt spray test for 600 h (a) CNC-0 and (b) CNC-3.

#### 4. Conclusions

Four types of PE/OMMT nanocomposites coating were synthesized by the in-situ polymerization with high speed homogenizer process at the various contents of organoclay to disperse into the polyester matrix. The absence of reflection pattern of organoclay by SAXS and TEM study revealed that exfoliated organoclay layers are well dispersed into the polymer chain. Mechanical property of PE/OMMT nanocomposites coatings improved 9 % of the maximum tensile strength. The viscoelastic behavior of PE/OMMT nanocomposites coatings was observed by dynamic mechanical analysis (DMA). When the content of organoclay was increased, the storage modulus of the PE/OMMT nanocomposites coatings increased considerably and  $T_g$  of each cured coatings shifted to a lower temperature.

Anti-corrosion property was examined by the salt spray test. CNC-3 had the highest amount of organoclay and it had little rust after 600 h. It implies that nano-sized layered silicate of organoclay effectively increases the length of the diffusion pathways water molecules. And nano-sized layered silicate of organoclay might be decreased the permeability and can make higher corrosion resistance of PE/OMMT nanocomposites coatings. From those results, CNC-3 which had 3 wt % of organoclay had good formability in the deep drawing and also had good anti-corrosion property. So, CNC-3 would be an appropriate PE/OMMT nanocomposites coatings as a primer for automotive pre-coated metals.

## **Chapter 4**

### **Synthesis and Characterization of Containing Cyclic Structure Contained Polyester Resin as a Basecoat for Automotive Pre-coated Metals**

## 1. Introduction

Stringent environmental legislations have been made around the world. These legislations also affect manufacturing sectors that employ coating processes. Pre-painted or coil-coated metals (PCM) provide an opportunity to eliminate coating processes (Jandel, 2005). Pre-painted or coil-coated metals (PCM) have been used in many applications, such as household electric appliances, building materials and others. In this system, the wet coating process can be eliminated by using a roll coating process, making it possible to circumvent the problem of air pollution arising from evaporation. One of the most important properties of PCM is formability. If the film on the coated PCM parts is damaged, the products are rendered useless (Moon *et al.*, 2012). Polyester resins crosslinked with melamine resins or isocyanates are widely used to improve resistance to abrasion and scratching.

The stone-chip resistance of automotive coatings is considered to be one of the important characteristics during service (Lonyuk *et al.*, 2008). Bendor has reported the stone-chip resistance and mechanical properties of polymer coating, and found that the glass transition temperature of the primer coating is the key factor in stone-chip resistance (Bendor *et al.*, 1971). The chip resistance has been decreased by increasing the glass transition temperature, such as by increasing the baking temperature, and decreasing the oil length..

A cycloaliphatic structure, such as 1,3-cyclohexanedicarboxylic acid (1,3-CHDA), or 1,4-cyclohexanedicarboxylic acid (1,4-CHDA), gives physical properties that are intermediate between aromatic and linear

aliphatic (Johnson *et al.*, 1993). The  $T_g$  of cycloaliphatic polyester is lower than that of aromatic polyester, but is higher than that of linear aliphatic polyester. The flexibility of cycloaliphatic polyester is also intermediate between the aromatic and linear aliphatic polyesters due to the cyclic structure, which can absorb energy through the interconversion of chair and boat conformations. When cross-linked with melamine–formaldehyde, 1,4-CHDA based polyesters provided better humidity and impact resistance (Li *et al.*, 2002).

In this study, we designed an improvement of the elasticity of coatings using 1,4-CHDA, which can give lower  $T_g$  and higher flexibility to polyester coatings, compared to isophthalic acid, because 1,4-CHDA has a cyclic structure consisting of a  $\text{CH}_2\text{-CH}_2$  component. Cyclic structure of 1,4-CHDA has better elasticity than the linear structure of adipic acid. Cyclic structure contained polyester resins were synthesized with different contents of 1,4-CHDA. The elongation, tensile strength and viscoelastic properties of synthesized resins of free-coated film were measured. The formability of PCMs was evaluated using a cylindrical drawing test. The stresses and strains of the coatings were calculated from the deep drawing results. Also, the relationship between the contents of 1,4-CHDA and the formability of the polyester coatings was discussed. Stone-resistance tests were measured, to assess their potential as a basecoat for automotive coatings.

## **2. Experimental**

### **2.1. Materials**

The polybasic acids used were 1,4-cyclohexanedicarboxylic acid (1,4-CHDA, Tokyo Chemical Industry, Japan), adipic acid (AA, Samchun Pure Chemical, Republic of Korea), and isophthalic acid (IPA, Junsei Chemical Corp., Japan), and the polybasic alcohols that were used were trimethylol propane (TMP, Tokyo Chemical Industry, Japan), 2,2,4-trimethyl-1,3-pentanediol (TMPD, Tokyo Chemical Industry, Japan), 1,6-hexandiol (1,6-HD, Samchun Pure Chemical, Republic of Korea), neopentyl glycol mono(hydroxypivalate) (HPHP, Tokyo Chemical Industry, Japan), and polycarbonate diol (PCDL,  $M_n = 500$ , Asahi Kasei Chemicals Corp., Japan), which were used without further purification. Butylstannoic acid (FASCAT 4100, Arkema Inc., USA) was used as a catalyst to catalyze polymerization, and to prevent a transesterification reaction during the polymerization (Hamada *et al.*, 1997).

Hexamethoxy-methylmelamine (HMMM, Cytec Industries Inc., USA) was used as the curing agent, and blocked acid catalyst (NACURE 1953, King Industries, Inc., USA) was used.

### **2.2. Synthesis of cyclic structure contained polyester resin**

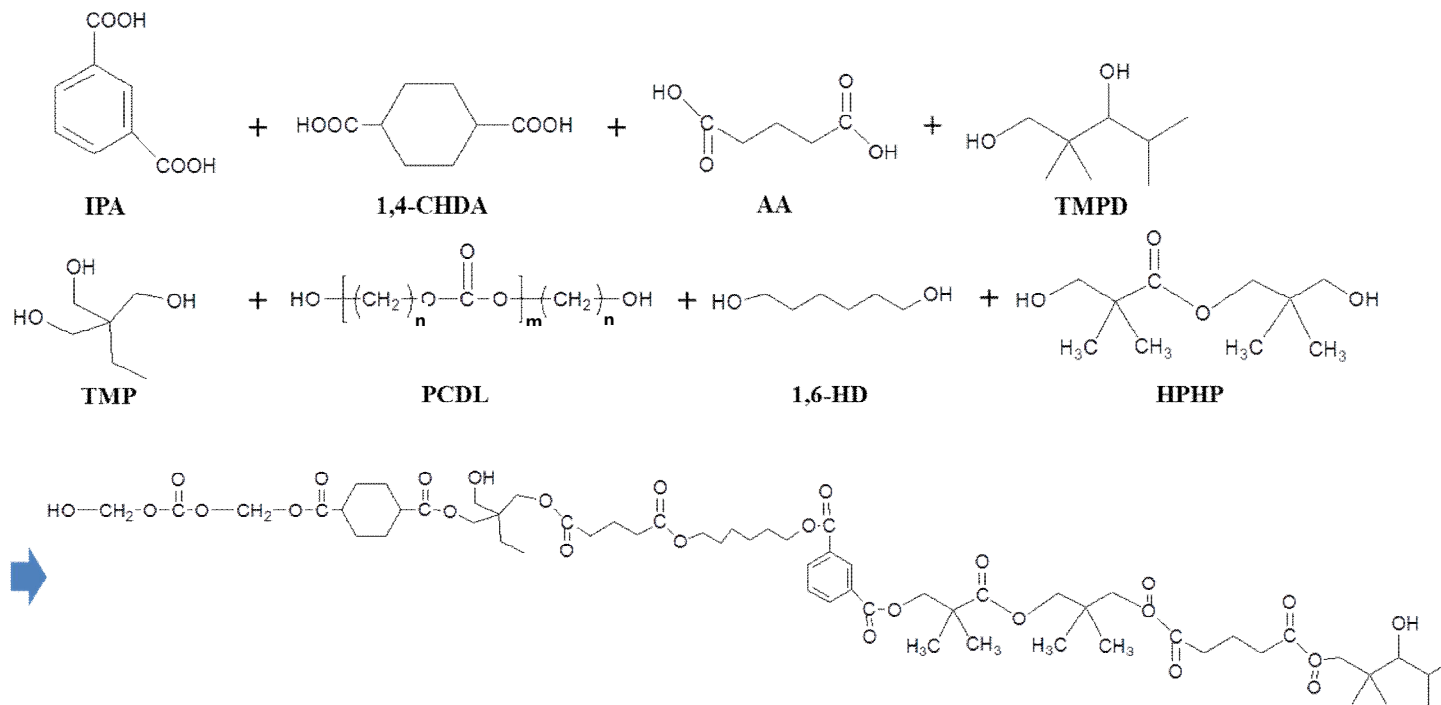
The synthesized scheme of cyclic structure contained polyester resin with 1,4-CHDA is shown in scheme 4-1 and the formulations are listed in Table 4-1. Polyester was synthesized from polybasic alcohols and polybasic acids with the following procedure, which consisted of two

synthetic processes. One was the fusion process, and the other was the solvent process. Synthesis equipments were same in chapter 2.

Isophthalic acid has two carboxyl groups, one of which reacts at around 190 °C, and the second one reacts at a temperature above 210 °C. It therefore requires a high reaction temperature. Polycarbonate diol could be decomposed around 210 °C. To avoid decomposition of polycarbonate diol, a modified synthesis process was carried out as follows.

Firstly, IPA, TMP, 1,6-HD, and HPHP were charged into a dried reactor, and the reaction temperature was set to 150 °C, with stirring for 2 h under N<sub>2</sub> purge. Subsequently, the reaction temperature was increased from 150 °C to 210 °C, at the rate of 0.5 °C/min. During the fusion process, all raw materials were melted, and the condensed water was collected. After that 1,4-CHDA, AA, and PCDL were charged into the reactor containing melt prepared from the preceding step, and the reaction temperature was set to 130 °C, with stirring for 2 h under N<sub>2</sub> purge. Subsequently, the reaction temperature was increased from 130 °C to 190 °C, at the rate of 0.3 °C/min. The reaction temperature was maintained for several hours, to collect condensed water.

The fusion process was converted into solvent process by adding xylene. The fusion process of synthesis was same in chapter 2.



Scheme 4-1. Synthesis scheme of cyclic structure contained polyester resin with 1,4-CHDA.

Table 4-1. Formulations used for synthesis of cyclic structure contained polyester resin.

(unit : mole of monomer)

Contents	CHDA-0	CHDA-5	CHDA-10	CHDA-20
Trimethylol propane	3	3	3	3
2,2,4-trimethyl-1,3-pentanediol	5	5	5	5
Polycarbonate diol	1	1	1	1
1,6-hexandiol	5	5	5	5
Neopentyl glycol mono (hydroxypivalate)	10	10	10	10
1,4-cyclohexanedicarboxylic acid	0	5	10	20
Isophthalic acid	20	15	10	0
Adipic acid	3	3	3	3

### **2.3. Preparation of cyclic structure contained polyester coatings**

Synthesized cyclic structure contained polyester resin was mixed with HMMM, additives, and solvents. Four different formulations were prepared, as listed in Table 4-2.

Free film: Preparing free films was same in chapter 2. The resulting films became the samples for tensile strength and dynamic mechanical analysis.

PCM: Cold roll steel sheets (thickness of 0.8 mm) were coated with primer, and baked at 180 °C for 10 min. The cured primer films were 15  $\mu\text{m}$  in thickness (white pigmented in CNC-3 in chapter 3). Then cyclic structure contained polyester coatings were coated on the cured primer, and then baked at 180 °C for 20 min. The thickness of those cured films was 25  $\mu\text{m}$ . The total film thickness was 40  $\mu\text{m}$ .

Table 4-2. Formulations of cyclic structure contained polyester resin as a basecoat.

(unit : wt %)

Contents	BCHDA-0	BCHDA-5	BCHDA-10	BCHDA-20
* CHDA-0	65.5	-		-
* CHDA-5	-	65.5		-
* CHDA-10	-	-	65.5	-
* CHDA-20	-	-		65.5
** Solvent	20.0	20.0	20.1	20.1
Black pigment	7.5	7.5	7.5	7.5
HMMM	5.4	5.4	5.3	5.3
Additives	1.0	1.0	1.0	1.0
Nacure	0.6	0.6	0.5	0.5

\* Solid content of polyester resin : 75 %

\*\* Solvent : solvesso #100

## 2.4. Characterization

### 2.4.1. Fourier transform infrared spectroscopy (*FT-IR*)

Infrared spectra were obtained using a JASCO FT/IR-6100 (Jasco, Japan) spectrometer that is equipped with a Miracle accessory, and attenuated total reflectance (ATR) setup. The measurement conditions were same in chapter 2.

### 2.4.2. Gel permeation chromatography (*GPC*)

The molecular weight and polydispersity of the synthesized silicone-modified polyester resins were measured using a YL9100 GPC SYSTEM (Young Lin, Republic of Korea) apparatus, consisting of a pump and a RI detector. The measurement conditions were same in chapter 2.

### 2.4.3. Dynamic mechanical analysis (*DMA*)

The glass transition temperature and viscoelastic properties of the polyester/melamine heat-cured films were analyzed using a dynamic mechanical analysis (Q800, TA Instruments). The crosslink density ( $\nu_c$ ) was derived from a following equation (Hill 1997; Stroisznigg *et al.*, 2009):

$$\nu_c = \frac{E'_{\min}}{3RT_{E'_{\min}}}$$

Rectangular specimens with 20 mm in length, 6.45 mm in width and 200  $\mu\text{m}$  in thickness were used for the test. The test conditions were same in chapter 2.

#### **2.4.4. Creep strain properties**

The creep strain of the free-coated films were performed using a dynamic mechanical analysis (Q800, TA Instruments). Rectangular specimens of 20 mm in length, 6.45 mm in width and 200  $\mu\text{m}$  in thickness were used for the test. The time-dependences of creep compliance of the free-coated films were obtained at a stress level of  $5.1 \times 10^6$  Pa. The tests were performed at 25 °C, and with a loading time of 90 s, which was designed to correspond to the deep drawing testing time.

#### **2.4.5. Tensile properties**

Tensile properties was measured using a Universal Testing Machine (Zwick Corp.) at a crosshead speed of 20 mm/min, which was designed to correspond to the deep drawing testing speed at an ambient temperature. The tensile specimens prepared from free-coated films were 40 mm in length (span length), 6.45 mm in width and 200  $\mu\text{m}$  in thickness. The test conditions were same in chapter 2.

#### **2.4.6. Deep drawing**

A cylindrical deep drawing test was performed to examine formability of the heat-cured coatings as shown Figure 2-1 and 2-2 in chapter 2. The shape of PCM before deep drawing was a disk of 105 mm diameter. The shape of the punch was a circle of 40 mm diameter, and the shoulder radius of the punch and the corner radius of the punch were 5 mm. Specific conditions of the deep drawing are shown in Table 2-3 in chapter 2.

#### **2.4.7. Chipping resistance test**

The Gravelometer is designed to evaluate the resistance of surface coatings (paint, clear coats, metallic plating, etc.) to chipping, caused by the impacts of gravel or other flying objects. The primary usage of this test is to simulate the effects of the impact of gravel or other debris on automotive parts.

A chipping resistance test is proposed to evaluate surface damages by stones, sands and NaCl salts. Before the chipping resistance test, specimens were set at  $-20 \pm 3$  °C for 3 h in the cold chamber. The tested pressure was  $4 \pm 0.2$  kgf/cm<sup>2</sup>, and the chip stone is listed in Table 4-3. The specimens prepared from the cold roll steel sheet coated films were 150 mm in length, 100 mm in width and 40  $\mu$ m in thickness.

#### **2.4.8 Video image enhanced evaluation of weathering (VIEEW)**

After the chipping resistance test, the surface damages were evaluated by the VIEEW<sup>TM</sup> system. VIEEW<sup>TM</sup> is capable of capturing digital images of samples under various lighting schemes that are optimized to highlight and enhance surface defects, to digitally process images. It is also capable of measuring and counting defects with a comprehensive statistical profile. The measurements were same in chapter 2.

Table 4-3. Chip stone types of chipping resistance test.

Type	Standard	Range of particles (mm)	Remarks
Stone number #7	JIS A5001	2.5 ~ 5	Pass through sieve 13 mm and remaining sieve 2.5 mm

### 3. Results and Discussion

#### 3.1. Characterization of cyclic structure contained polyester resin

Cyclic structure contained polyester resins were synthesized based on different contents of 1,4-CHDA. The aromatic ring and cyclic ring in the synthesized polyester resin were determined using FT-IR. As shown in Figure 4-1, the aromatic ring of isophthalic acid was detected at 728 and 1286  $\text{cm}^{-1}$ , and the intensity of these bands decreased with increasing content of 1,4-CHDA. The cyclic ring of 1,4-CHDA was detected at 1036 and 1138  $\text{cm}^{-1}$ , and the intensity of these bands increased with increasing content of 1,4-CHDA (Zhang *et al.*, 2012; Wang *et al.*, 2006).

Table 4-4 lists the molecular weight and polydispersity of the synthesized cyclic structure contained polyester resin. The theoretical hydroxyl number of polyester resin ( $n_{\text{OH}}$ ) was little decreased with increasing content of 1,4-CHDA, because ( $n_{\text{OH}}$ ) is dependent on the molecular weight of synthesized resin. Also, the ratio between the number average molecular weight and hydroxyl number ( $M_n/n_{\text{OH}}$ ) indicates the length of the repeating unit in the crosslink network of the synthesized polyester resin (Stroisznigg *et al.*, 2009). The ratio of  $M_n/n_{\text{OH}}$  was observed to increase with increasing content of 1,4-CHDA, thus indicating decreasing crosslinking density.

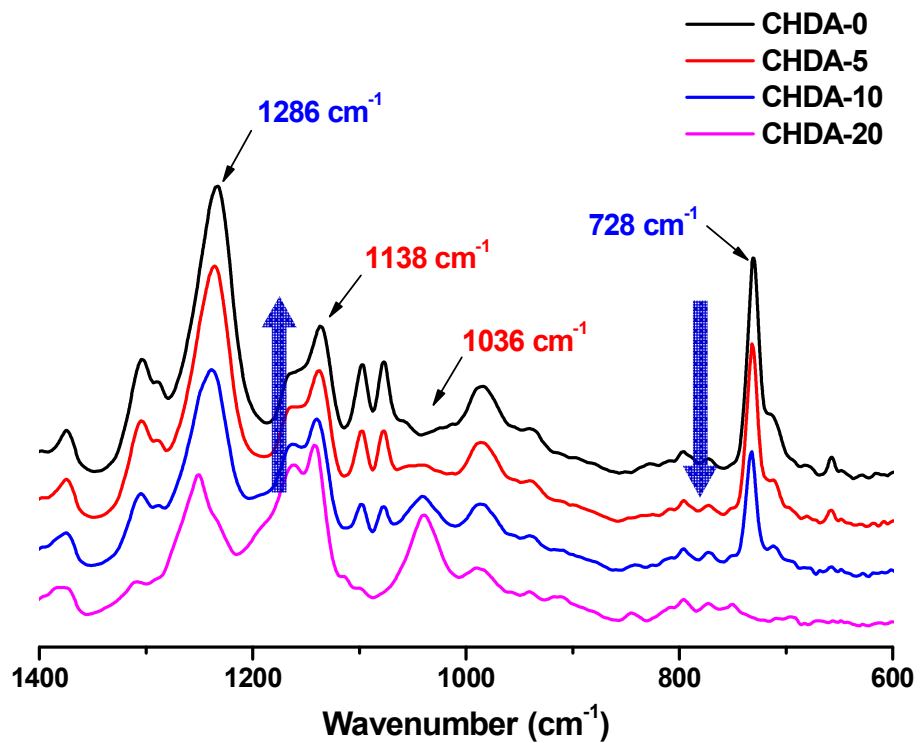


Figure 4-1. IR spectra of cyclic structure contained polyester resin with 1,4-cyclohexanedicarboxylic acid (aromatic ring : 728, 1286  $\text{cm}^{-1}$ , cyclic ring 1036, 1138  $\text{cm}^{-1}$ ).

Table 4-4. Characterization of cyclic structure contained polyester resin.

Property	CHDA-0	CHDA-5	CHDA-10	CHDA-20
Number average M.W. ( $M_n$ )	7,220	7,250	7,280	7,340
Polydispersity index ( $M_w/M_n$ )	2.9	3.1	3.3	2.8
* $n_{OH}$ (mg KOH/g)	38.8	38.6	38.5	38.1
$M_n/n_{OH}$ (g/mg KOH)	186	187	189	192
Crosslink density ( $10^{-3}$ mol/cm <sup>3</sup> )	0.47	0.35	0.25	0.16

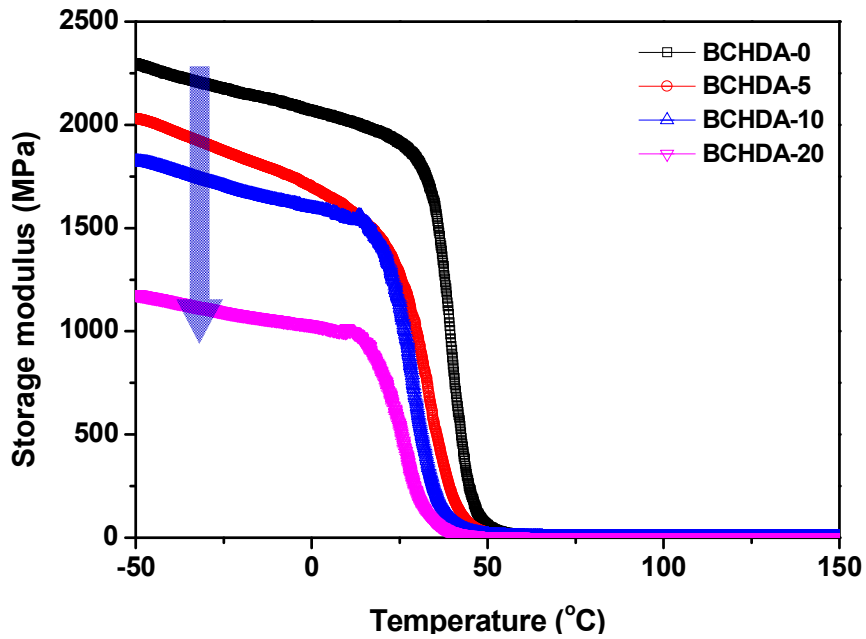
\*  $n_{OH}$  -Theoretical hydroxyl number of polyester resins

### 3.2. Viscoelastic behavior

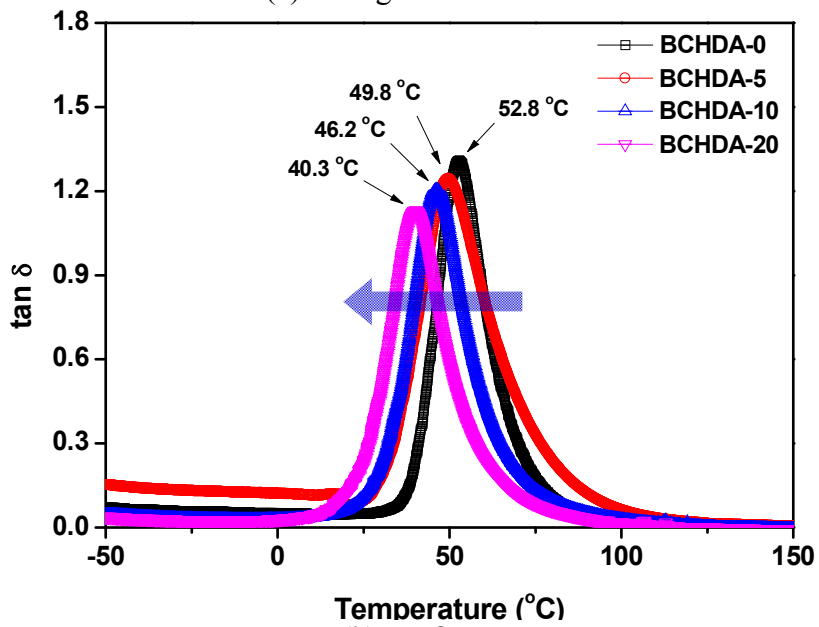
Dynamic mechanical analysis (DMA) is a convenient method to study thermal and mechanical viscoelastic properties of polymeric materials. The DMA data allow observations of changes in loss and storage modulus, glass transition temperature ( $T_g$ ), and crosslink density (Hou *et al.*, 2009).

Figure 4-2(a) shows the storage modulus as a function of temperature for synthesized polyester resins with 1,4-CHDA. The storage modulus decreased with increasing contents of 1,4-CHDA, i.e. BCHDA-0 > BCHDA-5 > BCHDA-10 > BCHDA-20. These results can be explained by the cyclic structure of 1,4-CHDA. Compared to isophthalic acid (IPA), the cyclic structure of 1,4-CHDA is more flexible than the conjugate structure of IPA, because 1,4-CHDA consists of only the  $\sigma$ -bond between  $\text{CH}_2$ - $\text{CH}_2$  components, and can be rotated and bent (Percec *et al.*, 199).

In addition, the storage modulus decreased with increase of the ratio between the number average molecular weight and hydroxyl number ( $M_n/n_{\text{OH}}$ ) (Stroisznnigg *et al.*, 2009). As listed in Table 4-4, a longer length between crosslinks corresponds to a lower crosslink density, thus explaining the lower modulus of the resin. Also, the  $T_g$  shifted to a lower temperature with increasing content of 1,4-CHDA, as shown in Figure 4-2(b) (Levine *et al.*, 2010). From the dynamic mechanical analysis, 1,4-CHDA could provide flexibility to the polyester coatings (Moon *et al.*, 2012).



(a) Storage modulus



(b) tan δ

Figure 4-2. Viscoelastic properties of cyclic structure contained polyester coatings (a) storage modulus and (b) tan δ. .

### 3.3. Flexibility

Flexibility is the most important property for the cutting, pressing and stamping processes in the pre-coated system. Tensile strength tests were carried out to study the basic mechanical properties of modulus, tensile strength, elongation at break, and toughness of polymeric materials (Levine *et al.*, 2010). Figure 4-3 presents the effects of the contents of 1,4-CHDA on tensile behaviors of the synthesized resins. The tensile strength decreased with increased content of 1,4-CHDA (BCHDA-0 > BCHDA-5 > BCHDA-10 > BCHDA-20). In contrast, the maximum strain increased when the content of 1,4-CHDA increased (BCHDA-0 < BCHDA-5 < BCHDA-10 < BCHDA-20).

The maximum stress of BCHDA-0 and BCHDA-5 was 25.8 MPa and 23.3 MPa, and the value of strain was 78 % and 100 %, respectively. However, in terms of elongation, the opposite trend to that of the stress appeared. Elongation of coatings generally increased with increasing content of 1,4-CHDA. In the case of BCHDA-10 and BCHDA-20, the maximum stress was 19.7 MPa and 12.9 MPa, and the value of strain was 123 % and 157 % respectively. These values could be explained by the cyclic structure between the ester linkages from the 1,4-CHDA. The cyclic structure of 1,4-CHDA was more flexible than the conjugate structure of IPA, because the cyclic structure consisted of only the  $\sigma$ -bond between CH<sub>2</sub>-CH<sub>2</sub> groups, and could be rotated and bent (Levine *et al.*, 2010). 1,4-CHDA could give the flexibility of a polymer network. Therefore it could be implied that 1,4-CHDA can give flexibility, and would provide lower stiffness to the polyester coatings (Li *et al.*, 2002).

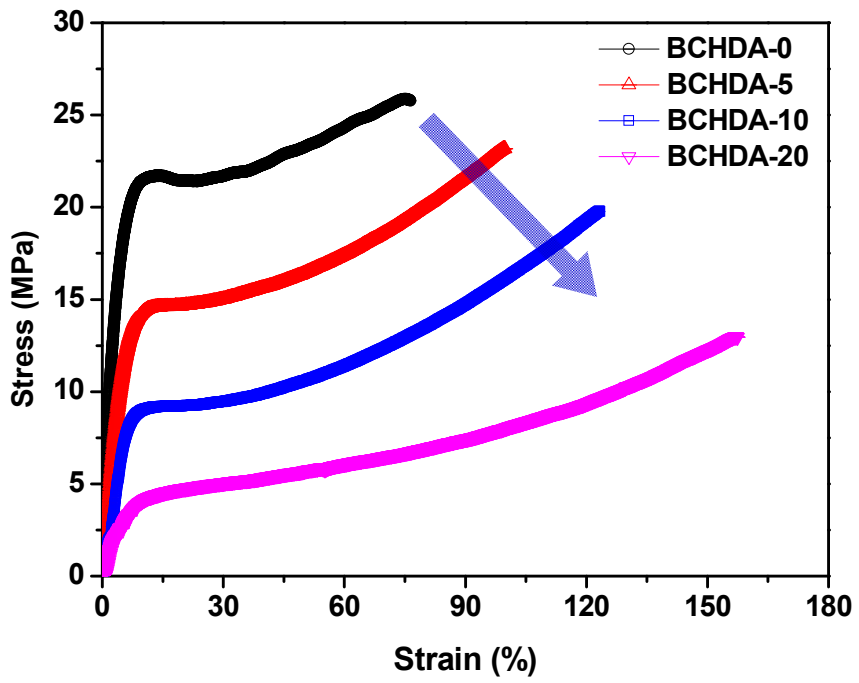


Figure 4-3. Stress-strain curve of cyclic structure contained polyester coatings.

### 3.4. Formability

The deep drawing test is a common method for determining formability in pre-coated metals. During the deep drawing test, which took 90 s to complete, the calculated stress was 5.1 MPa, and the strain on the PCM was 23.4 %.

Figure 4-4 shows the formability resulting from the deep drawing. The BCHDA-0 specimen had cracks and delamination, even though it exhibited a higher tensile strength value from the flexibility test. BCHDA-0 was not flexible enough to be stretched out during the deep drawing. The others exhibited good formability, because those specimens had sufficient tensile strength and elongation values, based on the flexibility test, and also had sufficient flexibility, based on the creep test, as shown in Figure 4-5. The developed strains of BCHDA-5, BCHDA-10 and BCHDA-20 were 23.6 %, 29.6 % and 43.2 %, respectively. In our previous study, formability could be predicted from the tensile test and creep test. A forming coefficient based on strain energy ( $F_U$ ) should be larger than 1, and a forming coefficient based on strain ( $F_\epsilon$ ) should be larger than 1 (Moon *et al.*, 2012).  $F_U$  and  $F_\epsilon$  were calculated, and are listed in Table 4-5. The  $F_U$  of BCHDA-0 was 0.71, and the  $F_\epsilon$  of BCHDA-0 was 0.79. So, BCHDA-0 was not flexible enough to stretch out during the deep drawing test. However, the  $F_U$  of BCHDA-5, BCHDA-10 and BCHDA-20 were larger than 1, and those of  $F_\epsilon$  were also larger than 1. So, those specimens can be stretched without being damaged during the deep drawing. Those results agreed with our previous study. The strain of polyester coatings should be larger than 23.4 % for 90 s, to have good formability. From the deep

drawing test, the cyclic structure of 1,4-CHDA of the CH<sub>2</sub>-CH<sub>2</sub> group could give the flexibility of polymer network, and could provide good formability.

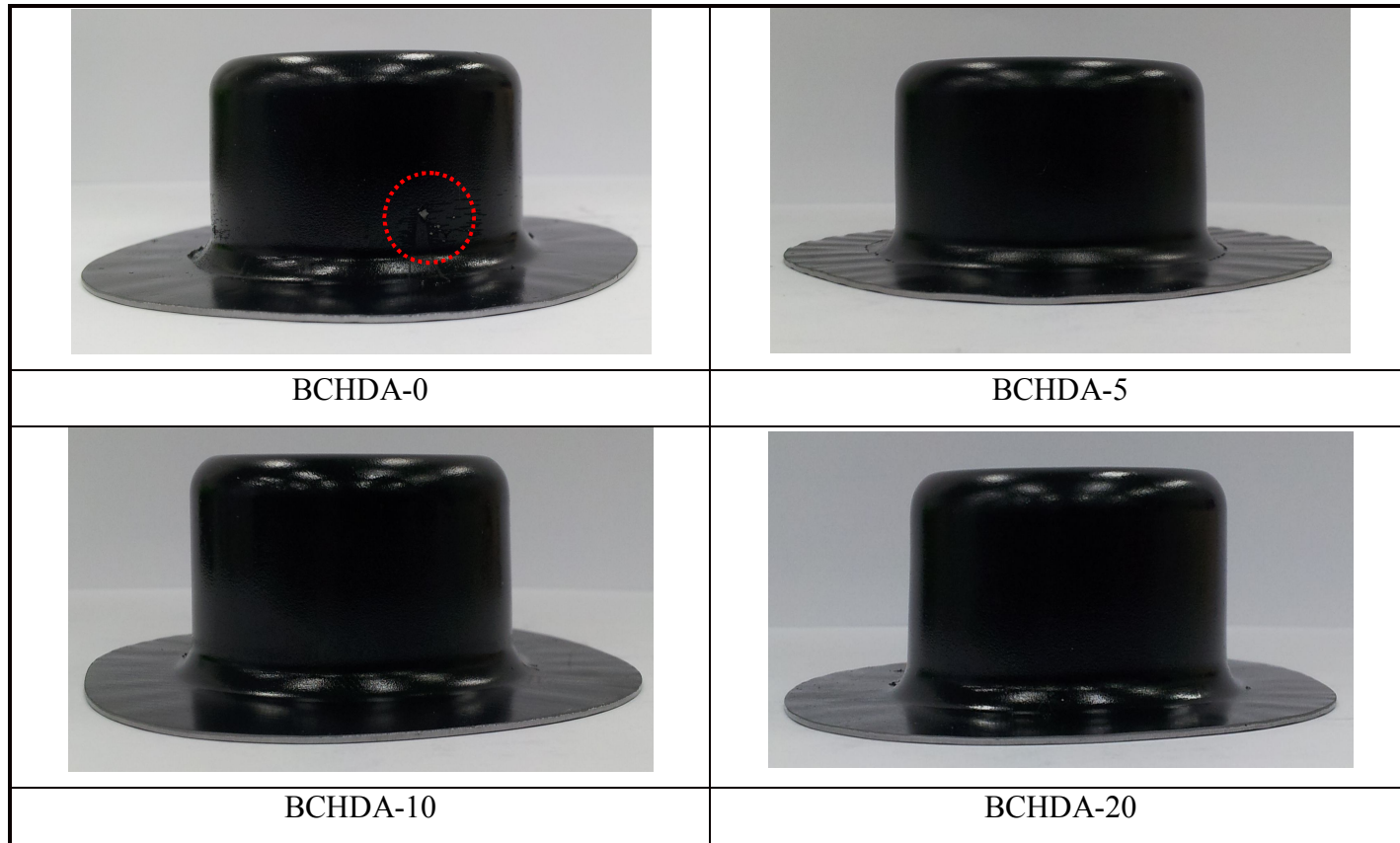


Figure 4-4. Formability of cyclic structure contained polyester coatings on the cold roll steel sheet.

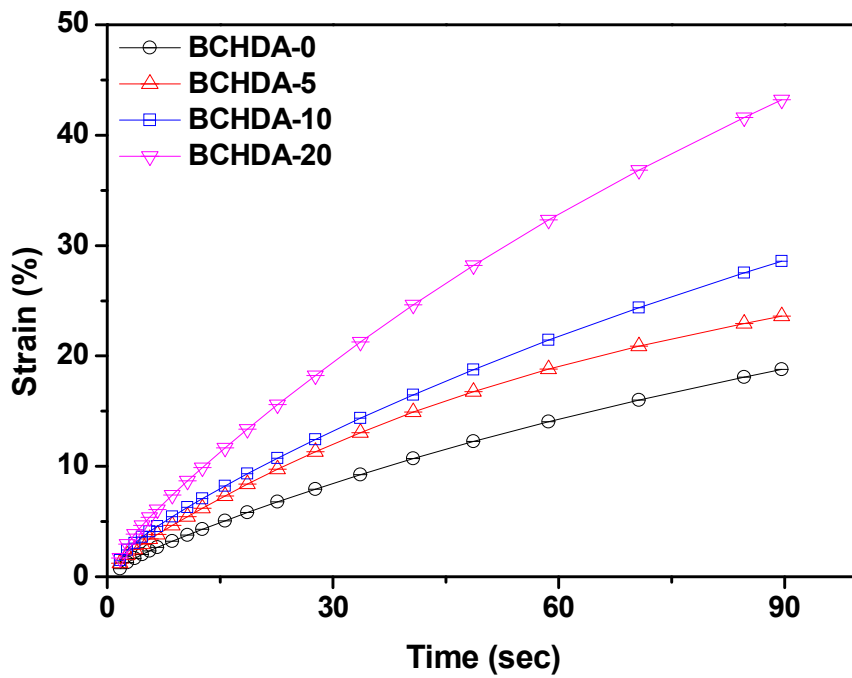


Figure 4-5. Strain of cyclic structure contained polyester coatings by the creep test.

Table 4-5. Calculated values from tensile test and creep test of cyclic structure contained polyester coatings (Moon *et al.*, 2012).

Sample	$U_T$	$U_C$	$F_U (U_C/U_T)$	$\varepsilon_C$ (%)	$F_\varepsilon (\varepsilon_C/R_f)$
BCHDA-0	205.7	145.7	0.71	18.5	0.79
BCHDA-5	183.6	190.1	1.03	23.6	1.08
BCHDA-10	152.5	220.2	1.44	29.6	1.27
BCHDA-20	100.1	242.5	2.42	43.2	1.85

$U_T$ : strain energy at 23.4% in tensile test

$U_C$ : strain energy of coating film in creep test

$F_U (U_C/U_T)$  : forming coefficient based on strain energy

$\varepsilon_C$ : strain at 5.1 MPa during the creep test

$F_\varepsilon (\varepsilon_C/R_f)$  : forming coefficient based on strain

### 3.5. Chipping resistance

Figure 4-6 shows the chipping resistance result as a function of the 1,4-CHDA content of synthesized polyester resins. With increasing 1,4-CHDA, synthesized polyester resins had increased cyclic structure in the polymer chain; and the cyclic structure affected a decrease in  $T_g$ , and increased flexibility. BCHDA-0 had 0 mol of 1,4-CHDA and 20 mol of IPA. It had the highest  $T_g$ , which meant that the heat-cured coating would be very hard. A chipping resistance test was carried out at  $4 \pm 0.2 \text{ kgf/cm}^2$  of pressure. Specimens were set to  $-20 \text{ }^\circ\text{C}$  for 3 h in a cold chamber, before the chipping resistance test. So, the polyester coating of BCHDA-0 could be easily damaged and removed by the stone chip. It had lots of removed areas, and large sized defects. However, by increasing the content of 1,4-CHDA, the removed areas were generally decreased. In the case of BCHDA-20, it had 20 mol of 1,4-CHDA and 0 mol of IPA. BCHDA-20 had the highest amount of 1,4-CHDA, so it had the highest amount of cyclic structure, which could give flexibility to the polymer chain of polyester. So, BCHDA-20 had little removed area and small sized defects. This means that the cyclic structure of 1,4-CHDA was more flexible than the conjugate structure of IPA.

Figure 4-7 shows the removed area (%) of specimens, which is calculated from the removed area by the tested area. The removed area was dramatically decreased. The removed area of BCHDA-0 was 3.70 %, but that of BCHDA-20 was 0.44 %.

From the chipping resistance test, the cyclic structure of 1,4-CHDA can give flexibility, and would provide lower stiffness than IPA to the

polyester coatings. It has better elasticity than aromatic structure, and can give better impact resistance.



Figure 4-6. Chipping resistance of cyclic structure contained polyester coatings on the cold roll steel (before test : -20 °C x 3 h).

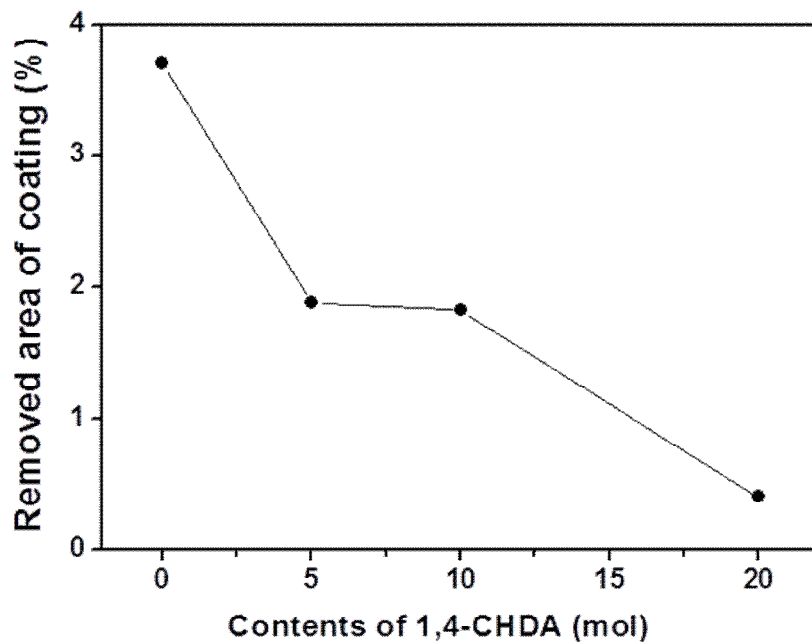


Figure 4-7. Calculated removed area of cyclic structure contained polyester coatings by the VIEEW.

#### 4. Conclusions

Four types of cyclic structure contained polyester resins with 1,4-CHDA were synthesized and formulated, to control formability for pre-coated metal systems. Those resins were designed to show the flexibility of the cyclic structure. The viscoelastic behavior, flexibility and formability were measured to determine the cyclic structure effect on the flexibility of the pre-coated metal system. When the content of cyclic structure of 1,4-CHDA was increased in the resins synthesized, the stiffness of the coatings generally decreased, and the  $T_g$  of each cured coatings shifted to a lower temperature. Therefore, 1,4-CHDA is a major factor in improving the flexibility and formability of polyester coatings. To ensure good formability of polyester coatings for the pre-coated metals, the tensile stress of the polyester coatings should be larger than 5.1 MPa, and the strain should stretch out by 23.4 % for 90 s.

The cyclic structure of 1,4-CHDA can give flexibility and would provide lower stiffness to the polyester coatings, and it has better elasticity than aromatic structure. So, it can give better chipping resistance. BCHDA-20 which had 20 mol of 1,4-CHDA had good formability in the deep drawing test, and also showed good chipping resistance in that test. So, BCHDA-20 would be appropriate coatings as a basecoat for automotive pre-coated metals.

## **Chapter 5**

### **Synthesis and Characterization of Silicone- modified Polyester as a topcoat for Automotive Pre-coated Metals**

## 1. Introduction

Pre-painted or coil-coated metals (PCM) have been used in many applications, such as household electric appliances, building materials and others. In this system, the wet coating process can be eliminated by using a roll coating process, making it possible to circumvent the problem of air pollution arising from evaporation. In addition, a pre-coated metal system offers other advantages, such as improved productivity and energy saving; thus the use of PCM has been spreading (Ueda *et al.*, 2001). One of the most important properties of PCM is its formability. If the film on coated PCM parts is damaged, the products are rendered useless (Moon *et al.*, 2012). Polyester resins crosslinked with melamine resins or isocyanates are widely used for improvement resistance to abrasion and scratching.

The interest in developing organic-inorganic hybrid coatings has been increasing, because of the unique properties obtained from combining inorganic and organic components into a single coating system. One approach is a sol-gel process, involving the hydrolysis and condensation reaction of metal alkoxydes (Frings *et al.*, 1998; Chen *et al.*, 2005). Sol-gel provides an easy, cost-effective and efficient way to incorporate inorganic components into an organic binder. The other is using nanoparticles dispersed in organic binder (Chen *et al.*, 2003; Zhou *et al.*, 2002). The incorporation of inorganic nanofillers in an organic coating is often reported. Organic-inorganic hybrid materials improve properties such as toughness, impact strength, tensile strength, and thermal stability (Chattopadhyay *et al.*, 2009)

In this study, we designed an organic-inorganic hybrid resin with a silicone intermediate. We synthesized a silicone-modified polyester resin between polyester resin and silicone intermediate, by methylool reaction between  $-OH$  and  $-CH_3$ . Silicone intermediate is an inorganic material, and branched polyester resin is organic material. Silicone modified polyester coatings are able to be used as a clearcoat for automotive coating. The surface free energy of the coating surface was calculated by the contact angle measurement. Also, the peel test was measured for the surface properties, and was used to determine any correlation with cleanable ability. The elongation, tensile strength and viscoelastic properties of synthesized resins of free-coated film were measured. The formability of PCMs was evaluated using a cylindrical drawing test. The stress and strain of the coatings were calculated from the deep drawing results. Finally, the relationship between the contents of silicone intermediate and the formability of the polyester coatings was discussed.

## 2. Experimental

### 2.1. Materials

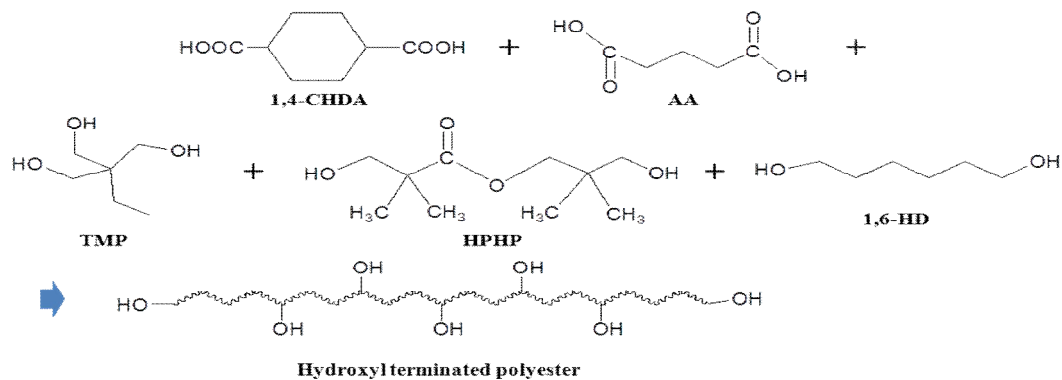
A silicone intermediate (DC 3037,  $M_n = 1,000$ , Dow Corning, USA) was prepared to control the flexibility of the main chain. 1,4-cyclohexanedicarboxylic acid (1,4-CHDA, Tokyo Chemical Industry, Japan), adipic acid (AA, Samchun Pure Chemical, Republic of Korea), trimethylol propane (TMP, Tokyo Chemical Industry, Japan), 1,6-hexandiol (1,6-HD, Samchun Pure Chemical, Republic of Korea), and neopentyl glycol mono(hydroxypivalate) (HPHP, Tokyo Chemical Industry, Japan) were used without further purification. Butylstannic acid (FASCAT 4100, Arkema Inc., USA) was used as a catalyst to catalyze polymerization, and to prevent a transesterification reaction during the polymerization (Hamada *et al.*, 1997).

Hexamethoxy-methylmelamine (HMMM, Cytec Industries Inc., USA) was used as the curing agent, and blocked acid catalyst (NACURE 1953, King Industries, Inc., USA) was used.

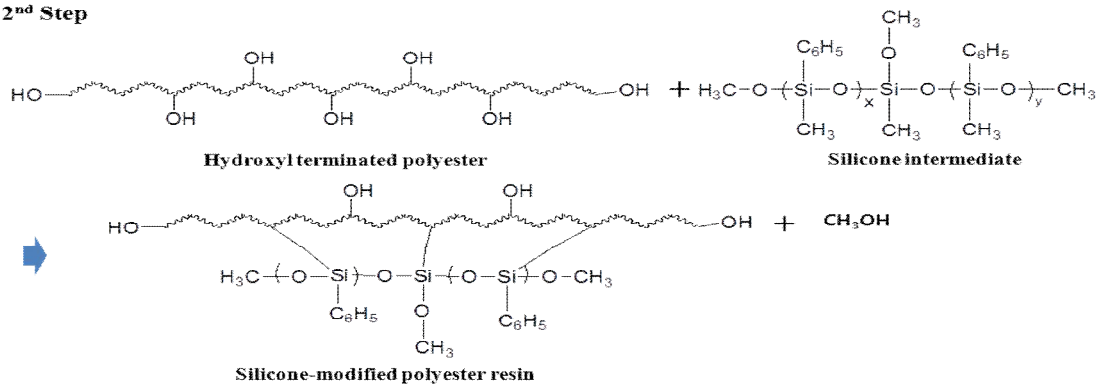
### 2.2. Synthesis of silicone-modified polyester resin

The synthesized scheme of silicone-modified polyester resin with silicone intermediate is shown in scheme 5-1 the formulations are listed in Table 5-1. Polyester was synthesized from polybasic alcohols and polybasic acids with the following procedure, which consisted of two synthetic processes. One was the fusion process, and the other was the solvent process. Synthesis equipments were same in chapter 2.

**1<sup>st</sup> Step**



**2<sup>nd</sup> Step**



Scheme 5-1. Synthesis scheme of silicone-modified polyester resin.

Table 5-1. Formulations used for synthesis of silicone-modified polyester resin.

(unit : mole of monomer)

Contents	SiPE-0	SiPE-1	SiPE-3	SiPE-5
Trimethylol propane	3	3	3	3
1,6-hexandiol	5	5	5	5
neopentyl glycol mono (hydroxypivalate)	8	8	8	8
1,4-cyclohexanedicarboxylic acid	13	13	13	13
Adipic acid	2	2	2	2
Silicone intermediate	0	0.1	0.3	0.5

The synthesis of polyester has two steps. The first step is to the synthesized base polyester resin remaining -OH group. 1,4-CHDA, AA, TMP, 1,6-HD, HPHP were charged into a dried reactor, and the reaction temperature was set to 150 °C with stirring for 2 h under N<sub>2</sub> purge. Subsequently, the reaction temperature was increased from 150 °C to 210 °C, at the rate of 0.5 °C/min. During the fusion process, all raw materials were melted, and the condensed water was collected. After finishing the fusion process, it was converted into solvent process, by adding xylene. The solvent process was carried out to collect condensed water, and to make a low acid value. The reaction temperature was set to 220 °C. During the solvent process, the acid value was measured by 0.1 N KOH. The reaction temperature was maintained for several hours, until the acid value was under 20 mg KOH/g resin (Hamada *et al.*, 1997).

The second step is a methylol reaction between the -OH group of polyester resin, and the -CH<sub>3</sub> of silicone intermediate, with catalyst. Silicone intermediated was charged into a synthesized polyester resin at a reactor, and the reaction temperature was set to 80 °C with stirring for 2 h under N<sub>2</sub> purge. Subsequently, the reaction temperature was increased from 80 °C to 160 °C, at the rate of 0.2 °C/min. During the methylol reaction, the by-product of methanol was collected by condenser. The reaction temperature was maintained for several hours to collect the methanol.

### **2.3. Preparation of silicone-modified polyester coatings**

Synthesized silicone-modified polyester resin was mixed with HMMM, additives, and solvents. Four different formulations were prepared, as listed in Table 5-2.

Free film: Preparing free films was same in chapter 2. The resulting films became the samples for tensile strength and dynamic mechanical analysis.

PCM: Cold roll steel sheets (thickness of 0.8 mm) were coated with primer, and baked at 180 °C for 10 min. The cured primer films were 15  $\mu\text{m}$  in thickness (white pigmented in CNC-3 in chapter 3). Then, basecoat was coated and baked at 180 °C for 10 min. The basecoat was BCHDA-20 in chapter 4. The cured basecoat films were 25  $\mu\text{m}$  in thickness. The silicone-modified polyester coatings as a topcoat were coated on the basecoat film, and then baked at 180 °C for 20 min. The thickness of the cured film was 25  $\mu\text{m}$ . The total film thickness was 65  $\mu\text{m}$ .

Table 5-2. Formulations of silicone-modified polyester coatings as a topcoat.

(unit : wt %)

Contents	CSiPE-0	CSiPE-1	CSiPE-3	CSiPE-5
SiPE-0 (70 %)	46.0	-		-
SiPE-1 (70 %)	-	46.8		-
SiPE-3 (50 %)	-	-	67.6	-
SiPE-5 (50 %)	-	-		69.5
* Solvent	21.5	21.4	2.1	1.1
TiO <sub>2</sub>	25.0	25.0	25.0	25.0
HMMM	5.9	5.3	4.2	3.1
Additives	1.0	1.0	1.0	1.0
Nacure	0.6	0.5	0.4	0.3

\*Solvent : solvesso #100

## 2.4. Characterization

### 2.4.1. Fourier transform infrared spectroscopy (FT-IR)

Infrared spectra were obtained using a JASCO FT/IR-6100 (Jasco, Japan) spectrometer, which is equipped with a Miracle accessory, and attenuated total reflectance (ATR) setup. The measurement conditions were same in chapter 2.

### 2.4.2. Gel permeation chromatography (GPC)

The molecular weight and polydispersity of the synthesized silicone-modified polyester resins were measured using a YL9100 GPC SYSTEM (Young Lin, Republic of Korea) apparatus, consisting of a pump and a RI detector. The measurement conditions were same in chapter 2.

### 2.4.3. Dynamic mechanical analysis (DMA)

The glass transition temperature and viscoelastic properties of the polyester/melamine heat-cured films were analyzed using a dynamic mechanical analysis (Q800, TA Instruments). The crosslink density ( $\nu_c$ ) was derived from a following equation (Hill 1997; Stroisznigg *et al.*, 2009):

$$\nu_c = \frac{E'_{\min}}{3RT_{E'_{\min}}}$$

Rectangular specimens with 20 mm in length, 6.45 mm in width and 200  $\mu\text{m}$  in thickness were used for the test. The test conditions were same in chapter 2.

#### **2.4.4. Creep strain properties**

The creep strain of the free-coated films was determined using a dynamic mechanical analysis (Q800, TA Instruments). Rectangular specimens with 20 mm in length, 6.45 mm in width and 200  $\mu\text{m}$  in thickness were used for the test. The time-dependence of creep strain of the free-coated films was obtained at a stress level of  $5.1 \times 10^6$  Pa. The measurement conditions were same in chapter 4.

#### **2.4.5. Tensile properties**

Tensile properties was measured using a Universal Testing Machine (Zwick Corp.) at a crosshead speed of 20 mm/min, which was designed to correspond to the deep drawing testing speed at an ambient temperature. The tensile specimens prepared from free-coated films were 40 mm in length (span length), 6.45 mm in width and 200  $\mu\text{m}$  in thickness. The measurement conditions were same in chapter 2.

#### **2.4.6. Deep drawing**

A cylindrical deep drawing test was performed to examine the formability of the heat-cured coatings, as shown in Figure 2-1 and 2-2 in chapter 2. The shape of the PCM before deep drawing was a disk, of diameter 105 mm. The shape of the punch was a circle of diameter 40 mm, and the shoulder radius of the punch and the corner radius of the punch were 5 mm. Specific conditions of the deep drawing are shown in Table 2-3 in chapter 2.

#### **2.4.7. Surface free energy**

The surface free energy of the heat-cured films was evaluated from

the static contact angles measured using a contact angle analyzer (SEO 300A, Surface & Electro-Optics Corp.). The temperature and relative humidity were  $23 \pm 2$  °C. The equilibrium contact angle is defined as the angle between the solid surface and a tangent drawn on the drop-surface, passing through the atmosphere-liquid-solid triple-point (Gindl *et al.*, 2001).

The surface free energy from contact angles was calculated based on Young's equation. In this study, the three liquids method was employed. This method was suggested by Good and van Oss, and has been widely used to examine the surface free energy of polymeric coating films. The test liquids used in this study were distilled water, formamide and diiodomethane. From these contact angles of the liquids, the surface free energy can be calculated using the following equations:

$$\begin{aligned}\gamma_{LV}(1 + \cos\theta_1) &= 2\sqrt{\gamma_S^{LW}\gamma_{LV1}^{LW}} + \sqrt{\gamma_S^+\gamma_{LV1}^-} + \sqrt{\gamma_S^-\gamma_{LV1}^+} \\ \gamma_{LV}(1 + \cos\theta_2) &= 2\sqrt{\gamma_S^{LW}\gamma_{LV2}^{LW}} + \sqrt{\gamma_S^+\gamma_{LV2}^-} + \sqrt{\gamma_S^-\gamma_{LV2}^+} \\ \gamma_{LV}(1 + \cos\theta_3) &= 2\sqrt{\gamma_S^{LW}\gamma_{LV3}^{LW}} + \sqrt{\gamma_S^+\gamma_{LV3}^-} + \sqrt{\gamma_S^-\gamma_{LV3}^+} \\ \gamma &= \gamma_S^{LW} + \gamma_S^{AB} = \gamma_S^{LW} + 2\sqrt{\gamma_S^+\gamma_S^-}\end{aligned}$$

where,  $LW$  is the Lifshitz-van der Waals force and  $AB$  is the acid-basic interaction, and  $\gamma$  is the surface free energy, acid-base interaction ( $\gamma^{AB}$ ).  $\gamma^+$  and  $\gamma^-$  are the Lewis acid parameter and the Lewis base parameter of the surface free energy, respectively (Lee *et al.*, 2002; Wang *et al.*, 2006; Geerken *et al.*, 2007)

#### **2.4.8. X-ray photoelectron spectroscopy (XPS)**

Chemical analysis was performed on the surface of cured coatings with an x-ray photoelectron spectroscopy (Sigma Probe, Thermo Scientific, U.S.A), equipped with spherical sector analyzer. The XPS spectra of the region corresponding to 0 - 700 eV. The signals of oxygen, carbon and silicone were observed at 530, 283 and 100 eV, respectively (Miao *et al.*, 2009).

#### **2.4.9. Measurement of cleanable characteristics using 180 ° peel test**

The cleanable characteristics of polymers were measured by using a contact angle measurement, which can be calculated from the surface free energy. According to these measurements, the surface free energy is decreased with fluorine or silicone derivatives. The peel test is a normal method to measure the adhesion of pressure sensitive adhesives (PSAs) when the coated film is removed from substrates. This method can be applied to determine the cleanable characteristics of silicone-modified coatings. The cleanable characteristics of silicone-modified coatings measured the adhesion between the coating surface and the PSAs. With decreasing surface free energy, the adhesion between different surfaces is decreased. The measurement of cleanable characteristics is illustrated in Figure 5-1 (Park *et al.*, 2008; Satas *et al.*, 2002).

SCOTCH No. 810 tape, which is a product of 3M, was prepared to evaluate the cleanable characteristic of coatings. Polyester coatings were coated on a stainless steel substrate, and cured at 150 °C for 30 min. After curing, a width of 18 mm PSA tape was attached to a coating

surface, and a 2 kg rubber roller was passed over it twice. The peel strength was measured using a Stable Micro Systems TA-XT2i Texture Analyzer (UK). The test was carried out at a speed of 300 mm/min at 20 °C, based on ASTM D 3330. The peel strength was recalculated from g/18mm to g/25mm (Park *et al.*, 2008; Satas *et al.*, 2002; Moon *et al.*, 2012).

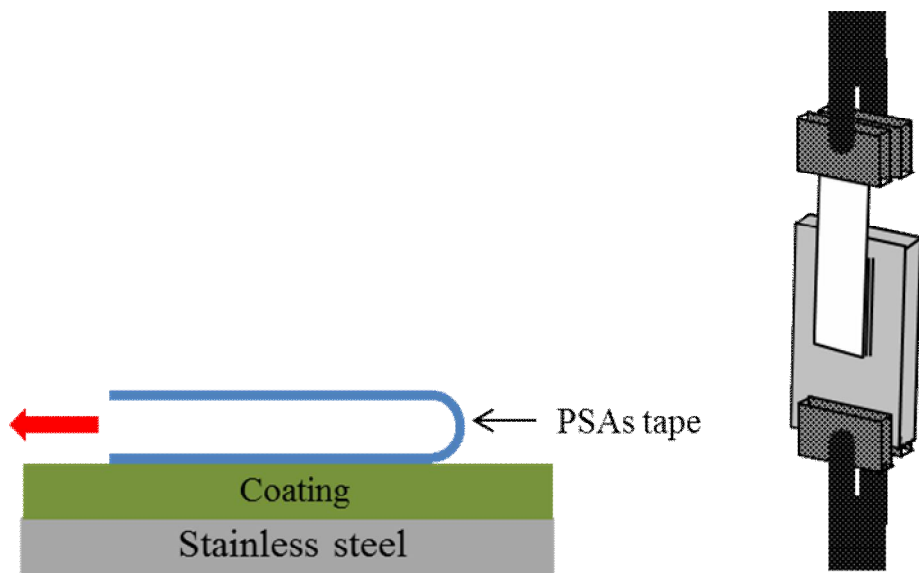


Figure 5-1. Measurement of cleanable characteristics using 180° peel test (Moon *et al.*, 2012).

### 3. Results and Discussion

#### 3.1. Characterizations of silicone-modified polyester resin

Silicone-modified polyester resins were synthesized based on different contents of silicone intermediate. The Si-O and Si-O-Si groups in the synthesized polyester resin were determined using FT-IR. As shown in Figure 5-2, the Si-O and Si-O-Si group that was from silicone intermediate was detected at 800 and 1083  $\text{cm}^{-1}$ , respectively, and the intensity of these bands increased with increasing content of silicone intermediate (Tian *et al.*, 2010).

Table 5-3 lists the molecular weight and polydispersity of the synthesized silicone-modified polyester resin. The theoretical hydroxyl number of polyester resin ( $n_{\text{OH}}$ ) decreased with increasing content of silicone intermediate, because ( $n_{\text{OH}}$ ) is dependent on the molecular weight of synthesized resin. Also, the ratio between the number average molecular weight and hydroxyl number ( $M_n/n_{\text{OH}}$ ) indicates the length of the repeating unit in the crosslink network of the synthesized polyester resin (Stroisznigg *et al.*, 2009). The value of  $M_n/n_{\text{OH}}$  was observed to increase with increasing content of silicone intermediate, and to indicate decreasing crosslinking density.

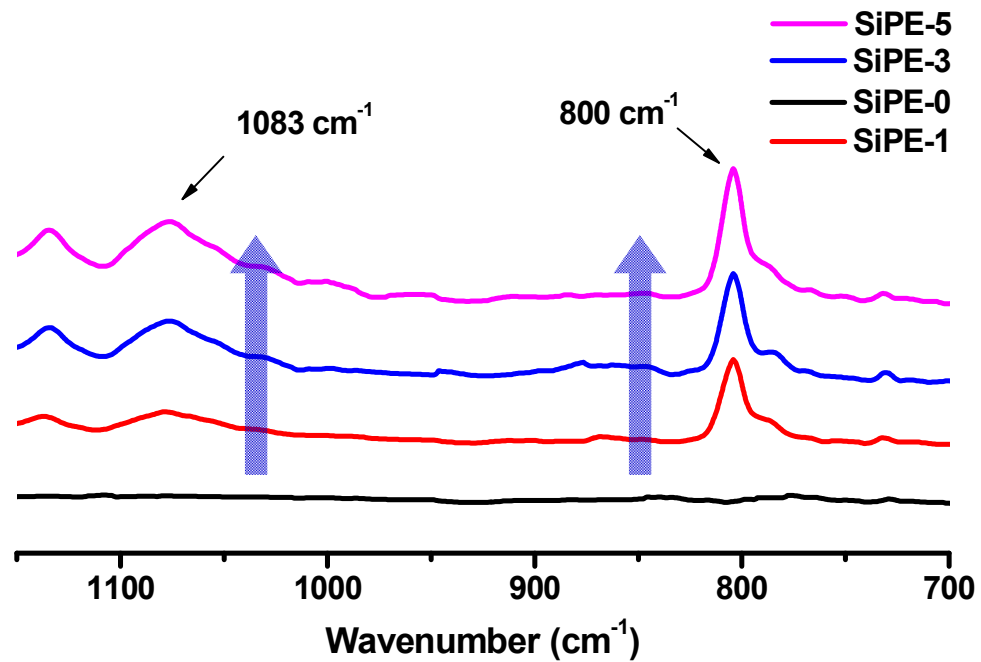


Figure 5-2. IR spectra of silicon-modified polyester resin (Si-O-Si :  $800 \text{ cm}^{-1}$ , Si-O :  $1083 \text{ cm}^{-1}$ ).

Table 5-3. Characterization of silicone-modified polyester resin.

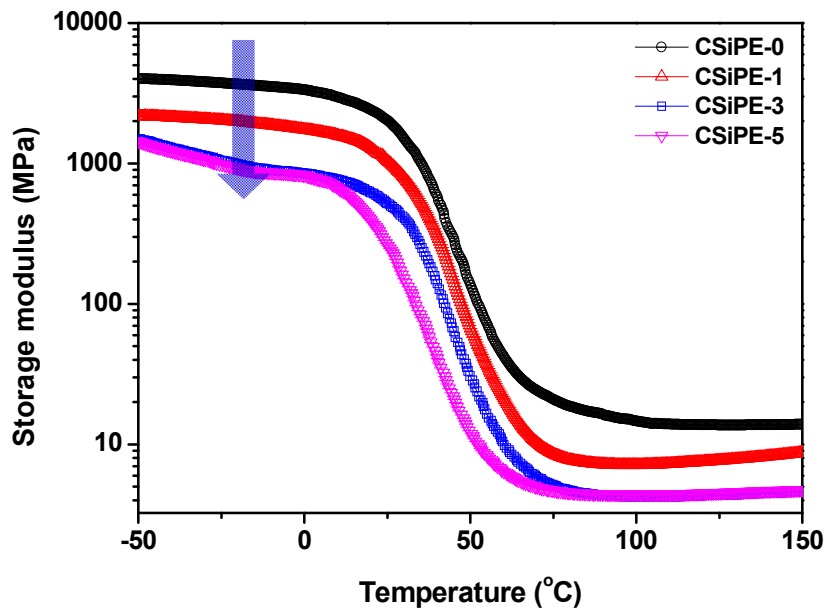
Property	SiPE-0	SiPE-1	SiPE-3	SiPE-5
Number average M. W. ( $M_n$ )	4,570	4,650	4,820	5,000
Polydispersity index ( $M_w/M_n$ )	2.9	3.4	3.3	3.2
* $n_{OH}$ (mg KOH/g)	61.4	54.3	40.8	30.4
$M_n/n_{OH}$ (g/mg KOH)	74	86	118	164
Crosslink density ( $10^{-3}$ mol/cm <sup>3</sup> )	1.38	1.02	0.69	0.47

\*  $n_{OH}$  -Theoretical hydroxyl number of polyester resins

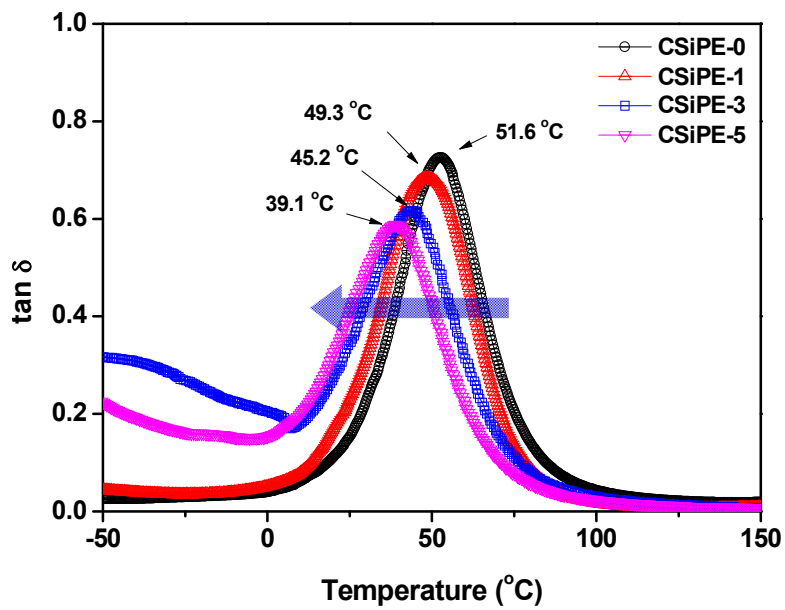
### 3.2. Viscoelastic behavior

Dynamic mechanical analysis (DMA) is a convenient method to study thermal and mechanical viscoelastic properties of polymeric materials. The DMA data allow observations of changes in loss and storage modulus, glass transition temperature ( $T_g$ ), and crosslink density (Hou *et al.*, 2005).

Figure 5-3(a) shows the storage modulus as a function of temperature for synthesized polyester coatings with different contents of silicone intermediate. The storage modulus of polyester coatings decreased with increasing contents of silicone intermediate, i.e. SiPE-0 > SiPE-1 > SiPE-3 > SiPE-5. Silicone intermediate has a long chain; it is generally recognized that the mobility and flexibility of polymer chain increases with the length of the linear chain segment (Moon *et al.*, 2012). In addition, the storage modulus decreased with the increase of the ratio between the number average molecular weight and hydroxyl number ( $M_n/n_{OH}$ ) (Stroisznnig *et al.*, 2009). As listed in Table 5-3, a longer length between crosslinks corresponds to a lower crosslink density, thus explaining the lower modulus of the resin. Also, the  $T_g$  shifted to a lower temperature with increasing content of silicone intermediate, as shown in Figure 5-3(b) (Hou *et al.*, 2009). From the dynamic mechanical analysis, silicone intermediate would provide lower stiffness and higher softness to the polyester coatings.



(a) Storage modulus



(b)  $\tan \delta$

Figure 5-3. Viscoelastic properties of silicone-modified polyester coatings (a) storage modulus and (b)  $\tan \delta$ .

### 3.3. Flexibility

Flexibility is the most important property for the cutting, pressing and stamping processes in the pre-coated system. Tensile strength tests were carried out to study basic mechanical properties - modulus, tensile strength, elongation at break, and toughness of polymeric materials (Levine *et al.*, 2010). Figure 5-4 presents the effects of the contents of silicone intermediate on the tensile behaviors of the synthesized resins. The tensile strength decreased with increasing content of silicone intermediate (CSiPE-0 > CSiPE-1 > CSiPE-3 > CSiPE-5). In contrast, the maximum strain increased when the content of silicone intermediate was higher (CSiPE-0 < CSiPE-1 < CSiPE-3 < CSiPE-5).

The maximum stress of CSiPE-0 and CSiPE-1 was 32.2 MPa and 24.8 MPa, and the value of the strain was 91 % and 109 %, respectively. However, in terms of elongation, the opposite trend to that of the stress appeared. The elongation of polyester coatings increased sharply with increasing content of silicone intermediate. In the case of CSiPE-3 and CSiPE-5, the strain value was over 150 %, and the stress was 12.2 MPa and 6.1 MPa. These values represent a high flexibility and high breaking strain, which were a consequence of the high stretchability imparted by the linear chains. Silicone intermediate would provide a linear chain that could give better mobility and flexibility to the polymer network. Therefore it could be implied that silicone intermediate can give flexibility, and would provide lower stiffness and higher softness to the polyester coatings (Moon *et al.*, 2012).

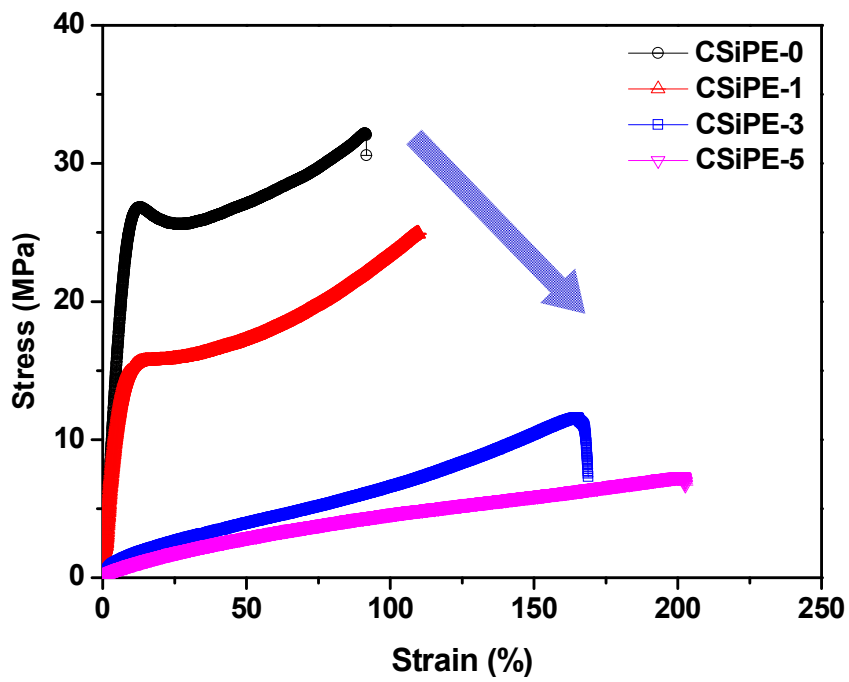


Figure 5-4. Stress-strain curve of silicone-modified polyester coatings.

### 3.4. Formability

The deep drawing test is a common method for determining the formability in pre-coated metals. During the deep drawing test, which took 90 s to complete, the calculated stress was 5.1 MPa, and the strain was 23.4 % on the PCM.

Figure 5-5 shows the formability resulting from the deep drawing. CSiPE-0 and CSiPE-1 had cracks and delamination, even though they exhibited higher tensile strength values from the flexibility test. CSiPE-0 and CSiPE-1 were not flexible enough to be stretched out during the deep drawing. CSiPE-3 and CSiPE-5 exhibited good formability, because those specimens had sufficient tensile strength and elongation values based on the flexibility test. They also had sufficient flexibility based on the creep test, as shown in Figure 5-6. The developed strain of CSiPE-3 and CSiPE-5 were over 30 % for 90 s by the creep strain. So, those specimens can be stretched, without being damaged during deep drawing. From the deep drawing test, the tensile strength of polyester coatings should be larger than 5.1 MPa to overcome tensile stress, and those of the strain should be larger than 23.4 % for 90 s to have good formability.

In our previous study, formability could be predicted from the tensile test and creep test. A forming coefficient based on strain energy ( $F_U$ ) should be larger than 1, and a forming coefficient based on strain ( $F_\epsilon$ ) should be larger than 1 (Moon *et al.*, 2012).  $F_U$  and  $F_\epsilon$  were calculated, and are listed in Table 5-4. The  $F_U$  of CSiPE-0 and CSiPE-1 was 0.33 and 0.51 respectively, and the  $F_\epsilon$  of CSiPE -0 and CSiPE-1 was 0.68 and 0.87. So, CSiPE -0 and CSiPE-1 were not flexible enough to

stretch out during the deep drawing test. However, the  $F_U$  of CSiPE -3 and CSiPE-5 were larger than 1, and those of  $F_\varepsilon$  were also larger than 1. So, those specimens can be stretched without being damaged during the deep drawing. Those results agreed with our previous study. Silicone intermediate would provide lower stiffness and higher softness to polyester coatings, but it would be made waken of polyester coatings.

	
<p>CSiPE-0</p>	<p>CSiPE-1</p>
	
<p>CSiPE-3</p>	<p>CSiPE-5</p>

Figure 5-5. Formability of silicone-modified polyester coatings on the cold roll steel sheet.

Table 5-4. Calculated values from tensile test and creep test of silicone-modified polyester coatings (Moon *et al.*, 2012).

Sample	$U_T$	$U_C$	$F_U (U_C/U_T)$	$\varepsilon_C$ (%)	$F_\varepsilon (\varepsilon_C/R_f)$
CSiPE-0	246.88	81.42	0.33	15.96	0.68
CSiPE-1	202.10	102.31	0.51	20.06	0.87
CSiPE-3	143.20	220.36	1.53	43.20	1.86
CSiPE-5	77.81	450.23	5.78	88.28	3.77

$U_T$ : strain energy at 23.4% in tensile test

$U_C$ : strain energy of coating film in creep test

$F_U (U_C/U_T)$  : forming coefficient based on strain energy

$\varepsilon_C$ : strain at 5.1 MPa during the creep test

$F_\varepsilon (\varepsilon_C/R_f)$  : forming coefficient based on strain

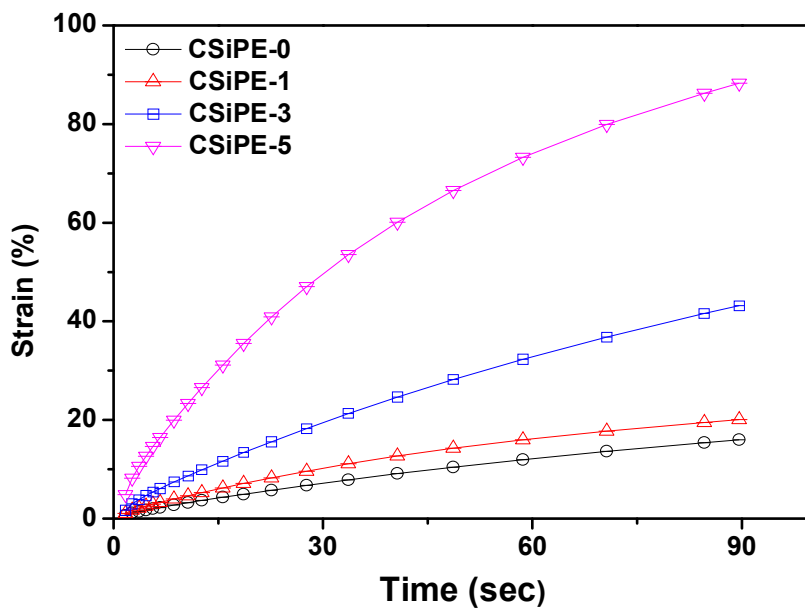


Figure 5-6. Strain of silicone-modified polyester coatings by the creep test.

### 3.5. Analysis of X-ray photoelectron spectroscopy

To analyze the amount of silicone component, XPS was used to detect O, C and Si atom on a cured coating surface. Photoemission peaks from O<sub>1s</sub>, C<sub>1s</sub> and Si<sub>2p</sub> core levels can clearly be observed, with bonding energies of 530, 283, 100 eV, respectively (Miao *et al.*, 2009). As shown in Figure 5-7, a silicone atom peak was not shown in the photoemission curve of CSiPE-0. The silicone atom to carbon ration increased with increasing content of silicone intermediate. The Si<sub>2p</sub> peak increased with increasing content of silicone intermediate. CSiPE-1, CSiPE-3, and CSiPE-5 have 0.1, 0.3 and 0.5 mol of silicone intermediate contents, while at the surface of the silicone group, the concentration was 8.5, 13.6 and 16.6 wt %, respectively. Those results implied that the silicone group can migrate to the surface of cured polyester coatings.

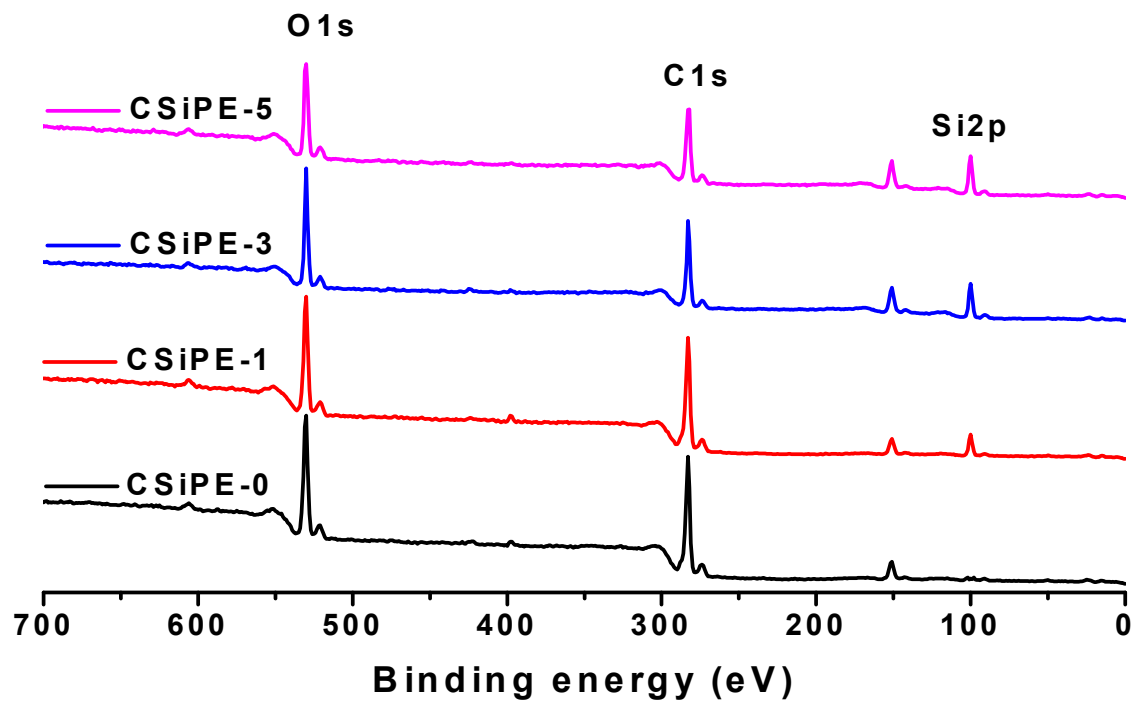


Figure 5-7. XPS curves of silicone-modified polyester coatings.

### **3.6. Surface free energy**

Figure 5-8 shows the surface energy calculated by the Lewis acid-base three liquids method. These results are summarized in Table 5-4. The contact angle of the film surface increased with increasing silicone content, which was incorporated to increase film hydrophobicity. The water contact angle and surface free energy of CSiPE-0 were 77.6° and 46.2 mN/m, respectively. CSiPE-5, which had the highest amount of silicone intermediate, had 93.5° of water contact angle, and had 26.5 mN/m of surface free energy. These results suggest that the Si-O and Si-O-Si groups in the flexible segment tailor to the outermost surface, and can be produced hydrophobicity on the cured film of the surface.

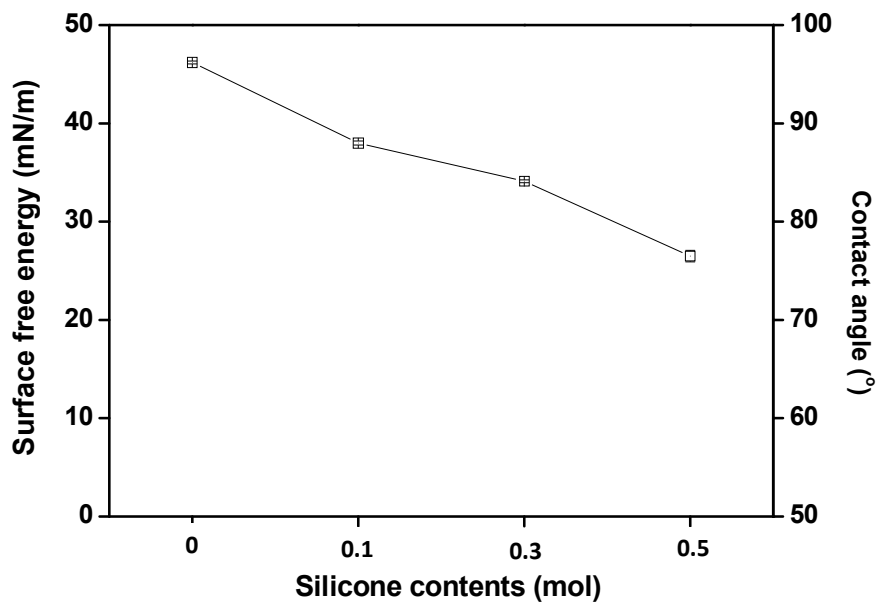


Figure 5-8. Surface free energy and contact angle of silicone-modified polyester coatings.

Table 5-5. Contact angle and surface free energy of silicone-modified polyester coatings.

Samples	Contact Angle (°)			Surface Free Energy (mN/m)		
	Water	Formamide	Diiodomethane	$\gamma_s$	$\gamma_s^d$	$\gamma_s^p$
CSiPE-0	77.6	46.4	29.8	46.2	43.1	3.4
CSiPE-1	82.7	55.6	45.1	38.0	34.7	3.2
CSiPE-3	89.5	62.8	51.9	34.1	31.9	2.1
CSiPE-5	93.5	72.3	67.5	26.5	24.3	2.0

### **3.7. Cleanable characteristics as a topcoat**

The peel test results for the evaluation of cleanable characteristics with the silicone group are shown in Figure 5-9. The maximum strength of CSiPE-0 was 8.5 N/25 mm, and that of SiPE-5 was 5.5 N/25mm. CSiPE-5 has the highest content of silicone; the value had a similar peel adhesion to that of semi-removable PSAs (pressure sensitive adhesives), as listed in Table 5-5 (Czech *et al.*, 2006). With the increasing silicone intermediate content, peel strength was gradually decreased. In the result of the peel test, the peel strength was steady decreased, with silicone intermediate content ranging from 0 to 0.5 mol. From those results, increasing contents of silicone intermediate to the silicone-modified polyester resin increased the contact angle of water, and decreased the peel strength of the cured silicone-modified polyester coatings.

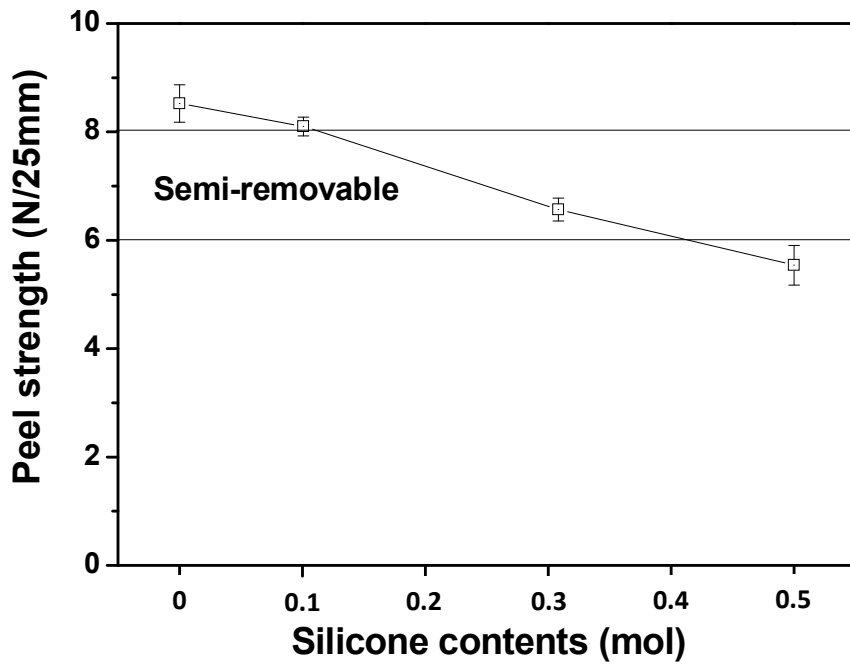


Figure 5-9. Peel strength of silicone-modified polyester coatings

Table 5-6. Classification of pressure-sensitive adhesive vs. peel adhesion (Czech *et al.*, 2006).

Kind of PSA	Adhesion of PSA [N/25 mm] (180° peel test)
Excellent permanent	>14
Permanent	10-14
Semi-removable	6-8
Removable	2-4
Excellent removable	<1

#### **4. Conclusions**

Four types of silicone-modified polyester resins with different contents of silicone intermediate were synthesized, and formulated to control formability for pre-coated metal systems. Those resins were designed to show the flexibility of the long chain of the silicone intermediate. The viscoelastic behavior, flexibility and formability were measured, to determine the long chain effect on the flexibility of the pre-coated metal system.

When the content of the long chain of silicone intermediate were increased in the resins synthesized, the stiffness of the product decreased considerably, and the  $T_g$  of each cured coatings shifted to the lower temperature. Therefore, silicone intermediate is a major factor in improving flexibility and formability of the polyester coatings. To make good formability of polyester coating for pre-coated metals, the tensile stress of the polyester coating should be larger than 5.1 MPa, and the strain should stretch out 23.4 % for 90 s.

Silicone intermediate can give low surface energy and cleanable characteristics to polyester coatings. The peel strength of CSiPE-5 was 5.5 N/25mm, which was that of semi-removable PSAs. CSiPE-5 which had 0.5 mol of silicone intermediate had good formability in the deep drawing, and also had low peel strength. So, CSiPE-5 would be an appropriate coating as a topcoat for automotive pre-coated metals.

# **Chapter 6**

## **Concluding remarks**

Currently, the automotive industry is faced with environmental regulations. These regulations demand reduction of solvent or wastes of industrial products, and to reuse or recycle end of life vehicles. In addition, the automotive market of developing countries, such as China, India and other nations, has increased quickly. Therefore, overcoming environmental regulations and satisfying the automotive trend of developing countries are important issues in the automotive industry.

Pre-coated metal system (PCM) is manufactured in a sheet or coil coating line and assembled in factories for household electric appliances, building materials and others. In this system, a wet coating process can be eliminated by the roll coating process, thereby the problem of solvent evaporation can be eliminated. In addition, PCM offers other advantages such as improving productivity and energy saving. Based on these reasons, the automotive pre-coated metal system (automotive PCM) has been investigated to remove the wet coating process, such as pre-treatment, dip coating and spray coating. In this system, all coating layers must have high flexibility and formability to overcome the harsh conditions due to the cutting, press and stamping process.

Polyesters are widely used in pre-coated metal sheet, especially for purposes of improved exterior durability and corrosion protection. In addition, polyesters can control physical properties and curing conditions using various curing agents such as melamine formaldehyde (MF) resin and blocked isocyanate pre-polymer. The main purpose of this study was to synthesize optimized polyester resins and to improve flexibility and formability for an automotive PCM.

## **Formability of flexible polyester coatings with polycarbonate diol for pre-coated metals**

Four types of flexible polyester resins with polycarbonate diol were synthesized and formulated to control formability for pre-coated metal systems. These resins were designed to show the flexibility of long alkyl chain. The viscoelastic behavior, flexibility and formability were measured to determine the long alkyl chain effect on the flexibility of the pre-coated metal system.

When the content of long alkyl chain of polycarbonate diol was increased in the resins synthesized, the stiffness of the product decreased considerably and  $T_g$  of each cured coatings shifted to a lower temperature. Therefore, polycarbonate diol is a major factor to improve flexibility and formability of the polyester coatings. To make good formability of polyester coating for the pre-coated metals, tensile stress of polyester coating should be larger than 5.1 MPa to overcome stressed during the deep drawing and strain should stretch out 23.4 % for 90 s.

CPC-2 which had 2 mol of polycarbonate diol had good formability in the deep drawing and also had good anti-corrosion property compared to electro deposition coating. So, CPC-2 would be an appropriate coating as a primer for automotive pre-coated metals.

## **Synthesis of polyester-nanocomposites and characterization of polyester-nanocomposites coatings for automotive pre-coated metals**

Four types of PE/OMMT nanocomposites were synthesized by the in-situ polymerization with high speed homogenizer process at the various contents of organoclay to disperse into the polyester matrix. The absence of refraction pattern of organoclay by SAXS and TEM study revealed that exfoliated organoclay layers are well dispersed into the polymer chain. Mechanical property of PE/OMMT nanocomposites coating improved 9 % of the maximum tensile strength. The viscoelastic behavior of PE/OMMT nanocomposites coating was observed by dynamic mechanical analysis (DMA). When the content of organoclay was increased, the storage modulus of the PE/OMMT nanocomposites coating increased considerably and  $T_g$  of each cured coatings shifted to a lower temperature.

Anti-corrosion property was examined by the salt spray test. CNC-3 had the highest amount of organoclay and it had little rust after 600 h. It implies that nano-sized layered silicate of organoclay effectively increases the length of the diffusion pathways water molecules. And nano-sized layered silicate of organoclay might be decreased the permeability and can make higher corrosion resistance of PE/OMMT nanocomposites coating. From those results, CNC-3 which had 3 wt % of organoclay had good formability in the deep drawing and also had good anti-corrosion property. So, CNC-3 would be an appropriate PE/OMMT nanocomposites coating as a primer for automotive pre-

coated metals.

### **Synthesis and characterization of cyclic structure contained polyester resin as a basecoat for automotive pre-coated metals**

Four types of cyclic structure contained polyester resins with 1,4-CHDA were synthesized and formulated, to control formability for pre-coated metal systems. Those resins were designed to show the flexibility of the cyclic ring. The viscoelastic behavior, flexibility and formability were measured to determine the cyclic structure effect on the flexibility of the pre-coated metal system. When the content of cyclic structure of 1,4-CHDA was increased in the resins synthesized, the stiffness of the product generally decreased, and the  $T_g$  of each cured coating shifted to a lower temperature. Therefore, 1,4-CHDA is a major factor in improving the flexibility and formability of polyester coatings. To ensure good formability of polyester coating for the pre-coated metals, the tensile stress of the polyester coating should be larger than 5.1 MPa, and the strain should stretch out by 23.4 % for 90 s.

The cyclic structure of 1,4-CHDA can give flexibility and would provide lower stiffness to the polyester coatings, and it has better elasticity than aromatic structure. So, it can give better chipping resistance. BCHDA-20 which had 20 mol of 1,4-CHDA had good formability in the deep drawing test, and also showed good chipping resistance in that test. So, BCHDA-20 would be an appropriate coating as a basecoat for automotive pre-coated metals.

## **Synthesis and characterization of silicone-modified polyester as a topcoat for automotive pre-coated metals**

Four types of silicone-modified polyester resins with different contents of silicone intermediate were synthesized, and formulated to control formability for pre-coated metal systems. Those resins were designed to show the flexibility of the long chain of the silicone intermediate. The viscoelastic behavior, flexibility and formability were measured, to determine the long chain effect on the flexibility of the pre-coated metal system.

When the contents of the long chain of silicone intermediate were increased in the resins synthesized, the stiffness of the product decreased considerably, and the  $T_g$  of each cured coating shifted to the lower temperature. Therefore, silicone intermediate is a major factor in improving flexibility and formability of the polyester coatings. To make good formability of polyester coating for pre-coated metals, the tensile stress of the polyester coating should be larger than 5.1 MPa, and the strain should stretch out 23.4 % for 90 s.

Silicone intermediate can give low surface energy and cleanable characteristics to polyester coatings. The peel strength of CSiPE-5 was 5.5 N/25mm, which was that of semi-removable PSAs. CSiPE-5 which had 0.5 mol of silicone intermediate had good formability in the deep drawing, and also had low peel strength. So, CSiPE-5 would be an appropriate coating as a topcoat for automotive pre-coated metals.

## References

H. S. Bendor, *J. Appl. Polym. Sci.* **13**: 1253-1264 (1969)

H. S. Bendor, *J. Paint Technol.* **48**: 51-57 (1971).

A. E. Tonelli, *Polymer* **15**: 194–196 (1974).

G. Hayward, C. J. Standen, M. J. Husbands, *A Manual of Resins for Surface Coatings*, SITA Technology, London (1987).

V. Percec, M. Zuber, *Polym. Bull.* **25**: 695-700 (1991).

G. P. Simon, P. E. M. Allen, D. R. G. Williams, *Polymer* **32**: 2577–2587 (1991).

Improved Coil Coating Performance with Eastman 1,4-CHDA,  
Eastman Publication N-327A (1995).

T. Hamada, H. Kanai, T. Koike, M. Fuda, *Prog. Org. Coat.* **30**: 271-278 (1997).

L. W. Hill, *Prog. Org. Coat.* **31**: 235-243 (1997).

K. Kanda, *J. Jpn. Soc. Colour Mater.* **71**: 328-338 (1998).

J. Yin, Y.-F. Ye, Z.-G. Wang, *Eur. Polym. J.* **34**: 1839-1843 (1998).

S. Frings, H. A. Meinema, C. F. Van Nostrum, R. Van der Linde, *Prog. Org. Coat.* **33**: 126-130 (1998).

S. Nakano, *Prog. Org. Coat.* **35**: 141-151 (1999).

R. L. Howard, S. B. Lyon, J. D. Scantlebury, *Prog. Org. Coat.* **37**: 91-98 (1999).

K. Ueda, H. Kanai, T. Suzuki, T. Amari, *Prog. Org. Coat.* **43**: 233-242 (2001).

M. Gindl, G. Sinn, W. Gindl, A. Reiterer, S. Tschegg, *Collo. Surf. A*, **181**: 279-287 (2001).

Y. K. Lee, H. J. Kim, M. Rafailovich, J. Sokolov, *Int J Adhes Adhes*, **22**: 375-384 (2002).

J. H. Chang, *Y. U. An. J. Polym. Sci., Part B : Polym. Phys.* **40**: 670-677 (2002).

H. Li, J. L. Daum, P. R. Thiltgen, M. D. Soucek, W. J. Simonsick, W. Zhong, A. D. Skaja, *Prog. Org. Coat.* **45**: 49-58 (2002).

K. Ueda, H. Kanai, T. Amari, *Prog. Org. Coat.* **43**: 267-272 (2002).

D. Satas, Handbook of Pressure Sensitive Adhesive Technology and Application, Satas & Associates Warwick, Rhode Island, USA (2002).

S. S. Ray, M. Okamoto, Prog. Polym. Sci. **28**: 1539-1641 (2003).

X. Chen, L. Wu, S. Zhou, B. You, Polym. Int. **52**: 993-998 (2003).

S. X. Zhou, L. M. Wu, J. Sun, W. D. Shen, J. Appl. Polym. Sci. **88**: 189-193 (2003).

W. J. Choi, S. H. Kim, Y. J. Kim, S.C. Kim, Polymer **45**: 6045–6057 (2004).

Y. W. Chen-Yang, H. C. Yang, G. J. Li, Y. K. Li, J. Polym. Res. **11**: 275–283 (2004).

A.-S. Jandel, B. Meuthen, Coil Coating, Vieweg & Sohn, Wiesbaden, (2005)

Y. Chen, S. Zhou, G. Chen, L. Wu, Prog. Org. Coat. **54**: 120-126 (2005).

A. Asif, W. F. Shi, X. F. Shen, K. M. Nie, Polymer **46**: 11066-11078 (2005).

J. H. Choi, H.-J. Kim, J. Ind. Eng. Chem. **12**: 412-417 (2006).

T. G. Mezger, The Rheology Handbook, 2<sup>nd</sup> Ed., VINCENTZ, Hannover (2006).

J. W. Wang, L. P. Wang, J. Fluor. Chem, **127**: 287-290 (2006).

Z. Czech, Int. J. Adhes. Adhes. **26**: 414-418 (2006).

L. Wang, Z. Xie, X. Bi, X. Wang, A. Zhang, Z. Chen, J. Zhou, Z. Feng, Polym. Degrad. Stab. **91**: 2220-2228 (2006).

M. R. Bagherzadeh, F. Mahdavi, Prog. Org. Coat. **60**: 117-120 (2007).

A. Tiwari and L. H. Hihrra, TRI-SERVICE Corrosion Conference (2007).

K. Wang, L. Chen, M. Kotaki, C. He, Comp. :Part A **38**: 192-197 (2007).

B. Ahmadi, M. Kassiriha, K. Khodabakhshi, E. R. Mafi, Prog. Org. Coat. **60**: 99-101 (2007).

M. J. Geerken, R. G.H. Lammertink, M. Wessling, Collo. Surf. A, **292**: 224-235 (2007).

M. Lonyuk, M. Bosma, C. A. M. Vijverberg, A. Baker, M. Janssen, Prog. Org. Coat. **61**: 305-315 (2008).

S. Lv, W. Zhou, S. Li, W. Shi, *Eur. Polym. J.* **44**: 1613–1619 (2008).

M. Spirkova, J. Brus, L. Brozova, A. Strachota, J. Baldrian, M. Urbanova, J. Kotek, B. Strachotova, M. Slouf, *Prog. Org. Coat.* **61**: 145–155 (2008).

Y. J. Park, D. H. Lim, H.-J. Kim, *J. Adhesion Sci. Technol.* **22**: 1401-1423 (2008).

Q. Hou, D. W. Grijpma, J. Feijen, *Acta Biomater.* **5**: 1543-1551 (2009).

D. K. Chattopadhyay, D. C. Webster, *Prog. Org. Coat.* **66**: 73-85 (2009)

H. Miao, L. Cheng and W. Shi, *Prog. Org. Coat.* **65**: 71-76 (2009).

M. B. Stroisznigg, G. M. Wallner, B. Straub, L. Jandel, R.W. Lang, *Prog. Org. Coat.* **65**: 44-48 (2009).

M. B. Stroisznigg, G. M. Wallner, B. Straub, L. Jandel, R.W. Lang, *Prog. Org. Coat.* **65**: 328-332 (2009).

F. Levine, J. La Scala, W. Kosik, *Prog Org Coat* **69**: 63-72 (2010).

R. Tian, O. Seitz, M. Li, W. W. Hu, Y. Chabal, *Langmuir* **26**: 4563-4566 (2010).

M. Heidarian, M. R. Shishesaz, S. M. Kassiriha, M. Nematollahi, Prog. Org. Coat. **68**: 180-188 (2010).

U. Konwar, M. Mandal, N. Karak, Prog. Org. Coat. **72**: 676-685 (2011).

J.-I Moon, Y.-H. Lee, H.-J. Kim, Prog. Org. Coat. **73**: 123-128 (2012).

J.-I Moon, Y.-H. Lee, H.-J. Kim, Polymer Testing **31**: 572–578 (2012).

Y.-H. Lee, H.-J. Kim, J.-Y. Shin, Prog. Org. Coat. POC-D-12-00184 (2012)

J.-I Moon, Y.-H. Lee, H.-J. Kim, S. Schwartz, M. Rafailovich, J. Sokolov, Polymer Testing **31**: 433–438 (2012).

J. Zhang, W. Tu, Z. Dai, Prog. Org. Coat. **75**: 579-583 (2012).

Standard Test Method for Tensile Properties of Plastics, ASTM D638-10.

[www.eccacoil.com](http://www.eccacoil.com):European Coil Coating Association (2006).

## 초 록

최근의 자동차 산업은 다양한 환경규제를 받기 시작했다. 이러한 환경규제는 휘발성이 강한 용제 사용의 억제, 산업 폐기물의 방출 제한 및 재활용 비율의 강제 등으로 인해 현재의 생산공정에 대한 변화를 요구하고 있다. 이러한 변화에 대응하기 위해 새로운 코팅 공정인 wet-on-wet coating과 roll coating이 적용되기 시작하였다.

Roll coating 공정이 적용되는 pre-coated metal (PCM)은 철판에 선도장 및 경화시킨 후 성형하는 방법으로 건축 재료, 전기·전자 및 백색 가전 등에 적용되고 있다. Roll coating 공정은 환경규제로 인해 문제가 되고 있는 습식 도장 공정에 비해 용제 및 도료의 회수와 도료 재사용이 가능하기 때문에 환경규제에 유리하게 대응할 수 있다. 또한 빠른 도장 속도와 도장 공정 라인 축소로 인한 생산성 향상과 에너지 절감이 가능하다. 이러한 장점으로 자동차용 PCM 공정은 최근 들어 연구가 활발히 진행되고 있다. 자동차용 PCM 공정은 선도장 후가공을 하기 모든 도막이 가혹한 성형 공정에 견딜 수 있는 높은 유연성 및 성형성을 보유하여야 한다. 폴리에스터 수지는 합성을 위한 원료가 다양하고 경화를 위한 경화제 선택이 자유롭기 때

문에 다양한 물리적 특성을 부여할 수 있다. 또한 내구성이 우수하기 때문에 PCM 공정에 주로 사용되고 있다.

본 연구에서는 자동차용 PCM를 위해 하도 도료용 수지, 중도 도료용 수지와 상도 도료용 수지를 합성하였으며, 합성된 수지를 이용하여 하도 도료, 중도 도료 및 상도 도료를 제조하였다. 제조된 도료들의 다양한 물성을 평가함으로써 자동차용 PCM 공정 연구에 도움이 되고자 하였다.

유연성이 향상된 폴리에스터 수지를 합성하기 위하여 긴 사슬로 구성되어 있는 폴리카보네이트 디올을 사용하였다. 합성된 수지의 분석과 점탄성적 특성 및 다양한 물리적 특성인 성형성과 내부식성을 분석하기 위하여 FT-IR, GPC, DMA, UTM, deep drawing test, EIS와 salt spray 등이 사용되었다. 폴리카보네이트 디올의 함량이 증가할수록 탄성계수가 감소하고 유리전이온도가 낮아지는 경향을 나타내었다. 이는 폴리카보네이트 디올 분자 사슬의 높은 움직임으로 인한 것으로 판단된다. 성형성과 내부식성 시험 결과 폴리카보네이트 디올의 함량이 2 mol인 CPC-2가 가장 우수한 결과를 나타내었으며, 이러한 결과를 통해 자동차용 PCM의 하도 도료로 적용이 가능할 것으로 판단된다.

하도 도료의 가장 중요한 특성인 내부식성능을 높이기 위해 유

기화처리된 organoclay를 폴리에스터 수지 분자내에 결합되도록 PE/OMMT nanocomposite를 합성하였다. Organoclay는 homogenizer를 사용하여 선 분산시켰으며, 합성된 PE/OMMT nanocomposite내에 organoclay의 분산 정도를 확인하기 위해 SAXS와 TEM을 사용하였다. 합성된 수지의 분석과 점탄성적 특성 및 다양한 물리적 특성을 분석하기 위하여 DMA, UTM, deep drawing test, EIS와 salt spray 등이 사용되었다. Organoclay의 함량이 증가할 수록 경화도막의 탄성 계수가 증가하였으나, 유리전이온도는 조금 낮아지는 것을 관찰하였고, 내부식능이 향상되는 것을 확인하였다. 이는 organoclay의 나노 크기의 layered silicate가 강성 부여 및 barrier 특성이 우수하기 때문이다. 성형성이 우수하기 위해서는 인장강도는 5.1 MPa 이상이고, 신율은 90 초 동안 23.4% 이상이어야 함을 확인하였다. 성형성과 내부식성 시험 결과 organoclay의 함량이 3 wt %인 CNC-3가 가장 우수한 결과를 나타내었으며, 이러한 결과를 통해 자동차용 PCM의 하도 도료로 적용이 가능할 것으로 판단된다.

자동차용 중도 도료의 주요 물성인 저온 stone-chipping 저항성을 향상시키기 위해 1,4-cyclohexanedicarboxylic acid의 함량을 조절하여 싸이클릭 구조가 많이 함유된 폴리에스터 수지를 합성하였다. 합성된 수지의 분석과 점탄성적 특성 및 다양한 물리적 특성을 분석

하기 위하여 GPC, DMA, UTM, deep drawing test와 저온 stone-chipping 시험 등을 사용하였다. 1,4-CHDA의 싸이클릭 구조의 양이 증가할 수록 경화도막의 탄성계수는 감소하고, 유리전이온도는 낮아짐을 관찰할 수 있었다. 이는 1,4-CHDA의 싸이클릭 구조는 벤젠링을 갖고 있는 isophthalic acid에 비해 폴리에스터 수지에 유연성과 탄성을 부여하였기 때문이다. 성형성과 저온 stone-chipping 시험 결과 1,4-CHDA의 함량이 20 mol인 BCHDA-20이 가장 우수한 결과를 나타내었다. 이러한 결과를 통해 싸이클릭 구조가 많이 함유된 폴리에스터 수지는 자동차용 PCM의 중도 도료로 적용이 가능할 것으로 판단된다.

자동차용 상도 도료의 주요 물성인 낮은 접촉각을 갖고 자기 세정이 가능한 실리콘 중간체를 이용하여 실리콘 변성 폴리에스터 수지를 합성하였다. 합성된 수지의 분석과 점탄성적 특성 및 다양한 물리적 특성을 분석하기 위하여 GPC, DMA, UTM, XPS, deep drawing test와 peel test 등을 사용하였다. 실리콘 중간체의 함량이 증가할 수록 경화도막의 탄성계수는 감소하고, 유리전이온도는 낮아짐을 관찰할 수 있었다. 경화 도막의 표면에 이동된 실리콘 원소의 함량이 증가하는 것을 XPS를 이용하여 확인하였으며, peel test를 이용하여 자기 세정 특성이 있음을 확인하였다. 실리콘 중간체의 함량이 0.5 mol

인 CSiPE-5는 성형성이 우수하고, peel test에서 semi-removable 특성을 갖는 낮은 peel 강도 결과를 나타내었다. 이러한 결과를 통해 실리콘 변성 폴리에스터 수지는 자동차용 PCM의 상도 도료로 적용이 가능할 것으로 판단된다.

**주요어** : 자동차 도료, 폴리에스터, Pre-coated metal (PCM), 유연성, 성형성, 성형성 시험, 폴리카보네이트 디올, 나노 클레이, 나노 복합체, 시클로헥산디카르복실산, 실리콘 중간체

학 번 : 2008-30330

## 감사의 글

오늘 제가 이 자리에 있기까지 박사과정 5년 동안 제 인생에서 가장 중요한 시간을 보냈고 개인적으로 열심히 노력한 것 같습니다. 그런데, 아직도 배울 것도 많고 부족한 점도 많아서 돌이켜 보면 한편으로는 아쉬움이 많이 남습니다. 아직 가야 할 길이 많이 남아 있기에 초심을 잃지 않고 다시 시작하는 마음으로 더욱 더 열심히 살아가겠습니다.

제가 대학원 생활을 하는 동안 많은 분들께서 도움을 주셨으며, 그 많은 분들의 도움이 있었기에 이 논문을 완성하게 되었습니다. 학위과정 동안 제가 본받고 따라야 할 모범을 보여주시고, 학문을 일깨워주신 지도 교수님인 김현중 교수님께 감사를 드립니다. 많이 바쁘심에도 불구하고 심사위원장님으로써 부족한 저의 논문을 지도하여 주신 서울대학교 화학생물공학부 장정식 교수님, 항상 곁에 계시면서 물심 양면으로 도와주신 최희천 겸임 교수님, 학과장님으로써 많이 바쁘심에도 불구하고 심사를 맡아주신 한양대학교 화학공학과 장영욱 교수님, 먼 길을 마다하지 않으시고 오셔서 논문 심사를 맡아주시고, 부족한 저의 논문을 처음부터 끝까지 세심하게 살펴보시고 조언하여 주신 한국화학연구원의 김영철 박사님께 진심으로 감사를 드립니다.

학위 과정 동안 많은 가르침과 관심을 기울여 주신 이전제 교수님, 이학래 교수님, 최인규 교수님, 윤혜정 교수님, 여환명 교수님, 최준원 교수님께 감사를 드립니다. 지난 대학원 생활 동안

가족보다 더 많은 시간을 함께해온 바이오복합재료 및 접착과학 연구실 모든 식구들에게도 많은 감사를 드립니다. 그리고, 연구실은 다르지만 모든 산림과학부 환경재료과학 전공 대학원생들에게도 감사를 드립니다.

제가 학위 논문과 연구 과제를 수행하는데 많은 도움과 조언을 주신 노루페인트의 연구원님들께 깊은 감사를 드립니다. 또한, 제가 학위를 무사히 마칠 수 있도록 많은 배려를 해주신 유니테크 이성호 사장님을 비롯한 모든 직원들에게도 깊은 감사를 드립니다. 늦은 나이에 공부하는 친구를 항상 응원해 주던 친구들에게도 이 자리를 빌어 감사의 마음을 전합니다. 제가 오늘 이 자리에 있을 수 있도록 도와주신 많은 분들에게 깊은 감사를 드리며, 도움을 주신 모든 분들의 은혜를 잊지 않고 사회에 보탬이 되는 연구자가 되도록 더욱더 노력하겠습니다.

그 무엇보다도 오늘의 제가 이 자리에 있기까지 항상 묵묵히 응원해 주신 가족들에게 깊은 미안함과 감사를 드립니다. 못난 자식을 항상 믿으시고 따뜻한 마음으로 격려해 주신 아버지, 어머님, 형님들, 누님에게 감사를 드립니다. 아버지, 어머님 사랑합니다. 끝으로 항상 믿고 따라준 사랑하는 아내 영옥에게 고맙고 미안한 마음뿐이며, 어려운 환경에서도 잘 키운 아들 용준이에게도 고마움을 전합니다.

이제까지 많은 분들에게서 도움을 받아 어려움을 이겨낼 수 있었기에 이제는 그 고마움을 베풀고 살아가는 사람이 되도록

노력하겠습니다.

2013년 1월, 사랑하고 고마운 분들에게 감사의 글을 올립니다.